

References

- Adriano, D.C. (1986). Trace elements in the terrestrial environment. *Springer-Verlag, New York.*
- Aftabi, A.; Ghodrati, Z. and Maclean, W.H. (in proof). Metamorphic textures and geochemistry of the Cyprus-type massive sulfide lenses at Zurabad, Khoy, Iran. *Journal of Asian earth sciences XX*, 1-11.
- Alymore, L.A.G.; Karim, M. and Quirk, J.P. (1967). Adsorption and desorption of sulphate ions by soil constituents. *Soil Science*, **103**, 10-15.
- Attridge, R.L. (1986). The Jacomynspan copper-nickel occurrence, Kenhardt District in Mineral Deposits of Southern Africa, II. In: C.R., Anhaeusser and S., Maske (Editors) *Geological Society of South Africa, Johannesburg*, 1539-1546.
- Badham, J.P.N. (1981). Shale- hosted Pb-Zn deposits: products of exhalation of formation waters? *Institution of Mining and Metallurgy, Transactions*, **90**, B71-B76.
- Bardshaw, P.M.D.; Thomson, I.; Smee, B.W. and Larsson, J.O. (1974). The application of different analytical extractions and soil profile sampling in exploration geochemistry. *Journal of Geochemical Exploration*, **3**, 209-225.
- Barton, E.S. and Burger, A.J. (1983). Reconnaissance isotopic investigation of the marginal zone of the Proterozoic Namaqua mobile belt, Upington Geotraverse. *Geological Society of South Africa, Special Publication*, **10**, 173-192.
- Beus, A.A. and Grigorian, S.V. (1977). Geochemical exploration methods for mineral deposits. *Applied Publishing LTD., U.S.A.*, 286 pp.
- Bonnet AL.; Corriveau L. and La Fleche MR. (2005). Chemical imprint of highly metamorphosed volcanic-hosted hydrothermal alterations in the La Romaine Supercrustal Belt, eastern Grenville Province, Quebec. *Canadian Journal of Earth Sciences*, **42**, 1783-1814.
- Bowers, T.S.; Von Damm, K.L. and Edmond, J.M. (1985). Chemical evolution of mid-ocean ridge hot springs. *Geochimica et Cosmochimica Acta*, **49**, 2239-2252.
- Bradshaw, P.M.D.; Thomson, I.; Smee, B.W. and Larsson, J.O. (1974). The application of different analytical extractions and soil traverse sampling exploration geochemistry. *Journal of Geochemical Exploration*, **3**, 209-225.

- Brauhart, C.W.; Huston, D.L. and Andrew, A.S. (2000). Oxygen isotope mapping in the Panorama VMS district, Pilbara Craton, Western Australia: applications to estimating temperatures of alteration and to exploration. *Mineralium Deposita*, **35**, 727-740.
- Bruker Advanced X-Ray Solutions. (2003). DIFFRAC^{plus}, EVA version 9.0, *Karlsruhe, Germany*.
- Cahen, L.; Snelling, N.J.; Delhal, J. and Vail, J.R. (1984). The geochronology and evolution of Africa. *Clarendon Press, Oxford*, 512 pp.
- Cameron, E.M.; Hamilton, S.M.; Leybourne, M.I. and Hall, G.E.M. (2004). Finding deeply buried deposits using geochemistry. *Geochemistry: Exploration, Environment, Analysis*, **4**, 7-32.
- Cameron, E.M. and Hattori, K. (1987). Archean sulphur cycle: Evidence from sulphate minerals and isotopically fractionated sulphides in superior province, Canada. *Chemical Geology, Isotope Geoscience section*, **65**, 341-358.
- Campbell, I.H.; Franklin, J.M.; Gorton, M.P.; Hart, T.R. and Scott, S.D. (1981). The role of subvolcanic sills in the generation of massive sulphide deposits. *Economic Geology*, **76**, 2248-2253.
- Canet, C.; Alfonso, P.; Melgarejo, J.C. and Belyatsky, B.V. (2004). Geochemical evidences of sedimentary-exhalative origin of the shale-hosted PGE-Ag-Au-Zn-Cu occurrences of the Prades Mountains (Catalonia, Spain): trace-element abundances and Sm-Nd isotopes. *Journal of Geochemical Exploration*, **82**, 17-33.
- Carlisle, D. (1980). Possible variations on the calcrete-gypcrete uranium model. *United State Department of Energy, open file Report GJBX 53(80), Subcontract 76-022-E, Bendix Field Engng. Corp. and University of California.*, Los Angeles, 38 pp.
- Cathles, L.M. (1983). An analysis of the hydrothermal system responsible for massive sulphide deposition in the Hokuroku basin of Japan. In: H. Ohmoto, and B.J. Skinner, (Editors) *Kuroko and related volcanogenic massive sulphide deposits. Economic Geology, Monograph 5*, 439-487.
- Chao, T.T. (1984). Use of partial dissolution techniques in geochemical exploration. *Journal of Geochemical Exploration*, **20**, 101-135.
- Chao, T.T.; Harward, M.E. and Fang, S.C. (1962a). Movement of ³⁵S tagged sulfate through soil columns. *Soil Science Society of America proceedings*, **26**, 27-32.

- Cilliers, F.H. (1987). Isotope characteristics of the sulphide-bearing sequence of the Areachap Group in the Boksputs area, Northwest Cape. *Unpublished M.Sc. thesis, University of Orange Free State, Bloemfontein*, 171 pp.
- Clark, J.R. (1997). Concepts and models for the interpretation of enzyme leach data for mineral and petroleum exploration. In: Enzyme leach: Model, Sampling Protocol and Case histories. *Activation Laboratories, Ontario*, 1-62.
- Clark, J.R. and Russ, G.P. (1991). A new enzyme partial leach enhances anomalies in pediment soils near buried gold deposits. *15th international Geochemical Exploration Symposium, Association of exploration Geochemists Reno, NV, 29 April-1 May 1991*.
- Cogley, J.G. (1985). Hypsometry of the continents. *Zeitschrift für Geomorphologie, Supplementbände*, **53**, 48 pp.
- Conradie, J.A. and Schoch, A.E. (1986). Petrological characteristics of the Koperberg Suite, South Africa: An analogy to massif-type anorthosites? *Precambrian Research*, **31**, 1570-188.
- Cornell, D.H.; Kroner, A.; Humphreys, H. and Griffin, G. (1990a). Age of origin of the polymetamorphosed Copperton Formation, Namaqua-Natal Province, by single grain zircon Pb-Pb dating. *South African Journal of Geology*, **93**, 709-714.
- Cornell, D.H.; Humphreys, H.C.; Theart, H.F.J. and Scheepers, D.J. (1992). A collision-related pressure-temperature-time path for Prieska copper mine, Namaqua-Natal tectonic Province, South Africa. *Precambrian Research*, **59**, 43-71.
- Cornell, D.H.; Theart, H.F.J. and Humphreys, H.C. (1990b). Dating a collision-related metamorphic cycle at Prieska copper mines, South Africa. In: P.G. Spry, & T. Bryndzia (Editor) Regional metamorphism of ore deposits and genetic implications, *VSP, Utrecht*, **11**, 97-116.
- Dawood YH.; Saleh GM. and EI-Naby HHA. (2005). Effects of hydrothermal alteration on geochemical characteristic of the EI Sakkari granite, Central eastern desert, Egypt. *International Geology Review*, **47**, 1316-1329.
- De Wit, MJ.; Roering, C.; Hart, RJ.; Armstrong, RA.; De Ronde, REJ.; Green RWE.; et al. (1992). Formation of an Archaean continent. *Nature*, **357**, 553-562.
- Dhir, RP.; Tandon, SK.; Sareen, BK.; Ramesh, R.; Rao, TKG.; Kailath, AJ. and Sharma, N. (2004). Calcretes in the Thar desert: genesis, chronology and palaeoenvironment.

- Proceedings of the Indian Academy of Sciences-Earth and Planetary Sciences*, **113**, 473-515.
- Dingle, R.V.; Siesser, W.G. and Newton, A.R. (1983). Mesozoic and Tertiary geology of Southern Africa. *A.A. Balkema, Rotterdam*, 375 pp.
- Fox, R.L.; Olson, R.A. and Rhoades, H.F. (1964). Evaluating the sulfur status of soils by plants and soil test. *Soil Science Society of America Proceedings*, **28**, 243-246.
- Francheteau, J.; Needham, H.D.; Choukroune, P.; Juteau, T.; Seguret, M.; Ballard, R.D.; Fox, P.J.; Normark, W.; Carranza, A.; Cordoba, D.; Guerrero, J.; Rangin, C.; Bougault, H.; Cambon, P. and Hekinian, R. (1979). Massive deep-sea sulphide ore deposits discovered on the East Pacific Rise. *Nature*, **227**, 523-528.
- Franklin, J.M.; Lydon, J.W. and Sangster, D.F. (1981). Volcanic associated massive sulphide deposits. *Economic Geology, 75th Anniversary Volume*, 485-627.
- Gaal, G. (1990). Tectonic styles of early Proterozoic ore deposition in the Fennoscandian Shield. *Precambrian Research*, **46**, 83-114.
- Genalysis Laboratory Services Pty Ltd. (© 2002, Cited 2005, Jan, 20). Terra leach™ Partial digest geochemistry (internat), TerraV6-0.doc, <http://www.genalysis.com.au>
- Geriner, G.J.; Botha, B.J.V.; Pretorius, J.J. and Ludick, D.J. (1987). Calc-alkaline volcanism along the eastern margin of the Namaqua mobile belt, South Africa-A possible middle proterozoic volcanic arc. *Precambrian Research*, **33**, 139-170.
- Geriner, G.J.; Humpherys, H.C. and Scheepers, D.J. (1994). Lithostratigraphy, protolithology, and tectonic setting of the Areachap group along the eastern margin of the Namaqua mobile belt, South Africa. *South African Journal of Geology*, **97**, 78-100.
- Geringer, G.J. and Ludick, D.J. (1990). Middle Proterozoic calc-alkaline, shoshonitic volcanism along the eastern margin of the Namaqua Mobile Belt, South Africa- implications for tectonic evolution in the area. *South African Journal of Geology*, **93**, 389-399.
- Geweke, J.F. and Singleton, K.J. (1980). Interpreting the likelihood ratio statistic in factor models when sample size is small. *Journal of the American Statistical Association*, **75**, 133-137.

- Goldberg, I.S. (1998). Vertical migration of elements from mineral deposits. *Journal of Geochemical Exploration*, **61**, 191-202.
- Goldfarb, M.S.; Converse, D.R.; Holland, H.D. and Edmond, J.M. (1983). The genesis of hot spring deposits on the East Pacific Rise, 21°N. In: H. Ohmoto, and B.J. Skinner (Editors) Kuroko and related volcanogenic massive sulphide deposits. *Economic Geology, Monograph 5*, 184-197.
- Goodfellow, W.D.; Lydon, J.W. and Turner, R.J.W. (1993). Geology and genesis of stratiform sediment-hosted (SEDEX) zinc-lead-silver sulphide deposits. In: R.V., Kirkham, W.D., Sinclair, R.I., Thorpe, J.M.S., Duke (Editors) Mineral Deposit Modeling. *Special Paper, Geological Association of Canada*, **40**, 201-251.
- Gorton, R.K. (1981). The petrology of the Kielder sulphide bodies and their wall rocks: District of Prieska, N. Cape, South Africa. *Unpublished M.Sc. thesis, University of Cape Town*, 153 pp.
- Grant, J.A. (1986). The isocon diagram-A simple solution to Gresens' equation for metasomatic alteration. *Economic Geology*, **81**, 1976-1982.
- Gray, D.J.; Wildman, J.E. and Longman, G.D. (1999). Selective and partial extraction analyses of transported overburden for gold exploration in the Yilgarn Craton, Western Australia. *Journal of Geochemical Exploration*, **67**, 51-66.
- Gresens, R.L. (1967). Composition- volume relationships of metasomatism. *Chemical Geology*, **2**, 47-55.
- Hajash, A. (1975). Hydrothermal processes along mid-ocean ridges: an experimental investigation. *Contributions to Mineralogy and Petrology*, **53**, 205-226.
- Hall, G.E.M.; Maclaurin, A.I. and Garrett, R.G. (1998). Assessment of the 1 M NH₄NO₃ extraction protocol to identify mobile forms of Cd in soils. *Journal of Geochemical Exploration*, **64**, 153-159.
- Harman, H.H. (1976). Modern factor analysis. *3rd Edition, Chicago, University of Chicago press*.
- Hartnady, C.J.H.; Joubert, P. and Stowe, C.W. (1985). Proterozoic crustal evolution in southwestern Africa. *Episodes*, **8**, 36-44.
- Haymon, R.M. (1983). Growth history of hydrothermal black smoker chimneys. *Nature*, **301**, 695-698.

- Haymon, R.M. and Kastner, M. (1981). Hot spring deposits on the East Pacific Rise at 21°N: preliminary description of mineralogy and genesis. *Earth and Planetary Science Letters*, **53**, 363-381.
- Hodgson, C.J. and Lydon, J.W. (1977). Geological setting of volcanogenic massive sulphide deposits and active hydrothermal systems: some implications for exploration. *Canadian Institution of Mining and Metallurgy, Bulletin*, **70**, 95-106.
- Hughes, C.J. (1972). Spilites, keratophytes and igneous spectrum. *Geological Magazine*, **109**, 513-527.
- Humphreys, H.C. (1993). Metamorphic evolution of amphibolite-bearing aluminous gneisses from the Eastern Namaqua Province, South Africa. *American Mineralogist*, **78**, 1041-1055.
- Humphreys, H.C.; Van Bever Donker, J.M.; Scott, W.D. and Van Schalkwyk, L. (1988a). The early deformational history of the eastern Namaqua Province: new evidence from Prieska copper mines. *South African Journal of Geology*, **91**, 174-183.
- Humphreys, H.C; Van Schalwyk, L. and Scott, W.D. (1988b). A geological and structural map of the Areachap Group succession at Prieska Copper Mines. *South African Journal of Geology*, **91**, 373-380.
- Hutchinson, R.W. (1973). Volcanogenic sulfide deposits and their metallogenetic significance. *Economic Geology*, **68**, 1223-1246.
- Ishikawa, Y.; Sawaguchi, T.; Iwaya, S. and Horiuchi, M. (1976). Delineation of prospecting targets for Kuroko deposits based on modes of volcanism of underlying dacite and alteration halos. *Mining Geology (in Japan with English abstract)*, **26**, 105-117.
- Iyengar, S.S.; Martens, D.C. and Miller, W.P. (1981). Distribution and plant availability of soil zinc fractions. *Soil Science Society of America Journal*, **45**, 735-739.
- Jacobs, J. and Weber, K. (1993). Accretion and indentation tectonics at the southern edge of the Kaapvaal craton during the Kibaran (Grenville) orogeny. *Geology*, **21**, 203-206.
- Janecky, D.R. and Seyfried, W.E., Jr. (1984). Formation of massive sulphide deposits on oceanic ridge crest: Incremental reaction models for mixing between hydrothermal solutions and seawater. *Geochimica et Cosmochimica Acta*, **48**, 2723-2738.

- Jenner, G.A. (1996). Trace element geochemistry of igneous rocks: geochemical nomenclature and analytical geochemistry. In: D.A. Wyman (Editors) Trace element geochemistry of volcanic rocks: Applications for massive sulphide exploration, Geological Association of Canada, *Short course notes volume 12*, 51-77.
- Jiang, SY. (2000). Controls on the mobility of high field strength elements (HFSE), U, and Th in an ancient submarine hydrothermal system of the Proterozoic Sullivan Pb-Zn-Ag deposit, British Columbia, Canada. *Geochemical Journal*, **34**, 341-348.
- Jimenez-Espinosa R. and Jimenez-Millan J. (2003). Calcrete development in Mediterranean colluvial carbonate systems from SE Spain. *Journal of Arid Environments*, **53**, 479-489.
- Kalogeropoulos, S.I. and Scott, S.D. (1983). Mineralogy and geochemistry of tuffaceous exhalites (tetsusekiei) of the Fukazawa mine. In: H., Ohmoto and B.J. Skinner (Editors) Kuroko and related volcanogenic massive sulphide deposits. *Economic Geology, Monograph 5*, 412-432.
- Kataba-Pendias, A. and Pendias, H. (1991). Trace elements in soil and plants. *2nd Edition, CRC Press, Inc., Boca Raton, Fl.*
- Kawakami, T. (2001). Tourmaline breakdown in the migmatite zone of the Ryoke metamorphic belt, SW Japan. *Journal of Metamorphic Geology*, **19**, 61-75.
- Khadkikar A.S.; Chemyal L.S. and Ramesh R. (2000). The character and genesis of calcrete in Late Quaternary alluvial deposits, Gujarat, western India, and its bearing on the interpretation of ancient climates. *Palaeogeography, Palaeoclimatology, Palaeoecology*, **162**, 239-261.
- Khadkikar A.S.; Merh S.S.; Malik J.N. and Chamyal L.S. (1998). Calcretes in semi-arid alluvial systems: formative pathways and sinks. *Sedimentary Geology*, **116**, 251-260.
- Kilmer, V.J. and Nerpass, D.C. (1960). The determination of available sulfur in soils. *Soil Science Society of America proceedings*, **24**, 337-340.
- Klau, W. and Large, D.E. (1980). Submarine exhalative Cu-Pb-Zn deposits- a discussion of their classification and metallogensis. *Geologisches Jahrbuch*, **40**, 13-58.
- Kowalik, J.; Rye, R. and Sawkins, F.J. (1981). Stable isotope study of the Buchans polymetallic sulphide deposits. In: E.A., Swanson, D.F., Strong and J.G., Thurlow

- (Editors) The Buchans orebodies: Fifty years of geology and mining. *Geological Association of Canada, Special Paper*, **22**, 229-254.
- Kshirsagar, A.M. (1972). Multivariate analysis. *New York, Marcel Dekker, Inc.*
- Kunckey, M.J. (1975). Geology of the Millenbach copper-zinc deposit, Noranda, Quebec, Canada. *Society of economic geologists-American institute of mining and metallurgical engineers, Annual general meeting*, Feb. 1975.
- Large, R.R. (1977). Chemical evolution and zonation of massive sulphide deposits in volcanic terrains. *Economic Geology*, **72**, 549-572.
- Large, R.; Doyle, M.; Raymond, O.; Cooke, D.; Jones, A. and Heasman, L. (1996). Evaluation of the role of Cambrian granites in the genesis of world class VHMS deposits in Tasmania. *Ore Geology Reviews*, **10**, 215-230.
- Large, R.; Gemmell, J.B.; Paulick, H. and Huston, D.L. (2001). The alteration box plot: A simple approach to understanding the relationship between alteration mineralogy and lithogeochemistry associated with volcanic-hosted massive sulphide deposits. *Economic Geology*, **96**, 957-971.
- Leake, B.E. (1964). The chemical distinction between ortho-amphibolite and para-amphibolites. *Journal of Petrology*, **5**, 238-254.
- Leinz, R.A. and Hoover, D.B. (1993). The Russian CHIM method electrically or diffusion driven collection of ions. *Explore*, **79**, 1-9.
- Levinson, A.A. (1974). Introduction to exploration geochemistry. *Applied publishing Ltd., Illinois, U.S.A.*, 924 pp.
- Liang, J.; Strwart, J.W.B. and Karamanos, R.E. (1991). Distribution and plant availability of soil copper fractions in Saskatchewan. *Canadian Journal of Soil Science*, **71**, 89-99.
- Lindsay, W.L. and Norvell, W.A. (1987). Development of a DTPA test for zinc, iron, manganese, and copper. *Soil Science Society of America Journal*, **42**, 421-428.
- Lombaard, A.F. and Schreuder, F.J.G. (1978). Distribution pattern and general geological features of steep structures, mega-breccias and basic rocks in the Okiep Copper district. In: W.J., Verwoerd (Editors) Mineralization in metamorphic terranes. *Geological Society of South Africa, Special Publication*, **4**, 269-295.

- Lott, D.A. (1999). Sedimentary exhalative nickel-molybdenum ores in south China. *Economic geology and bulletin of the society of economic geologists*, **94**, 1051-1066.
- Lowell, R.P. and Rona, P.A. (1985). Hydrothermal models for the generation of massive sulphide ore deposits. *Journal of Geophysical Research*, **90**, 8769-8783.
- Ludick, D.J. (1987). Die stratigrafie en tektoniese verwantskappe van die Areachap groep in die Upington-omgewing. *Unpublished M.Sc. thesis, University of Orange Free State, Bloemfontein*, 143 pp.
- Luoma, S.N. and Jenne, E.A. (1976). Estimating bio-availability of sediment-bound trace metals with chemical extractants. *Trace Substances in Environmental Health-X*, **10**, 343-351.
- Lydon, J.W. (1983). Chemical parameters controlling the origin and deposition of sediment-hosted stratiform lead-zinc deposits. In: D.F., Sangster (Editors) Sediment-hosted stratiform lead-zinc deposits, *Mineralogical Association of Canada, Short course handbook*, **9**, 175-250.
- Lydon, J.W. (1986). Models for the generation of metalliferous hydrothermal systems within sedimentary rocks and their applicability to the Irish Carboniferous Zn-Pb deposits. In: C.J., Andrew, R.W.A., Crowe, S., Finlay, W.M., Pennell and J.F., Pyne (Editors) Geology and genesis of mineral deposits in Ireland, *Irish Association for Economic Geology, Dublin*, 555-577.
- Lydon, J.W. (1998a). Volcanogenic massive sulphide deposit, part1: A descriptive model. In: R.G, Roberts and P.A., Sheahan (Editors) Ore deposit models, *Geoscience Canada*, 145-153.
- Lydon, J.W. (1998b). Volcanogenic massive sulphide deposit, part2: Genetic models. In: R.G, Roberts and P.A., Sheahan (Editors) Ore deposit models, *Geoscience Canada*, 155-181.
- Lydon, J.W. and Galley, A. (1986). Chemical and mineralogical zonation of the Mathiati alteration pipe, Cyprus, and its genetic significance. In: M.J., Gallagher, R.A., Ixer, C.R., Neary and H.M., Prichard (Editors) Metallogenesis of basic and ultrabasic rocks, *Institution of Mining and Metallurgy, London*, 49-68.

- Maes, A.; Vanthuyne, M.; Cauwenberg, P. and Engels, B. (2003). Metal partitioning in a sulfidic canal sediment: metal solubility as a function of pH combined with EDTA extraction in anoxic conditions. *The Science of the Total Environment*, **312**, 181-193.
- Malherbe, S.J. (1984). The geology of the Kalahari Gemsbok National Park. *Proceedings of a Symposium on the Kalahari Ecosystem*, 33-44.
- Mann, A.W.; Birrell, R.D.; Fedikow, M.A.F. and De Souza, H.A.F. (2005). Vertical ionic migration: mechanisms, soil anomalies, and sampling depth for mineral exploration. *Geochemistry: Exploration, Environment, Analysis*, **5**, 201-210.
- Mann, A.W.; Birrell, R.D.; Mann, A.T.; Humphreys D.B. and Perdrix, J.L. (1998). Application of the mobile metal ion technique to routine geochemical exploration. *Journal of Geochemical Exploration*, **61**, 87-102.
- Mann, A.W.; Birrell, R.D.; Perdrix, J.L.; Mann, A.T.; Humphreys, D.B. and Gry, L.M. (1995). Project M219: Mechanism of formation of mobile metal ion anomalies. *Meriwa report No. 153, Perth, W.A.*, 407 pp.
- Mann, A.W.; Mann, A.T.; Humphreys, D.B.; Dowling, S.E.; Staltari, S. and Myers, L. (1997). Soil geochemical anomalies-their dynamic nature and interpretation. *Meriwa report No. 184, Perth.*, 132 pp.
- Mardia, K.V.; Kent, J.T. and Biddy, J.M. (1979). Multivariate analysis. *London, Academic press, Inc.*
- McClung, A.C.; DeFreitas, L.M. and Lott, W.L. (1959). Analyses of several Brazilian soils in relation to plant responses to sulfur. *Soil Science Society of America proceedings*, **23**, 221-224.
- McQueen, K.G.; Hill, S.M. and Foster, K.A. (1999). The nature and distribution of regolith carbonate accumulations in southeastern Australia and their potential as a sampling medium in geochemical exploration. *Journal of Geochemical Exploration*, **67**, 67-82.
- Mehlich, A. (1984). Mehlich 3 soil test extractant: A modification of Mehlich 2 extractant. *Communications in Soil Science Plant Analysis*, **15**, 1409-1416.
- Middleton, R.C. (1976). The geology of the Prieska copper mines (Pty) Ltd. *Economic Geology*, **71**, 328-350.

- Miller, W.P.; Martens, D.C.; Zelazny, L.W. and Kornegay, E.T. (1986). Forms of solid phase copper in copper-enriched swine manure. *Journal of Environmental Quality*, **15**, 69-72.
- Miller, W.P. and McFee, W.W. (1983). Distribution of Cd, Zn, Cu and Pb in soils of industrial north western Indiana. *Journal of Environmental Quality*, **12**, 29-33.
- Miyashiro, A. (1994). Metamorphic petrology. *UCL press*, 404 pp.
- Morrison, D.F. (1976). Multivariate statistical methods. *2nd edition, New York, McGraw-Hill book Co.*
- Moen, H.F.G. (1988). 2820 Upington 1:250000 Geological Series. *Council for Geoscience, Pretoria, South Africa.*
- Moen, H.F.G. (1999). The Kheis tectonic subprovince, South Africa: A lithostratigraphic perspective. *South African Journal of Geology*, **102**, 27-42.
- Moore, J.M.; Reid, D.L. and Watkeys, M.K. (1990). The regional setting of the Aggenys/Gamsberg base metal deposits, Namaqualand, South Africa, In: P.G. Spry, & L.T. Bryndzia, (Editors) Regional metamorphism of ore deposits, 77-95.
- Moore, AE. (1999). A reappraisal of epirogenic flexure axes in southern Africa. *South African Journal of Geology*, **102**, 363-376.
- Mottl, M.J. and Holland, H.D. (1978). Chemical exchange during hydrothermal alteration of basalt by seawater: I. Experimental results for major and minor components of seawater and basalt. *Geochimica et Cosmochimica Acta*, **42**, 1103-1116.
- Nash, D.J. and McLaren, S.J. (2003). Kalahari valley calcretes: their nature, origins, and environmental significance. *Quaternary International*, **111**, 3-22.
- Nelisen, D.; Hoyt, P.B. and Mackenzi, A.F. (1986). Distribution of soil Zn fractions in British Columbia interior orchard soils. *Canadian Journal of Soil Science*, **66**, 445-454.
- Netterberg, F. (1970). Ages of calcretes in Southern African. *South African Archaeological Bulletin*, **24**, 88-92.
- Ohlander B.; Land M.; Ingri J. and Widerlund A. (1996). Mobility of rare earth elements during weathering of till in northern Sweden. *Applied Geochemistry*, **11**, 93-99.
- Ohmoto, H. and Rye, R.O. (1974). Hydrogen and oxygen isotopic compositions of fluid inclusions in the Kuroko deposits, Japan. *Economic Geology*, **69**, 947-953.

- Ohmoto, H. and Skinner, B.J. (1983). The Kuroko and related volcanogenic massive sulfide deposits. *Economic Geology, Monograph 5*, 604 pp.
- Oudin, E. (1981). Etudes mineralogique et geochemique des dépôts sulfures sous-marins actuels de la ridge est-pacifique (21° N). *Documents du BRGM 25*, 241 pp.
- Oudin, E. (1983). Hydrothermal sulphide deposits of the East Pacific Rise (210° N) Part 1: Descriptive mineralogy. *Marine Mining*, **4**, 39-72.
- Pan, Y. and Fleet, M.E. (1995). Geochemistry and origin of cordierite-orthoamphibole gneiss and associated rocks at an Archaean volcanogenic massive sulphide camp: Manitouwadge, Ontario, Canada. *Precambrian Research*, **74**, 73-89.
- Partridge, T.C. and Maud, R.R. (1987). Geomorphic evolution of Southern Africa since the Mesozoic, *South African Journal of Geology*, **90**, 179-208.
- Piercey, S.J.; Pardis, S.; Murphy, D.C. and Mortensen, J.K. (2001). Geochemistry and Paleotectonic setting of felsic volcanic rocks in the Finlayson Lake volcanic-hosted massive sulphide District, Yukon, Canada. *Economic Geology*, **96**, 1877-1905.
- Pottorf, R.J. and Barnes, H.J. (1983). Mineralogy, geochemistry, and ore genesis of hydrothermal sediments from the Atlantis II deep, Red Sea. In: H., Ohmoto and B.J., Skinner (Editors) Kuroko and related volcanogenic massive sulphide deposits. *Economic Geology, Monograph 5*, 198-223.
- Pupin, J.P. (1980). Zircon and granite petrology. *Contributions to Mineralogy and Petrology*, **73**, 207-220.
- Rao, C.R. (1964). The use and interpretation of principal component analysis in applied research. *Sankhy A*, **26**, 329-358.
- Reed, M.H. (1983). Seawater-basalt reaction and the origin of greenstones and related ore deposits. *Economic Geology*, **78**, 446-485.
- Richards, H.G. and Boyle, J.F. (1986). Origin, alteration and mineralization of inter-lava metalliferous sediments of the Troodos ophiolite, Cyprus. In: M.J., Gallagher, R.A., Ixer, C.R., Neary and H.M., Prichard (Editors) Metallogeny of basic and ultrabasic rocks, *Institue of Mining and Metallurgy, London*, 21-31.
- Ringrose S.; Downey B.; Genecke D.; Sefe F. and Vink B. (1999). Nature of sedimentary deposits in the Western Makgadikgadi basin, Botswana. *Journal of Arid Environments*, **43**, 375-397.

- Rossouw, D. (2003). A technical risk evaluation of the Kantienpan volcanic-hosted massive sulphide deposit and its financial viability. *Unpublished M.Sc. thesis, University of Pretoria*, 118 pp.
- Ruiz, C.; Arribas, A. and Arribas Jr., A. (2002). Mineralogy and geochemistry of the Masa Valverde blind massive sulphide deposit, Iberian Pyrite Belt (Spain). *Ore Geology Reviews*, **19**, 1-22.
- Ryan, P.J.; Lawrence, R.D.; Lipson, R.D.; Moore, J.M.; Paterson, A.; Stedman, D. P. and Van Zyl, D. (1986). The Aggeneys base metal sulphide deposits, Namaqualand District, Mineral Deposits of Southern Africa. In:C.R., Anhaeusser and S., Maske (Editors) *Geological Society of South Africa, Johannesburg*, 1447-1473.
- Salomons, W. and Forstner, U. (1984). Metals in the hydrocycle. *Springer-Verlag, Berlin*.
- Sangster, D.F. (2002). The role of dense brines in the formation of vent distal sedimentary-exhalative (SEDEX) lead-zinc deposits: field and laboratory evidence. *Mineralium Deposita*, **37**, 149-157.
- Sanchez-Espana, J.; Velasco, F. and Yusta, I. (2000). Hydrothermal alteration of felsic volcanic rocks associated with massive sulphide deposition in the northern Iberian Pyrite Belt (SW Spain). *Applied Geochemistry*, **15**, 1265-1290.
- Sangster, D.F. (1972). Precambrian volcanogenic massive sulphide deposits in Canada: A review. *Geological Survey of Canada, paper 72-22*, 44 pp.
- Sangster, D.F. and Scott, S.D. (1976). Precambrian, strata-bound, massive Cu-Zn-Pb sulphide ores of North America. In: K.H., Wolf (Editors) Handbook of stratabound and stratiform ore deposits. *Elsevier Scientific Publishing Co., Amsterdam*, **6**, 130-221.
- SAS® V 8.2 (2003). Integrated system of software providing control of data management, analysis, and presentation. *SAS Institute, Cary, North Carolina, USA*.
- Sawkins, F.J. (1976). Massive sulphide deposits in relation to geotectonics. In: D.F., Strong (Editors) Metallogenesis and plate tectonics. *Geological Association of Canada, Special Paper 14*, 221-240.
- Sawkins, F.J. (1984). Ore genesis by episodic dewatering of sedimentary basins: Application to giant Proterozoic lead-zinc deposits. *Geology*, **5**, 451-454.

- Schade, J.; Cornell, D.H. and Theart, H.F.J. (1989). Rare earth element and isotopic evidence for the genesis of the Prieska massive sulphide deposit, South Africa. *Economic Geology*, **84**, 49-63.
- Schnitzer, M. (1978). Humic substances: Chemistry and reactions. In: M. Schnitzer and S.U. Khan (Editors) *Soil organic matter*. Elsevier, Amsterdam, 1-64
- Seyfried, W.E., Jr. and Bischoff, J.L. (1979). Low temperature basalt alteration by seawater: an experimental study at 70°C and 150°C. *Geochimica et Cosmochimica Acta*, **43**, 1937-1947.
- Shapiro, S.S. and Wilk, M.B. (1965). An analysis of variance test for normality (complete samples). *Biometrika*, **52**, 591-611.
- Shpak, A.P.; Kalinichenko, A.M.; Bagmut, N.N.; Kalinichenko, Y.A.; Karbiv'sky, V.L. and Trashchan, Y.A. (2003). Influencing of isomorphic replacements on electron distribution in point defects of oxygen-phosphorous compounds of calcium and strontium. *Metallofizika I Noveishie Teknologii*, **25**, 699-712.
- Shuman, L.M. (1983). Sodium hypochlorite methods for extracting microelements associated with soil organic matter. *Soil Science Society of America Journal*, **47**, 656-660.
- Sibson, R.H.; Moore, J.Mc.M. and Rankin, A.H. (1975). Seismic pumping- a hydrothermal fluid transport mechanism. *Journal of the Geological Society of London*, **131**, 653-659.
- Sillitoe, R.H. (1973). Environments of formation of volcanogenic massive sulphide deposits. *Economic Geology*, **68**, 1321-1325.
- Sinclair, A.J. (1976). Applications of probability graphs in mineral exploration. *The association of exploration geochemists, Special volume No. 4, Richmond printers LTD.*
- Smmerfield, M.A. (1985). Plate tectonics and landscape development on the African continent, In: M. Morisawa, & J.J. Hack (Editors) *Tectonic Geomorphology*. Allen and Unwin, Boston, 390 pp.
- Solomon, M. (1976). Volcanic massive sulphide deposits and their host rocks- a review and an explanation. In: K.H., Wolf (Editors) *Handbook of stratabound and stratiform ore deposits*. Elsevier, Amsterdam, **2**, 21-50.

- Soltanpour, P.N. (1991). Determination of nutrient availability and elemental toxicity by AB-DTPA soil test and ICPS. *Advances in Soil Science*, **16**, 165-190.
- Soltanpur, P.N.; Jones, J.B., Jr. and Workman, S.M. (1982). Optical emission spectrometry. In: A.L., Page et al., (Editors). Methods of soil analysis, part 2, 2nd Ed, *Agron. Monogr. 9. ASA and SSSA, Madison, WI*.
- Speiss, F.N.; Macdonald, K.C.; Atwater, T.; Ballard, R.; Carranza, A.; Cordoba, D.; Cox, C.; Diaz Garcia, V.M.; Francheteau, J.; Guerrero, J.; Hawhins, J.; Haymon, R.; Hessler, R.; Juteau, T.; Kastner, M.; Larson, R.; Luyendyke, B.; Macdougall, J.D.; Miller, S.; Normark, W.; Orcutt, J. and Rangin, C. (1980). East Pacific Rise; hot springs and geophysical experiments. *Science*, **207**, 1421-1433.
- Spooner, E.T.C. (1977). Hydrodynamic model for the origin of the ophiolite cupriferous pyrite ore deposits of Cyprus, in volcanic processes in ore genesis. *Geological Society of London, Special Publication* **7**, 58-71.
- Stanford, J.O. and Lancaster, J.D. (1962). Biological and chemical evalution of the readily available sulfur status of Mississippi soils. *Soil Science Society of America Proceedings*, **26**, 63-65.
- Stover, R.C.; Sommers, L.E. and Silviera, D.J. (1976). Evaluation of metals in wastewater sludge. *Journal of Water. Pollution Control Federation* **48**, 2165-2175.
- Stowe, C.W. (1983). The Upington geotraverse and its implications for Craton margin tectonics. In: Botha, B.J.V. (ED.), Namaqualand metamorphic complex. *Geological Society of South Africa, Special Publication*, **10**, 147-171.
- Sundblad, K. (1991). Lead isotopic evidence for the origin of 1.8-1.4 Ga ores and granitoids in the southeastern part of the Fennoscandian Shield. *Precambrian Research*, **51**, 265-281.
- Tabatabai, M.A. and Lafen, J.M. (1976a). Nitrogen and sulfur content and pH of precipitation in Iowa. *Journal of Environmental Quality*, **5**, 108-112.
- Tauson, V.L. (1999). Isomorphism and endocrypty: Novel approaches in studies of behavior of microelements in mineral systems. *Geologyia I Geofizika*, **40**, 1488-1494.
- Tessier, A.; Campbell, P.G.C. and Bisson, M. (1979). Sequential extraction procedure for the speciation of particular trace metals. *Analytical Chemistry*, **51**, 844-851.

- Theart, H.F.J. (1985). Copperton-Areachap Cu-Zn mineralization, *Unpublished Ph.D. thesis, University of Stellenbosch*, 329 pp.
- Theart, H.F.J.; Cornell, D.H. and Schade, J. (1989). Geochemistry and metamorphism of the Prieska Zn-Cu deposit, South Africa. *Economic Geology*, **84**, 34-49.
- Thomas, M.A. (1981). The geology of the Kalahari in the northern Cape Province (Areas 2620 and 2720). *Unpublished M.Sc. thesis, University of the Orange Free State, Bloemfontein*.
- Thomas, R.J.; Agenbacht, A.L.D.; Cornell, D.H. and Moore, J.M. (1994b). The Kibaran of Southern Africa: Tectonic evolution and metallogeny. *Ore Geology Reviews*, **9**, 131-160.
- Thomas, R.J.; Cornell, D.H.; Moore, M.J. and Jacobs, J. (1994a). Crustal evolution of the Namaqua-Natal metamorphic Province, Southern Africa. *South African Journal of Geology*, **97**, 8-14.
- Tivey, M.K. and Delaney, J.R. (1986). Growth of large sulphide structures on the Endeavour segment of the Juan de Fuca Ridge. *Earth and Planetary Science Letters*, **77**, 303-317.
- Tornos, F. (2006). Environment of formation and styles of volcanogenic massive sulphides: The Iberian Pyrite Belt. *Ore Geology Reviews*, **28**, 259-307.
- Ulrich, T.; Golding, S.D.; Kamber, B.S.; Zam, K. and Taube, A. (2002). Different mineralization styles in a volcanic-hosted ore deposit: the fluid and isotopic signatures of the Mt Morgan Au-Cu deposit, Australia. *Ore Geology Reviews*, **22**, 61-90.
- Van Niekerk, HS.; Beukes, NJ. and Gutzmer, J. (1999). Post-Gondwana pedogenic ferromanganese deposits, ancient soil profiles, African land surfaces and palaeoclimatic change on the Highveld of South Africa. *Journal of African Earth Sciences*, **26**, 761-781.
- Van Zyl, C.Z. (1981). Structural and metamorphic evolution in the transitional zone between craton and mobile belt, Upington geotraverse. *Chamber of mines Precambrian research unit, Bulletin 31, University of Cape Town*.

- Vermaak, J. J. (1984). Aspects of the secondary dispersion of ore-related elements in calcrete-environments of the Northern Cape Province. *Unpublished M.Sc. thesis, University of the Orange Free State, Bloemfontein*, 549.1145 VER.
- Voet, H.W. and King, B.H. (1986). The Areachap copper-zinc deposit, Gordonia district., In: S. Maske (Editors) Mineral Deposits of southern Africa, *Geological Society of South Africa*, **2**, 1529 pp.
- Vokes, F.M. (1969). A review of metamorphism of sulphide deposits. *Earth Science Review*, **5**, 99-143.
- Wagener, J.H.F. and Van Schalkwyk, L. (1986). The Prieska zinc-copper deposit, north-western Cape Province, Mineral Deposits of Southern Africa, II . In:C.R., Anhaeusser and S., Maske (Editors). *Geological Society of South Africa, Johannesburg*, 1503-1527.
- Walker, R.N.; Logan, R.G. and Binnekamp, J.G. (1977). Recent geological advances concerning the H.Y.C and associated deposits, Mcarthur River, N.T. *Journal of the Geological Society of Australia*, **24**, 365-380.
- Wang, X. (1998). Leaching of mobile forms of metals in overburden: development and application. *Journal of Geochemical Exploration*, **61**, 39-55.
- Ward, J.D., Seely, M.K. and Lancaster, I.N. (1983). On the antiquity of the Namib. *South African Journal of Science*, **79**, 175-183.
- Wear, J.I. and Evans, C.E. (1968). Relationship of zinc uptake by corn and sorghum to soil zinc measured by three extractants. *Soil Science Society of America Proceedings*, **32**, 543-546
- Watanabe, M. and Sakai, H. (1983). Stable isotope geochemistry of sulfates from the Neogene ore deposits in the Green Tuff region, Japan. In: H., Ohmoto and B.J., Skinner (Editors) Kuroko and related volcanogenic massive sulphide deposits. *Economic Geology, Monograph 5*, 282-291.
- Whitbread, M.A. and Moore, C.L. (2004). Two lithogeochemical approaches to the identification of alteration patterns at the Elura Zn-Pb-Ag deposit, Cobar, New South Wales, Australia: use of Pearce Element Ratio analysis and isocon analysis. *Geochemistry: Exploration, Environment, Analysis*, **4**, 129-141.

- Williams, C.H. and Steinbergs, A. (1962). The valuation of plant-available sulphur in soils: I. The chemical nature of sulphates in some Australian soils. *Plant Soil* **17**, 279-294.
- Wilson, M.G.C. and Anhaeusser, C.R. (1998). The mineral resources of South Africa. *Handbook 16, Sixth edition, Council for Geosciences*.
- Young, R.A. (1996). The Rietveld method, IUCr Monographs on Crystallography, 5. *International Union of Crystallography, Oxford Science Publications*, 298 pp.
- Xueqiu, W. (1998). Leaching of mobile forms of metals in overburden: development and application. *Journal of Geochemical Exploration* , **61**, 39-55.

Appendix A

Cross sections and extra figure

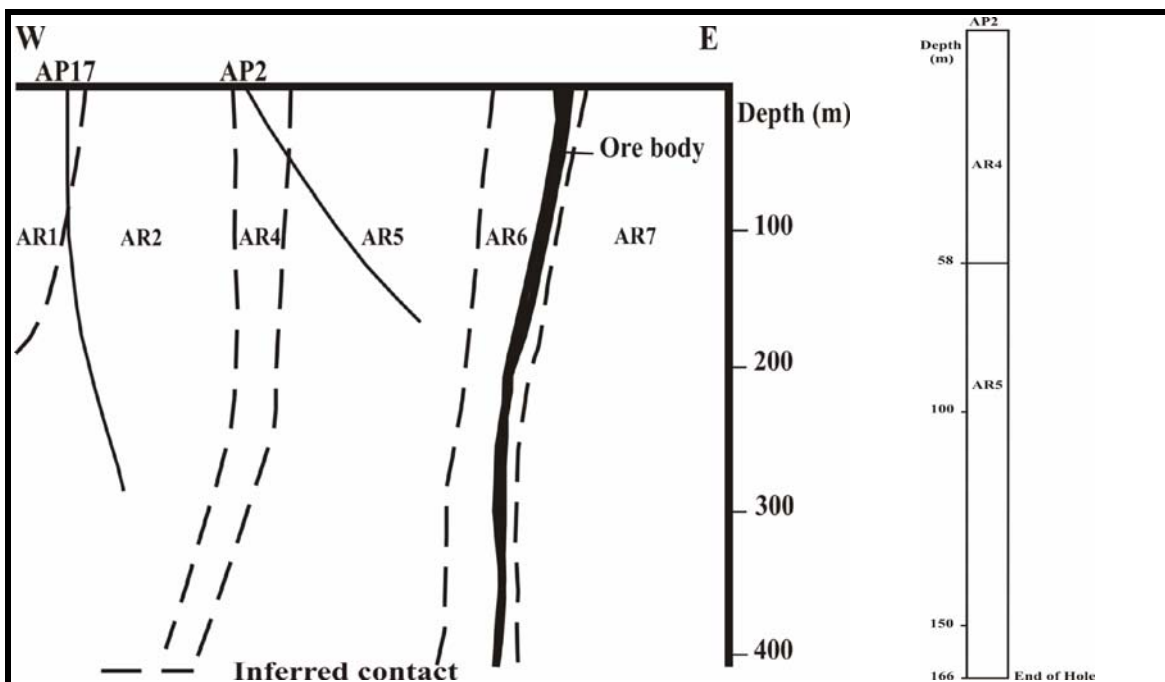


Figure A.1: Cross section includes borehole AP2 and sample locations

Table A.1: Depth of samples in drill hole AP2, Areachap

Sample No.	Depth (m)	Sample No.	Depth (m)	Sample No.	Depth (m)
AP2/1	62.2	AP2/9	92.5	AP2/18	112.4
AP2/2	71.2	AP2/14	92.6	AP2/16	113.2
AP2/3	74.4	AP2/12	97.8	AP2/15	118.0
AP2/4	81.2	AP2/10	105.7	AP2/22	120.1
AP2/5	82.5	AP2/11	106.3	AP2/24	122.1
AP2/6	87.1	AP2/21	107.5	AP2/23	124.1
AP2/7	91.1	AP2/20	108.7	AP2/25	141.1
AP2/13	91.1	AP2/19	111.7	AP2/26	153.7
AP2/8	92.2	AP2/17	112.2	AP2/27	165.0

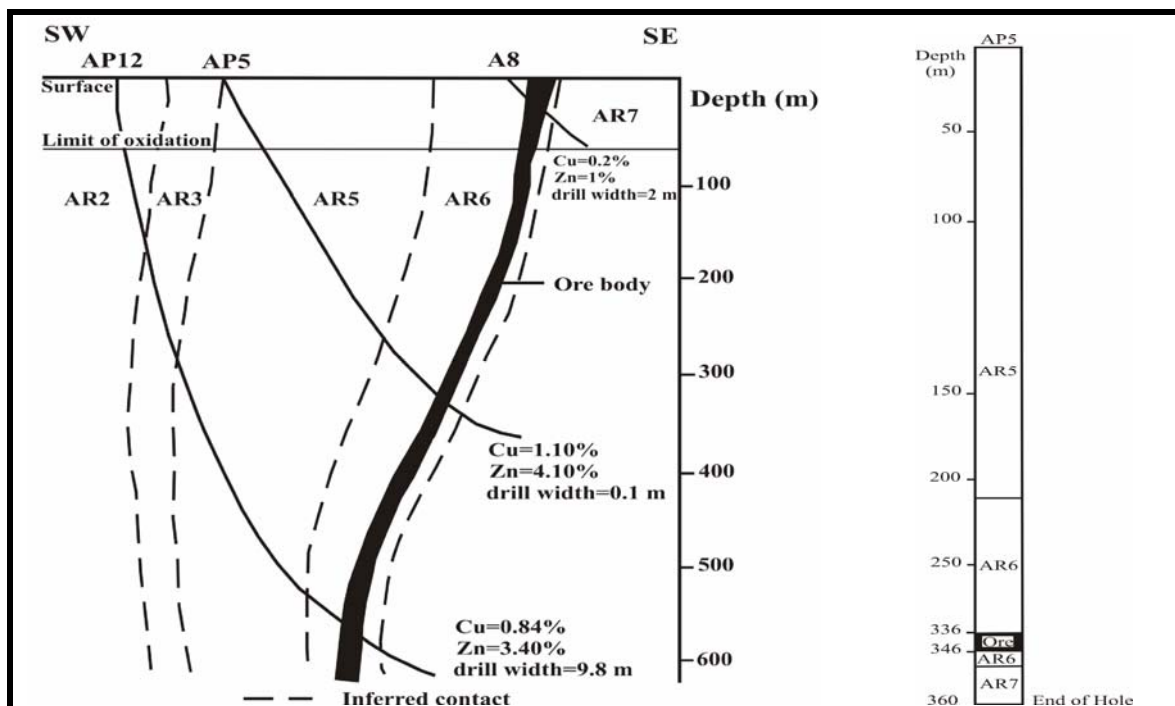


Figure A.2: Cross section includes borehole AP5 and sample locations.

Table A.2: Depth of samples in drill hole AP5, Areachap

Sample No.	Depth (m)						
AP5/2	29.7	AP5/11	177.9	AP5/25	298.5	AP5/34	335.7
AP5/3	33.5	AP5/14	188.1	AP5/27	306.1	AP5/33	336.8
AP5/4	46.2	AP5/15	196.6	AP5/26	311.5	AP5/40	338.0
AP5/5	60.8	AP5/16	206.9	AP5/29	317.4	AP5/39	339.0
AP5/1	79.2	AP5/17	219.3	AP5/28	318.8	AP5/41	341.4
AP5/6	84.8	AP5/18	228.0	AP5/30	318.9	AP5/42	343.7
AP5/7	108.6	AP5/19	243.2	AP5/31	322.7	AP5/43	344.7
AP5/8	120.8	AP5/20	253.4	AP5/32	326.8	AP5/44	349.0
AP5/9	145.8	AP5/21	269.9	AP5/38	327.4	AP5/45	354.8
AP5/10	154.6	AP5/23	277.6	AP5/37	328.4	AP5/46	360.1
AP5/12	176.2	AP5/24	281.4	AP5/36	331.3		
AP5/13	176.5	AP5/22	282.7	AP5/35	334.2		

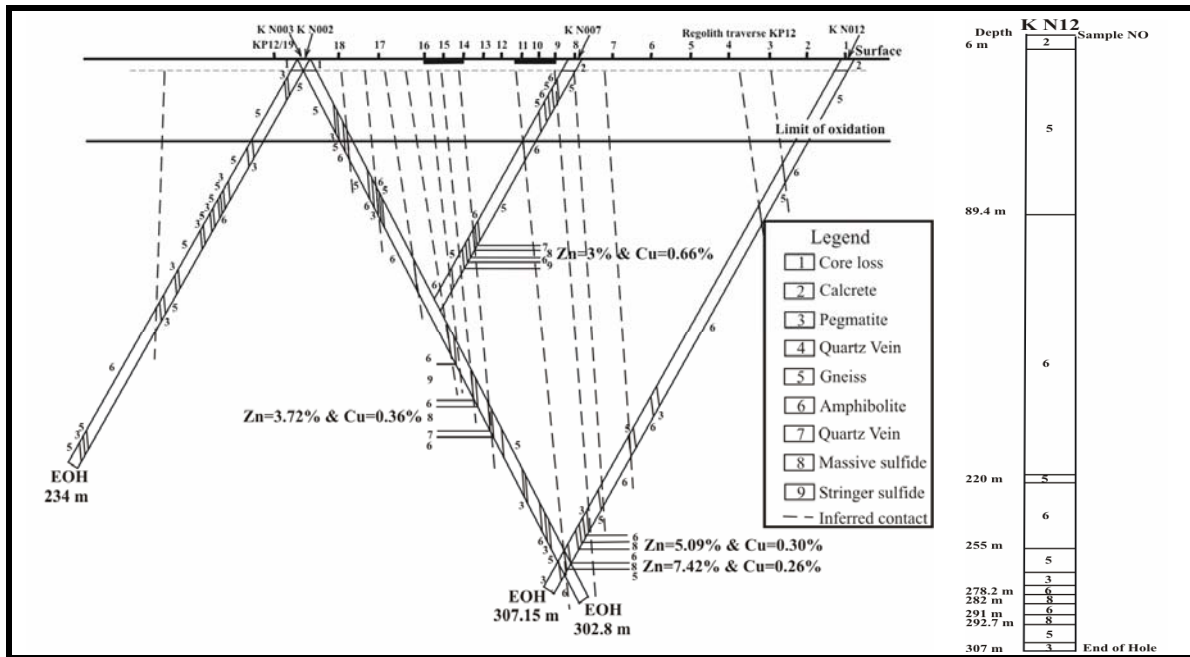


Figure A.3: Cross section includes borehole KN12 and sample locations.

Table A.3: Depth of samples in drill hole KN12, Kantienpan

Sample No.	Depth (m)						
KN12/1	175.68	KN12/11	233.67	KN12/22	278.5	KN12/33	291.29
KN12/2	179.78	KN12/12	239.8	KN12/19	278.7	KN12/32	292
KN12/3	188.27	KN12/14	250.62	KN12/23	279.41	KN12/34	292.65
KN12/4	190.12	KN12/13	253.95	KN12/24	280.28	KN12/35	293.03
KN12/5	194.67	KN12/15	255.82	KN12/25	280.74	KN12/36	293.8
KN12/6	203.23	KN12/16	262.1	KN12/26	281.8	KN12/37	295.1
KN12/7	209.93	KN12/17	266.8	KN12/28	283.32	KN12/38	297.2
KN12/8	216.76	KN12/18	274.8	KN12/29	285.32	KN12/39	299.1
KN12/9	221.15	KN12/20	276.5	KN12/30	287.25		
KN12/10	228.83	KN12/21	277.97	KN12/31	290.8		

Note: KN12/27: missing sample

Table A. 4: Lithological description of borehole KN12 (Rossouw, 2003)

Depth (m)	Lithological description of borehole KN12
0.00-6.00	Calcrete
6.00-89.40	Light grey-beige, weathered to 17.80 m, medium-grained, and granular to weakly banded quartzo-feldspathic gneiss with intercalated bands of feldspathic amphibolite
89.40-219.60	Dark-grey, fine-grained and weakly foliated feldspathic amphibolite
219.60-222.40	Light grey-beige, very weathered, medium-grained, granular to weakly banded quartzo-feldspathic gneiss
222.40-255.23	Dark-grey, fine-grained and weakly foliated feldspathic amphibolite
225.23-267.52	Pale-grey, strongly banded feldspar-quartz-amphibole gneiss with a quartzo-feldspathic gneiss marker and a garnetiferous layer at the bottom
267.52-274.73	Pegmatite
274.73-278.24	Dark-grey, fine-grained and weakly foliated feldspathic amphibolite
278.24-278.34	Chert
278.34-282.04	Massive sulphides (80%) and wall-rock clasts (20% - gneiss and quartz). Bronze coloured and medium- to coarse-grained. Sulphides: pyrrhotite ($\pm 30\%$), sphalerite ($\pm 7\%$), pyrite ($\pm 60\%$) and chalcopyrite ($\pm 3\%$). Two barren zones of gneiss with disseminated pyrite (3%) start at 280.12 and 280.62 m with varying thickness of 7 and 19 cm respectively. Thin chert topping (10 cm).
282.04-290.82	Grey, fine-grained, weakly banded feldspathic amphibolite. Spotty alteration and weakly defined foliation and a gradational bottom contact with massive sulphide
290.82-292.70	Massive sulphides (30%) and wall-rock clasts (80% - chlorite and quartz). Bronze coloured and medium- to coarse-grained. Sulphides: pyrrhotite ($\pm 20\%$), sphalerite ($\pm 2\%$), pyrite ($\pm 80\%$) and chalcopyrite ($\pm 1\%$)
292.70-300.07	Grey, polymict medium- to coarse-grained, moderately banded quartzo-feldspathic gneiss. Few fractured and a gradational bottom contact with pegmatite
300.07-307.15	Pegmatite
307.15	End of Hole

Table A. 5: Lithological description of borehole KN7 (Rossouw, 2003)

Depth (m)	Lithological description of borehole KN7
0.00-5.89	Calcrete
5.89-12.91	Pegmatite
12.91-39.50	Light grey-beige, weathered to a depth of 25.26m, medium-grained, and granular to weakly banded quartzofeldspathic gneiss with intercalated bands of feldspathic amphibolite
39.50-54.70	Dark-grey, slightly weathered fine-grained feldspathic amphibolite
54.70-83.82	Dark-grey, medium-grained feldspar-quartz-amphibole gneiss
83.82-98.89	Pale-grey, strongly banded feldspar-quartz-amphibole gneiss. Weakly defined foliation with ± 2% pyrrhotite and pyrite
98.89-104.52	Quartzofeldspathic gneiss marker with a garnetiferous layer
104.52-105.86	Dark-grey, fine-grained and weakly foliated feldspathic amphibolite with a 1m mineralised brecciated zone at the top
105.86-105.96	Chert
105.96-111.35	Massive sulphides (70%) and wall-rock clasts (30% - chlorite, epidote and quartz). Sulphides: Pyrrhotite (±60%), sphalerite (±10%), pyrite (±30%) and chalcopyrite (±2%)
111.35-112.96	Grey, fine-grained, weakly banded feldspathic amphibolite. Spotty alteration, garnetiferous and weakly defined foliation with disseminated sulphides (±3% pyrite)
112.96-113.55	Massive sulphides (70%) and wall-rock clasts (30% - chlorite, epidote and quartz). Sulphides: Pyrrhotite (±60%), sphalerite (±10%), pyrite (±30%) and chalcopyrite (±2%)
113.55-116.54	Stinger sulphides in medium-grained garnet-cordierite-feldspathic amphibolite. Spotty alteration, moderately banded and weakly defined foliation with disseminated sulphides (±5% pyrite). A carbon shale layer occurs between 114.82-116.54m with ±10% disseminated sulphides (pyrite)
116.54-126.64	Grey, polymict medium- to coarse-grained, moderately banded quartzofeldspathic gneiss
126.64-140.00	Dark-grey, fine-grained, weakly banded biotite with some intercalated thin metaquartzites and a garnet marker
140.00	End of Hole

Table A. 6: Lithological description of borehole KN3 (Rossouw, 2003)

Depth (m)	Lithological description of borehole KN3
0.00-4.67	Core loss
4.67-5.47	Calcrete
5.47-49.70	Light-grey, moderately banded medium-grained quartzofeldspathic gneiss. Weathered to a depth of 41.80m
49.70-57.77	Dark-grey, fine-grained, weakly banded feldspathic amphibolite with a pink pegmatite vein
57.77-76.15	Light-grey, moderately banded coarse-grained quartzofeldspathic gneiss
76.15-120.45	Dark-green, fine-grained, weakly banded biotite amphibolite with intercalated bands of gneiss, a sugary metaquartzite vein and pegmatite veins
120.45-163.35	Grey, coarse-grained, moderately banded quartzofeldspathic gneiss
163.35-169.01	Dark-grey, medium-grained feldspathic amphibolite
169.01-189.91	Stringer sulphides in a medium-grained feldspathic amphibolite. Spotty alteration and moderately banded. Gradational bottom contact with massive sulphides
189.91-190.75	Massive sulphides ($\pm 70\%$) and wall-rock clasts (30% - chlorite, epidote and quartz). Sulphides: Pyrrhotite 60%, pyrite 40%, sphalerite 1% and chalcopyrite 1% (pyrite crystals in a matrix of pyrrhotite)
190.75-192.27	Light-green and fine-grained amphibolite. Sharp bottom contact with massive sulphides
192.27-204.60	Massive sulphides (80%) and wall-rock clasts (20% - chlorite, epidote and quartz). Bronze coloured and unweathered. Blebs of chalcopyrite are more frequent at the bottom 2m of the zone. Sulphides: Pyrrhotite ($\pm 50\%$), sphalerite ($\pm 15\%$), pyrite ($\pm 30\%$) and chalcopyrite ($\pm 3\%$). Sphalerite matrix to pyrrhotite and pebbly and coarse blebby pyrite replaces both
204.60-206.15	Chert
206.15-219.85	Dark-grey, fine-grained and weakly foliated feldspathic amphibolite. Gradational bottom contact with gneiss
219.85-230.60	Grey medium-grained quartzofeldspathic gneiss marker with garniferous layer (220-226m)
230.60-236.38	Pale-grey, strongly banded feldspar-quartz-amphibole gneiss. Weakly defined foliation
236.38-285.44	Dark-grey, medium-grained feldspar-quartz-amphibole gneiss
285.44-302.80	Dark-grey, slightly weathered fine-grained feldspathic amphibolite. A weakly defined foliation
302.80	End of Hole

Table A. 7: Lithological description of borehole KN2 (Rossouw, 2003)

Depth (m)	Lithological description of borehole KN2
0.00-5.50	Core loss
5.50-6.00	Calcrete
6.00-18.65	Light-grey, moderately banded, weathered, medium- to coarse-grained quartzofeldspathic gneiss. Moderately defined foliation with a gradational bottom contact with the pegmatite
18.65-21.22	Pegmatite
21.22-78.98	Pale-grey, moderately banded, medium- to coarse-grained quartzofeldspathic gneiss. Weathered to a depth of 39.83m Moderately defined foliation with pink pegmatite veins. Few fractures and a gradational bottom contact with pegmatite
78.98-83.33	Pegmatite
83.33-86.56	Pale-grey, moderately banded, medium-grained quartzofeldspathic gneiss. Weakly defined foliation with disseminated sulphides (<1%). Few fractures and a gradational bottom contact with amphibolite
86.56-88.42	Dark grey and fine grained. A sharp bottom contact with grey gneiss
88.42-146.09	Pale-grey, moderately banded, medium-grained quartzofeldspathic gneiss. Weakly defined foliation with pink pegmatite veins with a gradational bottom contact with pink pegmatite
146.09-148.12	Pegmatite
148.12-223.60	Dark-grey, fine-grained, moderately banded feldspathic amphibolite. Pink pegmatite veins with a gradational bottom contact with gneiss
223.60-234.03	Pale-grey, moderately banded, medium-grained quartzofeldspathic gneiss. Weakly defined foliation with a pink pegmatite vein
234.03	End of Hole

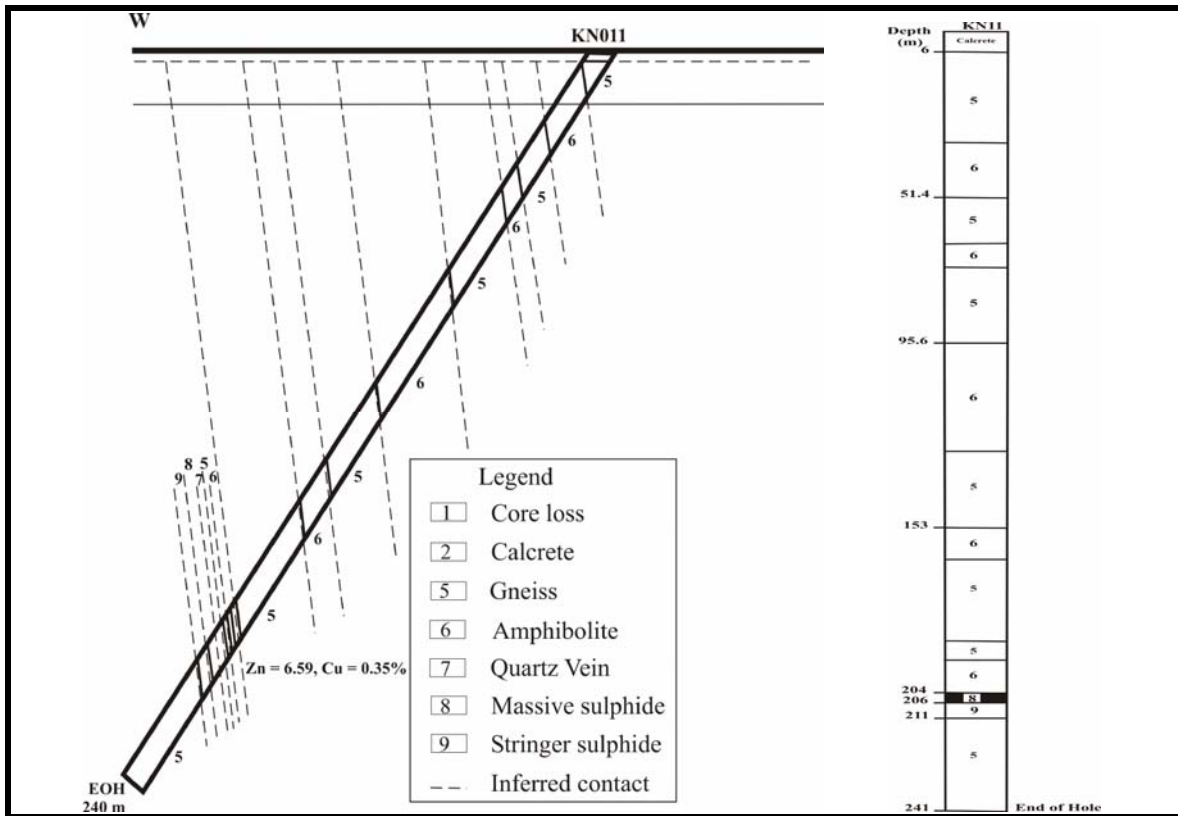


Figure A.4: Cross section of KN11 and location of samples.

Table A.8: Depth of samples in drill hole KN11, Areachap

Sample No.	Depth (m)						
KN11/2	22.1	KN11/14	101.3	KN11/26	172.2	KN11/38	210.7
KN11/1	24.2	KN11/15	108.3	KN11/27	175.8	KN11/39	212.2
KN11/3	27.2	KN11/16	112.5	KN11/28	182.4	KN11/40	216.2
KN11/4	42.0	KN11/17	120.1	KN11/29	188.3	KN11/41	217.7
KN11/6	42.8	KN11/18	126.1	KN11/30	195.4	KN11/42	217.8
KN11/5	48.9	KN11/19	130.2	KN11/31	196.8	KN11/43	218.2
KN11/7	60.5	KN11/20	136.8	KN11/32	198.8	KN11/45	224.1
KN11/8	68.4	KN11/21	142.7	KN11/33	205.0	KN11/44	226.7
KN11/9	72.0	KN11/22	149.6	KN11/34	206.6	KN11/47	229.3
KN11/10	78.1	KN11/23	154.4	KN11/35	207.0	KN11/46	231.2
KN11/11	84.7	KN11/24	159.6	KN11/36	208.3	KN11/48	237.7
KN11/12	90.0	KN11/25	165.7	KN11/37	209.2	KN11/49	239.3
KN11/13	97.7						

Table A. 9: Lithological description of borehole KN11 (Rossouw, 2003)

Depth (m)	Lithological description of borehole KN11
0.00-6.00	Calcrete
6.00-33.70	Light grey-beige, weathered to 33.70m, medium-grained, and granular to weakly banded quartzofeldspathic gneiss with pegmatite veins. Weakly defined foliation with a 25° angle to the core axis. Feldspar
33.70-51.14	Dark-grey, fine-grained feldspathic amphibolite. Disseminated sulphide of pyrite and pyrrhotite ($\pm 2\%$). A few fractures occur with a gradational bottom contact with the gneiss
51.14-65.26	Grey and medium grained quartzofeldspathic gneiss. Weakly defined foliation with a few fractures and a gradational bottom contact with amphibolite
65.26-72.17	Dark-grey, fine-grained feldspathic amphibolite. Garnetiferous and $\pm 3\%$ disseminated sulphide of pyrite and pyrrhotite at the bottom ± 1.5 m of this section
72.17-95.58	Light grey-beige, very weathered, medium-grained, granular to weakly banded quartzofeldspathic gneiss
95.58-129.56	Dark-grey, fine-grained feldspathic amphibolite
129.56-153.00	Light grey-beige, very weathered, medium-grained, granular to weakly banded quartzofeldspathic gneiss with intercalated bands of feldspathic amphibolite. Few fractures with a sharp bottom contact with the amphibolite
153.00-163.17	Dark-grey, weakly foliated fine-grained feldspathic amphibolite
163.17-188.35	Pale-grey, medium-grained strongly banded feldspar-quartz-amphibole gneiss. Disseminated sulphide of pyrite ($\pm 2\%$)
188.35-193.05	Quartzofeldspathic gneiss marker with garnetiferous layer (192.00-193.05m)
193.05-204.07	Dark-grey, fine-grained and weakly foliated feldspathic amphibolite
204.07-206.70	Massive sulphides (80%) and wall-rock clasts (20% - chlorite and quartz). Bronze coloured. Sulphides: Pyrrhotite ($\pm 55\%$), sphalerite ($\pm 7\%$), pyrite ($\pm 35\%$) and chalcopyrite ($\pm 3\%$). Thin chert topping (10cm)
206.70-211.02	Stinger sulphides in medium-grained garnet-cordierite-feldspathic amphibolite. Spotty alteration and moderately banded with disseminated sulphides of pyrite ($\pm 10\%$). A 14cm carbon shale layer occurs at 207.28m
211.02-239.52	Grey, polymict medium- to coarse-grained, moderately banded quartzofeldspathic gneiss. Weakly defined foliation with occasional garnet porphyroblasts and $\pm 1\%$ disseminated sulphide of pyrite
239.52	End of Hole

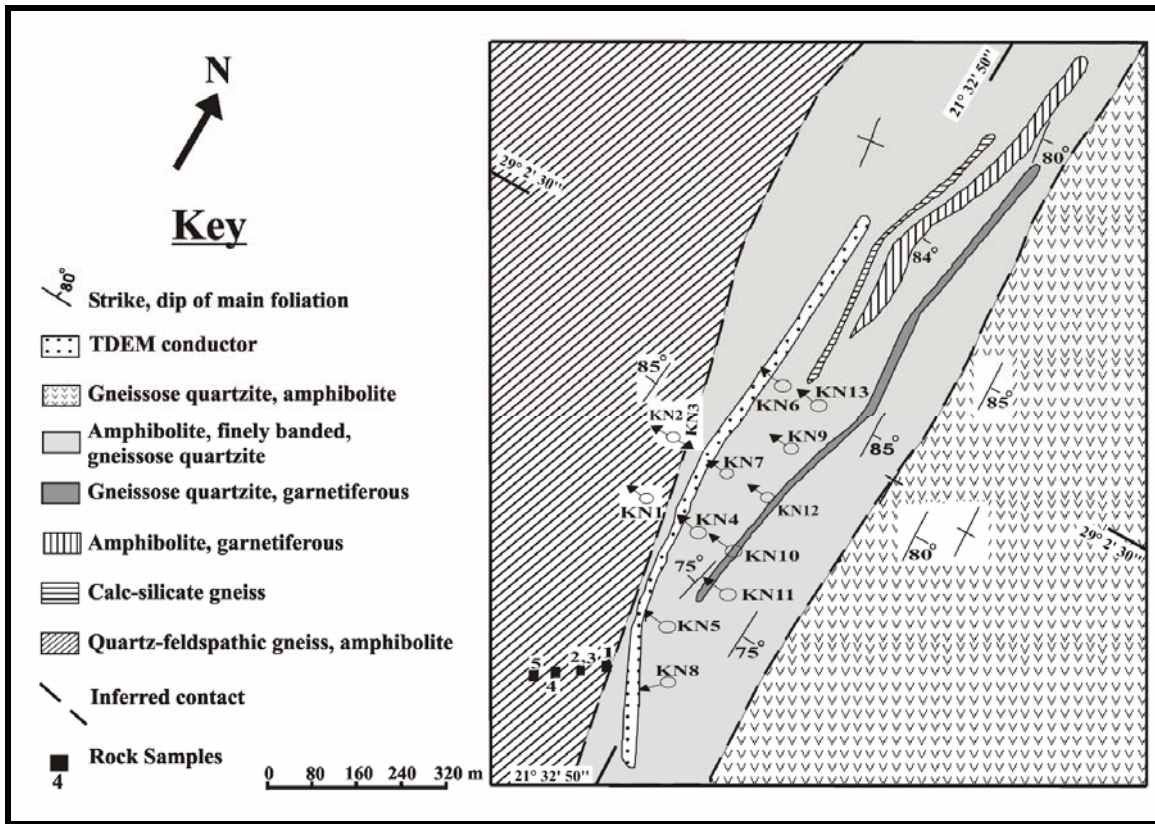
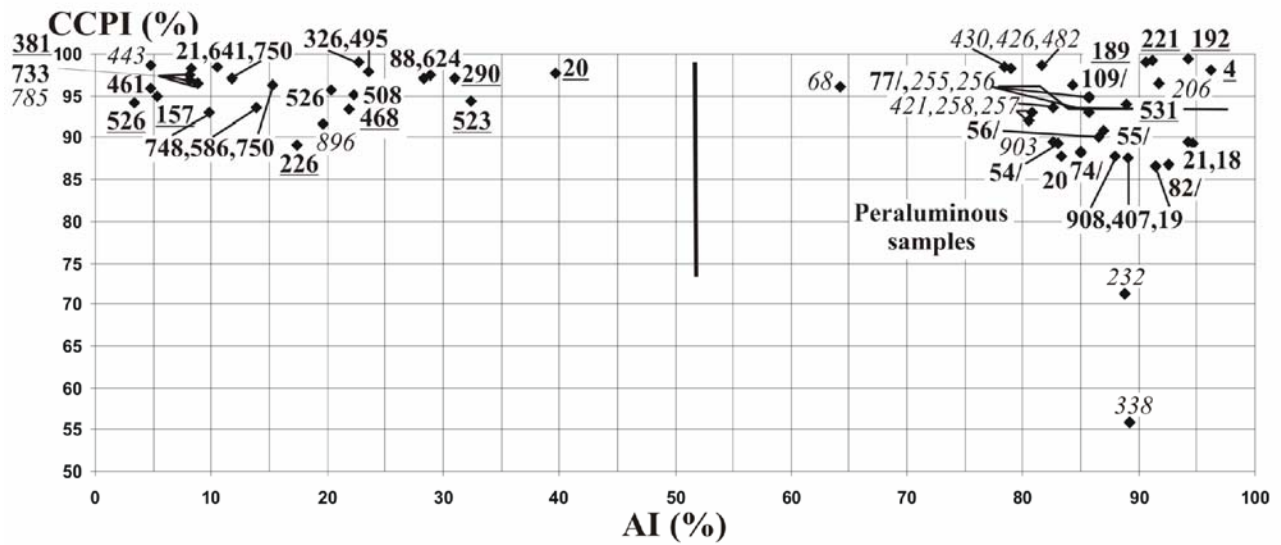


Figure A.5: Geology map of the Kantienpan area (after Rossouw, 2003) and locations of rock samples (TDEM: Time domain electro-magnetic conductor).

Extra Figures



Note 4: Kantienpan (Boks); 19: Bokspuit (Kant); 68: south of Upington (BeUp) and 82/: north of Upington (UpUp).

Figure A.6: Box plot of final results of regional data set (Figure 5.18).

Appendix B

Micropore Analyses

Micropore analyses here were done by using a energy dispersion spectrometer (EDS), or a wavelength dispersion spectrometer (WDS). EDS was used as a qualitative method for fast determination of mineral composition, whereas WDS was used for quantitative mineral analyses.

A CAMECA EPMA- SX 100 was used to analyse minerals such as biotite, feldspars, chlorite, pyroxenes, amphiboles, cordierite (pinite), and garnets. The analytical results for selected samples from boreholes KN11 and KN12 from the Kantienpan and AP2 and AP5 from the Areachap deposit are summarized in tables B.1 to B.7.

Table B.1: Chemical composition of feldspar grains adjacent to the ore zone (Areachap and Kantienpan)

	Sample No.	SiO ₂	Al ₂ O ₃	MgO	FeO	MnO	CaO	K ₂ O	Na ₂ O	F	Cl	Total	TiO ₂	ZnO	Cr ₂ O ₃	NiO
<i>Areachap</i>																
FW	AP5_22A_P2_Plug	62.58	22.50	0.00	0.02	0.00	3.83	0.05	9.05	0.00	0.00	98.11	0.00	0.00	0.00	0.01
FW	AP5_22A_P2_alt_Plug	63.42	22.58	0.22	0.48	0.00	0.75	2.10	8.91	0.01	0.02	98.53	0.00	0.00	0.00	0.00
HW	AP5_44_P4_alt_Plug	69.23	19.41	0.00	0.03	0.00	0.10	0.06	11.20	0.03	0.00	100.07	0.00	0.00	0.01	0.00
HW	AP5_44_P3_UN	64.79	18.24	0.00	0.13	0.02	0.00	15.57	0.19	0.00	0.00	98.96	0.00	0.00	0.00	0.00
<i>Kantienpan</i>																
HW	KN11_20_P2_Plug	62.73	23.49	0.07	0.00	0.01	4.88	0.44	8.34	0.06	0.00	100.04	0.02	0.00	0.01	0.00
HW	KN11_27B_P1_Plug	59.29	25.33	0.06	0.00	0.00	7.13	0.17	7.42	0.00	0.00	99.50	0.03	0.00	0.01	0.00
HW	KN11_27B_P3_Plug	60.38	25.10	0.08	0.00	0.00	6.83	0.24	7.39	0.00	0.01	100.07	0.01	0.00	0.00	0.00
HW	KN11_28_P2_Plug	63.20	22.27	0.00	0.02	0.01	3.88	0.49	8.80	0.02	0.01	98.78	0.02	0.00	0.01	0.00
HW*	KN11_32_P2_Plug	54.15	29.12	0.00	0.17	0.01	10.96	0.12	4.84	0.01	0.00	99.44	0.02	0.00	0.00	0.00
HW*	KN11_33_2_P5_Plug	57.82	26.45	0.03	0.31	0.02	8.17	0.05	6.62	0.00	0.00	99.53	0.00	0.00	0.00	0.00
FW	KN11_40_P6_Plug	48.81	32.35	0.20	0.00	0.02	15.72	0.08	2.46	0.04	0.01	99.76	0.02	0.00	0.02	0.00
FW	KN11_44_P1_Plug	58.15	26.50	0.00	0.07	0.00	8.36	0.13	6.54	-0.02	0.01	99.82	0.02	0.01	0.00	0.00

Note: HW*: Amphibolite, HW: Gneiss and HW: hangingwall

Table B.2: Chemical composition of pyroxene grains near the ore zone (Areachap and Kantienpan)

	Sample No.	SiO ₂	Al ₂ O ₃	MgO	FeO	MnO	CaO	K ₂ O	Na ₂ O	F	Cl	Total	TiO ₂	ZnO	Cr ₂ O ₃	NiO
<i>Areachap</i>																
FW	AP5_38A_P2_Opx	53.65	1.16	16.95	22.51	1.01	1.24	0.01	0.10	0.07	0.00	96.82	0.04	0.07	0.00	0.00
<i>Kantienpan</i>																
HW	KN11_20_P4_Opx	50.06	1.16	12.82	33.26	1.63	0.22	0.00	0.02	0.00	0.00	99.37	0.11	0.07	0.00	0.01
HW	KN11_27B_P3_Opx	51.17	4.04	21.78	19.62	2.65	0.15	0.00	0.02	0.00	0.00	99.68	0.15	0.07	0.00	0.01
HW	KN11_27B_P4_Opx	52.11	2.90	22.21	19.17	2.66	0.16	0.00	0.02	0.09	0.00	99.56	0.09	0.13	0.02	0.00
HW*	KN11_32_P2_Cpx	53.34	1.40	13.91	8.11	0.71	20.97	0.01	0.31	0.07	0.01	99.02	0.14	0.00	0.00	0.00
Ore	KN12_35A_P2_mica	55.69	2.82	24.10	13.73	1.34	0.15	0.44	0.23	0.42	0.00	99.21	0.01	0.28	0.00	0.00
Stringer	KN11_38_P2_opx	48.92	4.77	16.29	26.87	1.78	0.19	0.00	0.01	0.03	0.00	98.97	0.02	0.07	0.02	0.01
FW	KN11_39_P3_opx	50.51	3.89	19.32	25.10	0.78	0.11	0.00	0.02	0.00	0.00	99.82	0.03	0.05	0.00	0.00
FW	KN11_40_P1_Opx	49.53	3.96	16.07	28.62	1.13	0.20	0.01	0.00	0.00	0.00	99.83	0.03	0.24	0.00	0.00
FW	KN11_40_P4_Chl?	52.60	3.94	16.77	20.80	1.52	0.23	0.05	0.30	0.28	0.01	96.58	0.01	0.07	0.00	0.00
FW	KN11_40_P5_Opx	49.74	3.47	27.93	16.64	1.12	0.20	0.00	0.02	0.03	0.00	99.40	0.03	0.20	0.01	0.00
FW	KN11_40_P6_Opx	49.34	4.16	27.91	16.42	1.10	0.22	0.00	0.03	0.03	0.00	99.48	0.02	0.22	0.00	0.00
FW	KN11_44_P3_Opx	51.45	3.41	20.79	22.10	1.57	0.20	0.01	0.01	0.03	0.00	99.70	0.04	0.08	0.00	0.00

Note: HW*: Amphibolite, HW: Gneiss and HW: hangingwall

Table B.3: Chemical composition of cordierite grains close to the ore zone (Areachap and Kantienpan)

	Sample No.	SiO ₂	Al ₂ O ₃	MgO	FeO	MnO	CaO	K ₂ O	Na ₂ O	F	Cl	Total	TiO ₂	ZnO	Cr ₂ O ₃	NiO
<i>Areachap</i>																
FW	AP5_23_Cord	48.92	32.71	8.64	7.34	0.34	0.00	0.01	0.19	0.02	0.00	98.21	0.00	0.01	0.00	0.00
FW	AP5_25_P5_(Bio-Cord,alt)	40.17	32.80	5.24	9.81	0.10	0.14	0.78	0.10	0.10	0.02	89.30	0.00	0.02	0.01	0.00
FW	AP5_29A_P3_Bio	42.45	31.27	4.76	6.94	0.13	0.15	1.61	0.09	0.10	0.00	87.55	0.02	0.02	0.00	0.00
FW	AP5_32_P1_Cord	49.32	32.98	9.93	5.09	0.42	0.01	0.00	0.18	0.00	0.01	98.00	0.02	0.01	0.00	0.00
FW	AP5_32_P1_alt Cord?	38.93	29.65	5.20	12.70	0.20	0.13	2.54	0.06	0.10	0.01	89.55	0.01	0.02	0.00	0.00
FW	AP5_23_P6_Sill	36.98	61.63	0.05	0.53	0.01	0.00	0.01	0.01	0.13	0.00	99.36	0.00	0.00	0.00	0.00
<i>Kantienpan</i>																
HW	KN11_27B_P5_Cord	49.69	33.15	10.57	4.01	0.57	0.02	0.07	0.13	0.00	0.00	98.26	0.00	0.00	0.00	0.00
HW*	KN11_33_2_P4_Cord	50.09	33.41	11.06	3.56	0.54	0.01	0.00	0.19	0.01	0.01	98.99	0.00	0.09	0.00	0.00
Ore	KN11_34B_P3_Cord	50.05	33.48	11.60	2.44	0.73	0.01	0.00	0.10	0.09	0.01	98.59	0.00	0.05	0.01	0.00
Stringer	KN11_38_P4_cord	49.23	33.07	9.25	6.68	0.33	0.02	0.01	0.08	0.01	0.00	98.71	0.00	0.02	0.01	0.00
FW	KN11_39_P4_Cord	49.91	33.41	10.36	4.84	0.28	0.03	0.00	0.11	0.00	0.00	98.98	0.01	0.00	0.00	0.00
FW	KN11_40_P3_cord	49.56	33.07	9.26	6.64	0.28	0.00	0.01	0.11	0.00	0.01	99.00	0.00	0.04	0.01	0.00
FW	KN11_41_P3_Cord	48.62	32.62	8.39	7.64	0.31	0.01	0.00	0.37	0.03	0.00	98.06	0.02	0.00	0.02	0.00
FW	KN11_42_P3_Cor	49.07	32.89	8.57	7.07	0.44	0.01	0.01	0.17	0.00	0.00	98.31	0.00	0.06	0.00	0.00
FW	KN11_43_P2_Cord	49.35	33.06	9.32	6.13	0.42	0.05	0.00	0.19	0.00	0.00	98.59	0.01	0.04	0.00	0.00

Note: HW*: Amphibolite, HW: Gneiss and HW: hangingwall

Table B.4: Chemical composition of garnet grains adjacent to the ore zone (Areachap)

	Sample No.	SiO ₂	Al ₂ O ₃	MgO	FeO	MnO	CaO	K ₂ O	Na ₂ O	F	Cl	Total	TiO ₂	ZnO	Cr ₂ O ₃	NiO
	AP5_20_P2_Garn	37.68	20.86	3.96	24.66	12.52	0.25	0.00	0.01	0.00	0.01	100.00	0.02	0.00	0.00	0.00
FW	AP5_22A_P3_Gar	37.26	20.44	2.67	33.08	5.41	0.87	0.00	0.03	0.05	0.00	99.85	0.02	0.00	0.00	0.00
FW	AP5_23_P1_Gar?	35.36	23.48	3.30	30.88	6.21	0.78	0.01	0.01	0.00	0.01	100.23	0.01	0.12	0.00	0.00
FW	AP5_23_P4_Gar	37.09	23.55	3.26	30.04	5.90	0.72	0.00	0.01	0.02	0.00	100.69	0.00	0.02	0.01	0.00
FW	AP5_25_P1_Gar	37.23	20.87	2.63	35.85	2.43	0.52	0.00	0.02	0.00	0.00	99.62	0.00	0.00	0.02	0.00
FW	AP5_28_B_P4_Garn	37.78	20.91	3.28	36.58	0.90	0.60	0.00	0.03	0.00	0.00	100.15	0.02	0.01	0.00	0.00
FW*	AP5_38A_P7_Garn	37.62	21.30	4.40	34.56	1.38	0.56	0.00	0.02	0.00	0.01	99.84	0.01	0.00	0.01	0.00
HW	AP5_42_P1_Gar	37.00	19.89	1.14	24.20	13.24	3.52	0.00	0.04	0.00	0.00	99.11	0.02	0.00	0.01	0.00
HW	AP5_43_P3_Garn	37.21	19.99	1.27	24.99	11.60	4.32	0.00	0.03	0.01	0.00	99.49	0.02	0.02	0.01	0.00

FW*: Unaltered footwall, FW: Altered footwall

Table B.5: Chemical composition of biotite grains near the ore zone (Areachap and Kantienpan)

	Sample No.	SiO ₂	Al ₂ O ₃	MgO	FeO	MnO	CaO	K ₂ O	Na ₂ O	F	Cl	Total	TiO ₂	ZnO	Cr ₂ O ₃	NiO
<i>Areachap</i>																
FW	AP5_23_P3_Bio	36.19	18.09	12.29	16.74	0.10	0.00	7.87	0.63	0.55	0.02	93.94	1.46	0.00	0.00	0.00
FW	AP5_22A_P3_Bio	36.32	18.42	11.07	18.27	0.06	0.00	8.07	0.41	0.51	0.00	94.73	1.56	0.02	0.00	0.00
FW	AP5_30B_P2_bio	38.32	17.94	15.34	12.42	0.13	0.01	8.21	0.42	0.74	0.02	95.10	1.48	0.06	0.00	0.02
FW	AP5_32_P4_Bio	37.33	18.53	15.57	13.46	0.21	0.00	7.04	0.44	0.53	0.01	93.55	0.39	0.04	0.00	0.00
FW*	AP5_35_P8_Bio	35.23	15.45	6.12	25.00	0.83	0.01	8.76	0.13	0.12	0.05	94.21	2.40	0.09	0.00	0.00
<i>Kantienpan</i>																
HW	KN11_20_P5_Bio	35.07	14.93	21.90	9.07	0.14	0.05	8.49	0.05	0.24	0.01	94.18	4.20	0.02	0.00	0.00
HW	KN11_27B_P2_Bio	37.97	16.85	11.56	15.68	0.35	0.00	9.56	0.05	1.00	0.02	95.85	2.79	0.02	0.00	0.00
HW	KN11_28_P4_Bio	35.79	17.48	14.88	12.74	0.49	0.00	8.51	0.09	0.27	0.10	93.12	2.76	0.00	0.00	0.00
FW	KN11_38_P3_bio	36.86	17.86	14.40	13.78	0.15	0.00	8.82	0.15	1.45	0.02	94.63	1.17	0.00	0.01	0.00
FW	KN11_39_P2_Bi	38.12	16.41	10.39	18.39	0.09	0.00	8.45	0.25	2.00	0.01	94.40	0.25	0.03	0.00	0.01
FW	KN11_41_P2_Bio	36.94	19.10	15.49	12.96	0.12	0.01	8.47	0.31	0.92	0.05	95.44	1.02	0.04	0.00	0.01
FW	KN11_43_P2_Bio	36.76	18.68	14.67	13.34	0.20	0.02	7.95	0.31	1.11	0.06	94.19	1.06	0.04	0.00	0.00
FW	KN11_44_P1_Bio	37.83	15.93	11.32	17.10	0.21	0.00	8.84	0.14	1.27	0.03	95.15	2.43	0.04	0.00	0.00

FW: Altered footwall and FW*: Unaltered footwall

Table B.6: Chemical composition of gahnite (spinel group) grains close the ore zone (Kantienpan)

	Sample No.	SiO ₂	Al ₂ O ₃	FeO	MgO	MnO	CaO	K ₂ O	Na ₂ O	F	Cl	Total	TiO ₂	ZnO	Cr ₂ O ₃	NiO
Ore Zone	KN11_34B_P5_Spin	0.03	59.02	5.39	6.26	0.46	0.00	0.00	0.66	0.00	0.01	101.27	0.00	29.39	0.01	0.00
FW	KN11_42_P1_Spin	0.21	56.12	13.71	2.30	0.23	0.00	0.01	0.63	0.06	0.00	99.73	0.01	26.43	0.01	0.00
FW	KN11_43_P4_Spin	0.23	56.31	12.04	2.47	0.23	0.00	0.00	0.69	0.00	0.00	100.71	0.01	28.69	0.01	0.00
Ore Zone	KN12_32_P2_Gah	0.42	56.39	9.50	4.28	0.22	0.00	0.00	0.63	0.02	0.00	99.42	0.00	27.94	0.01	0.00
Ore Zone	KN12_35A_P3_SP	0.01	59.94	16.60	8.56	0.39	0.00	0.01	0.31	0.00	0.01	99.97	0.02	14.10	0.00	0.00

FW: Altered footwall

Table B.7: Chemical composition of chlorite grains near the ore zone (Areachap and Kantienpan)

	Sample No.	SiO ₂	Al ₂ O ₃	MgO	FeO	MnO	CaO	K ₂ O	Na ₂ O	F	Cl	Total	TiO ₂	ZnO	Cr ₂ O ₃	NiO
<i>Areachap</i>																
HW	AP5_40_P3_Bio	29.07	16.90	12.57	27.94	0.42	0.04	0.89	0.05	0.13	0.02	88.48	0.39	0.04	0.00	0.01
HW	AP5_42_P3_Bio	27.00	17.01	6.68	34.06	0.88	0.14	1.04	0.04	0.00	0.00	87.72	0.79	0.07	0.00	0.00
HW	AP5_44_P2_Chl	26.21	18.46	9.48	33.31	0.68	0.02	0.02	0.01	0.05	0.00	88.31	0.04	0.01	0.00	0.00
HW	AP5_45_P4_Bio	26.55	18.23	12.41	28.71	1.05	0.09	0.08	0.01	0.05	0.00	87.45	0.17	0.06	0.00	0.00
<i>Kantienpan</i>																
Ore	KN11_36_P2_alt(chl or pin)	30.22	12.57	38.05	4.94	0.76	0.13	0.08	0.02	0.00	0.01	86.82	0.00	0.02	0.00	0.02
FW	KN11_41_P4_Amp	25.43	23.09	16.71	21.01	0.31	0.01	0.02	0.01	0.12	0.01	86.81	0.03	0.03	0.01	0.01

FW: Altered footwall and HW: Hangingwall

The calculated mineral formulae from the analyses of plagioclase, pyroxene, cordierite and garnet grains are given in Table B.8 to B. 11.

Table B.8: Chemical composition and unit formulae of plagioclase grains close to the ore zone (Areachap and Kantienpan).

Sample No.	Plagioclase Analyses									
	AP5_22A [P2_Plug (FW)]	AP5_22A [P2_alt_Plug (FW)]	AP5_44 [P4_alt_Plug (HW)]	KN11_27B [P1_Plug (HW)]	KN11_27B [P3_Plug (HW)]	KN11_28 [P2_Plug (HW*)]	KN11_32 [P2_Plug (HW*)]	KN11_33 [2_P5_Plug (Ore Zone)]	KN11_40 [P6_Plug (FW)]	KN11_44 [P1_Plug (FW)]
Mineral	Oligoclase	Albite	Albite	Andesine	Andesine	Oligoclase	Labradorite	Andesine	Bytownite	Andesine
SiO ₂	62.58	63.42	69.23	59.29	60.38	63.20	54.15	57.82	48.81	58.15
Al ₂ O ₃	22.50	22.58	19.41	25.33	25.10	22.27	29.12	26.45	32.35	26.50
FeO	0.02	0.48	0.03	0.00	0.00	0.02	0.17	0.31	0.00	0.07
TiO ₂	0.00	0.00	0.00	0.03	0.01	0.02	0.02	0.00	0.02	0.02
MgO	0.00	0.22	0.00	0.06	0.08	0.00	0.00	0.03	0.20	0.00
CaO	3.83	0.75	0.10	7.13	6.83	3.88	10.96	8.17	15.72	8.36
Na ₂ O	9.05	8.91	11.20	7.42	7.39	8.80	4.84	6.62	2.46	6.54
K ₂ O	0.05	2.10	0.06	0.17	0.24	0.49	0.12	0.05	0.08	0.13
MnO	0.00	0.00	0.00	0.00	0.00	0.01	0.01	0.02	0.02	0.00
FeO	0.00	0.01	0.03	0.00	0.00	0.02	0.01	0.00	0.04	0.00
Total	98.11	98.53	100.07	99.50	100.07	98.78	99.44	99.53	99.76	99.82
Based on 32(O)										
Si	11.26	11.38	12.06	10.63	10.74	11.31	9.82	10.40	8.96	10.42
Al	4.77	4.78	3.98	5.35	5.26	4.70	6.22	5.61	6.99	5.60
Fe ⁺²	0.00	0.07	0.00	0.00	0.00	0.00	0.03	0.05	0.00	0.01
Ti	0.00	0.00	0.00	0.00	0.00	0.00	0.00	0.00	0.00	0.00
Mg	0.00	0.06	0.00	0.02	0.02	0.00	0.00	0.01	0.05	0.00
Ca	0.74	0.14	0.02	1.37	1.30	0.74	2.13	1.57	3.09	1.60
Na	3.16	3.10	3.78	2.58	2.55	3.05	1.70	2.31	0.88	2.27
K	0.01	0.48	0.01	0.04	0.05	0.11	0.03	0.01	0.02	0.03
Ca+Na+K	3.91	3.73	3.81	3.99	3.90	3.91	3.86	3.89	3.98	3.91
Ab	80.81	83.22	99.16	64.68	65.27	78.11	44.10	59.28	21.97	58.16
An	18.90	3.87	0.49	34.35	33.34	19.03	55.18	40.43	77.56	41.08
Or	0.29	12.91	0.35	0.98	1.39	2.86	0.72	0.29	0.47	0.76

Note: HW*: amphibolite, HW: gneiss, HW: hangingwall, FW: footwall, Plag: plagioclase, and AP5_22A [P2_Plug (FW)] means borehole AP5_sample No. 22A_[analysis point No_in plagioclase (from the footwall zone)].

Table B.9: Chemical composition and unit formulae of pyroxene grains close to the ore zone (Areachap and Kantienpan).

Sample No.	Pyroxene Analyses												
	AP5_38A [P2_OPX (FW)]	KN11_20 [P4_Opx (HW)]	KN11_27B [P3_Opx (HW)]	KN11_27B [P4_Opx (HW)]	KN11_32 [P2_Cpx (Ore)]	KN12_35A [P2_mica (Ore)]	KN11_38 [P2_opx (Stringer)]	KN11_39 [P3_opx (FW)]	KN11_40 [P1_Opx (FW)]	KN11_40 [P4_Ch?] (FW)]	KN11_40 [P5_Opx (FW)]	KN11_40 [P6_Opx (FW)]	KN11_44 [P3_Opx (FW)]
Mineral	Clino-Enstatite	Clino-Ferrosilite	Clino-Enstatite	Clino-Enstatite	Augite	Clino-Enstatite	Clino-Enstatite	Clino-Enstatite	Pigeonite	Clinoenstaite-Ferrosilite	Clino-Enstatite	Clino-Enstatite	Clino-Enstatite
SiO₂	53.65	50.06	51.17	52.11	53.34	55.69	48.92	50.51	49.53	52.60	49.74	49.34	51.45
Al₂O₃	1.16	1.16	4.04	2.90	1.40	2.82	4.77	3.89	3.96	3.94	3.47	4.16	3.41
TiO₂	0.04	0.11	0.15	0.09	0.14	0.01	0.02	0.03	0.03	0.01	0.03	0.02	0.04
FeO	22.51	33.26	19.62	19.17	8.11	13.73	26.87	25.10	28.62	20.80	16.64	16.42	22.10
MgO	16.95	12.82	21.78	22.21	13.91	24.10	16.29	19.32	16.07	16.77	27.93	27.91	20.79
MnO	1.01	1.63	2.65	2.66	0.71	1.34	1.78	0.78	1.13	1.52	1.12	1.10	1.57
CaO	1.24	0.22	0.15	0.16	20.97	0.15	0.19	0.11	0.20	0.23	0.20	0.22	0.20
Na₂O	0.10	0.02	0.02	0.02	0.31	0.23	0.01	0.02	0.00	0.30	0.02	0.03	0.01
K₂O	0.01	0.00	0.00	0.00	0.01	0.44	0.00	0.00	0.01	0.05	0.00	0.00	0.01
Cr₂O₃	0.00	0.00	0.00	0.02	0.00	0.00	0.02	0.00	0.00	0.00	0.01	0.00	0.00
NiO	0.00	0.01	0.01	0.00	0.00	0.00	0.01	0.00	0.00	0.00	0.00	0.00	0.00
F	0.07	0.00	0.00	0.09	0.07	0.42	0.03	0.00	0.00	0.28	0.03	0.03	0.03
Total	96.82	99.37	99.68	99.56	99.02	99.21	98.97	99.82	99.83	96.58	99.40	99.48	99.70

Note: Mg*=100Mg/(Mg+Fe+Mn), Opx: ortho-pyroxene, chl: Chlorite, FW: footwall, HW: hangingwall and AP5_38A [P2_OPX (FW)] means borehole AP5 – sample No. 38A [analysis point No. in orthopyroxene(from the footwall zone)].

Table B.9: Continued

Sample No.	Pyroxene Analyses												
	AP5_38A [P2_Opx (FW)]	KN11_20 [P4_Opx (HW)]	KN11_27B [P3_Opx (HW)]	KN11_27B [P4_Opx (HW)]	KN11_32 [P2_Cpx (Ore)]	KN12_35A [P2_mica (Ore)]	KN11_38 [P2_oxp (Stringer)]	KN11_39 [P3_oxp (FW)]	KN11_40 [P1_Opx (FW)]	KN11_40 [P4_Chl? (FW)]	KN11_40 [P5_Opx (FW)]	KN11_40 [P6_Opx (FW)]	KN11_44 [P3_Opx (FW)]
Mineral	Clino-Enstatite	Clino-Ferrosilite	Clino-Enstatite	Clino-Enstatite	Augite	Clino-Enstatite	Clino-Enstatite	Pigeonite	Clinoenstaite-Ferrosilite	Clino-Enstatite	Clino-Enstatite	Clino-Enstatite	
Based on 6(O)													
Si	2.07	1.99	1.91	1.94	2.00	2.02	1.90	1.91	1.92	2.02	1.84	1.82	1.93
Al	0.00	0.01	0.09	0.06	0.00	0.00	0.10	0.09	0.08	0.00	0.15	0.18	0.07
Al	0.05	0.04	0.09	0.07	0.06	0.12	0.12	0.08	0.10	0.18	0.00	0.00	0.08
Ti	0.00	0.00	0.00	0.00	0.00	0.00	0.00	0.00	0.00	0.00	0.00	0.00	0.00
Fe⁺²	0.73	1.11	0.61	0.60	0.25	0.42	0.87	0.79	0.93	0.67	0.51	0.51	0.69
Cr	0.00	0.00	0.00	0.00	0.00	0.00	0.00	0.00	0.00	0.00	0.00	0.00	0.00
Mn	0.03	0.05	0.08	0.08	0.02	0.04	0.06	0.03	0.04	0.05	0.04	0.03	0.05
Ni	0.00	0.00	0.00	0.00	0.00	0.00	0.00	0.00	0.00	0.00	0.00	0.00	0.00
Mg	0.97	0.76	1.21	1.23	0.78	1.30	0.94	1.09	0.93	0.96	1.54	1.54	1.16
Ca	0.05	0.01	0.01	0.01	0.84	0.01	0.01	0.00	0.01	0.01	0.01	0.01	0.01
Na	0.01	0.00	0.00	0.00	0.02	0.02	0.00	0.00	0.00	0.02	0.00	0.00	0.00
K	0.00	0.00	0.00	0.00	0.00	0.02	0.00	0.00	0.00	0.00	0.00	0.00	0.00
Atomic Percentages													
Mg+Fe+Ca	1.75	1.87	1.83	1.84	1.87	1.72	1.82	1.89	1.86	1.64	2.06	2.05	1.86
Mg	55.63	40.52	66.21	67.14	41.48	75.52	51.71	57.70	49.80	58.63	74.66	74.87	62.37
Fe⁺²	41.45	58.98	33.46	32.51	13.57	24.14	47.85	42.06	49.76	40.80	24.96	24.71	37.20
Ca	2.93	0.50	0.33	0.35	44.95	0.34	0.43	0.24	0.45	0.58	0.38	0.42	0.43
Mg*	56.21	39.56	63.51	64.42	73.74	74.01	50.31	57.08	49.04	57.23	73.69	73.94	61.00

Note: Mg* = 100Mg/(Mg+Fe+Mn), Opx: ortho-pyroxene, chl: Chlorite, FW: footwall, HW: hangingwall and AP5_38A [P2_Opx (FW)] means borehole AP5_sample No. 38A_[analysis point No_in orthopyroxene(from the footwall zone)].

Table B.10: Chemical composition and unit formulae of cordierite grains near the ore zone (Areachap and Kantienpan).

	Cordierite Analyses													
Sample No.	AP5_23 [Cord (FW)]	AP5_25 [P5_(Bio- alt Cord,) (FW)]	AP5_29A [P3_Bio (FW)]	AP5_32 [P1_Cord (FW)]	AP5_32 [P1_alt Cord? (FW)]	KN11_27 B [P5_Cord (HW)]	KN11_33 _2 [P4_Cord (HW*)]	KN11_34 B [P3_Cord (Ore)]	KN11_38 [P4_cord (Stringer)]	KN11_39 [P4_Cord (FW)]	KN11_40 [P3_cord (FW)]	KN11_41 [P3_Cord (FW)]	KN11_42 [P3_Cord (FW)]	KN11_43 [P2_Cord (FW)]
Mineral	Cordierite	Cordierite	Cordierite	Cordierite	Cordierite	Cordierite	Cordierite	Cordierite	Cordierite	Cordierite	Cordierite	Cordierite	Cordierite	Cordierite
SiO₂	48.92	40.17	42.45	49.32	38.93	49.69	50.09	50.05	49.23	49.91	49.56	48.62	49.07	49.35
Al₂O₃	32.71	32.80	31.27	32.98	29.65	33.15	33.41	33.48	33.07	33.41	33.07	32.62	32.89	33.06
TiO₂	0.00	0.00	0.02	0.02	0.01	0.00	0.00	0.00	0.00	0.01	0.00	0.02	0.00	0.01
FeO	7.34	9.81	6.94	5.09	12.70	4.01	3.56	2.44	6.68	4.84	6.64	7.64	7.07	6.13
MgO	8.64	5.24	4.76	9.93	5.20	10.57	11.06	11.60	9.25	10.36	9.26	8.39	8.57	9.32
MnO	0.34	0.10	0.13	0.42	0.20	0.57	0.54	0.73	0.33	0.28	0.28	0.31	0.44	0.42
Na₂O	0.19	0.10	0.09	0.18	0.06	0.13	0.19	0.10	0.08	0.11	0.11	0.37	0.17	0.19
CaO	0.00	0.14	0.15	0.01	0.13	0.02	0.01	0.01	0.02	0.03	0.00	0.01	0.01	0.05
K₂O	0.01	0.78	1.61	0.00	2.54	0.07	0.00	0.00	0.01	0.00	0.01	0.00	0.01	0.00
F	0.02	0.10	0.10	0.00	0.10	0.00	0.01	0.09	0.01	0.00	0.00	0.03	0.00	0.00
Cl	0.00	0.02	0.00	0.01	0.01	0.00	0.01	0.01	0.00	0.00	0.01	0.00	0.00	0.00
Total	98.21	89.30	87.55	98.00	89.55	98.26	98.99	98.59	98.71	98.98	99.00	98.06	98.31	98.59
Based on 18(O)														
Si	5.03	4.66	4.95	5.03	4.65	5.03	5.03	5.02	5.02	5.03	5.03	5.02	5.03	5.03
Al	0.97	1.34	1.05	0.97	1.35	0.97	0.97	0.98	0.98	0.97	0.97	0.97	0.97	0.97
Al	2.99	3.14	3.24	2.99	2.83	2.99	2.98	2.98	2.99	2.99	2.99	3.00	3.01	3.01
Ti	0.00	0.00	0.00	0.00	0.00	0.00	0.00	0.00	0.00	0.00	0.00	0.00	0.00	0.00
Fe⁺²	0.63	0.95	0.68	0.43	1.27	0.34	0.30	0.20	0.57	0.41	0.56	0.66	0.61	0.52
Mg	1.32	0.91	0.83	1.51	0.93	1.60	1.65	1.74	1.40	1.55	1.40	1.29	1.31	1.41
Mn	0.03	0.01	0.01	0.04	0.02	0.05	0.05	0.06	0.03	0.02	0.02	0.03	0.04	0.04
Na	0.04	0.02	0.02	0.04	0.01	0.03	0.04	0.02	0.02	0.02	0.02	0.07	0.03	0.04
Ca	0.00	0.02	0.02	0.00	0.02	0.00	0.00	0.00	0.00	0.00	0.00	0.00	0.00	0.01
K	0.00	0.12	0.24	0.00	0.39	0.01	0.00	0.00	0.00	0.00	0.00	0.00	0.00	0.00
Mg#	67.72	48.77	55.01	77.67	42.19	82.45	84.70	89.44	71.17	79.23	71.31	66.19	68.36	73.05

Note: HW*: amphibolite, HW: gneiss, HW: hangingwall, FW: footwall, Mg# = 100*Mg/(Mg+Fe), Bio: biotite, Cord: cordierite, alt: altered and AP5_25 [P5_(Bio- alt Cord,) (FW)] means borehole AP5_ sample No. 25_[analysis point No_ in biotite or altered cordierite (from the footwall zone)].

Table B.11: Chemical composition and unit formulae of garnet grains near the ore zone (Areachap).

Sample No.	Garnet Analyses									
	AP5_20 [P2_Garn]	AP5_22A [P3_Garn (FW)]	AP5_23 [P1_Garn? (FW)]	AP5_23 [P4_Garn (FW)]	AP5_25 [P1_Garn (FW)]	AP5_28_B [P4_Garn (FW)]	AP5_38A [P7_Garn (FW*)]	AP5_42 [P1_Garn (HW)]	AP5_43 [P3_Garn (HW)]	
Mineral	Almandine	Almandine	Almandine	Almandine	Almandine	Almandine	Almandine	Almandine	Almandine	Almandine
SiO ₂	37.68	37.26	35.36	37.09	37.23	37.78	37.62	37.00	37.21	
Al ₂ O ₃	20.86	20.44	23.48	23.55	20.87	20.91	21.30	19.89	19.99	
Cr ₂ O ₃	0.00	0.00	0.00	0.01	0.02	0.00	0.01	0.01	0.01	
FeO	24.66	33.08	30.88	30.04	35.85	36.58	34.56	24.20	24.99	
TiO ₂	0.02	0.02	0.01	0.00	0.00	0.02	0.01	0.02	0.02	
MgO	3.96	2.67	3.30	3.26	2.63	3.28	4.40	1.14	1.27	
MnO	12.52	5.41	6.21	5.90	2.43	0.90	1.38	13.24	11.60	
CaO	0.25	0.87	0.78	0.72	0.52	0.60	0.56	3.52	4.32	
K ₂ O	0.00	0.00	0.01	0.00	0.00	0.00	0.00	0.00	0.00	
Na ₂ O	0.01	0.03	0.01	0.01	0.02	0.03	0.02	0.04	0.03	
F	0.00	0.05	0.00	0.02	0.00	0.00	0.00	0.00	0.01	
Total	100.00	99.85	100.23	100.69	99.62	100.15	99.84	99.11	99.49	
Based on 24(O)										
Si	6.04	6.05	5.69	5.87	6.04	6.07	6.01	6.08	6.07	
Al	3.94	3.91	0.31	0.13	3.99	3.96	4.01	3.85	3.85	
AI	0.00	0.00	4.15	4.26	0.00	0.00	0.00	0.00	0.00	
Cr	0.00	0.00	0.00	0.00	0.00	0.00	0.00	0.00	0.00	
Fe ⁺²	3.31	4.49	4.16	3.98	4.86	4.91	4.62	3.32	3.41	
Ti	0.00	0.00	0.00	0.00	0.00	0.00	0.00	0.00	0.00	
Mg	0.95	0.65	0.79	0.77	0.64	0.79	1.05	0.28	0.31	
Mn	1.70	0.74	0.85	0.79	0.33	0.12	0.19	1.84	1.60	
Ca	0.04	0.15	0.13	0.12	0.09	0.10	0.10	0.62	0.76	
Mol per cent end-members										
Mg+Fe+Mn+Ca	6.00	6.03	5.93	5.66	5.93	5.92	5.95	6.06	6.08	
Pyrope	15.78	10.71	13.35	13.59	10.74	13.26	17.62	4.60	5.08	
Almandine	55.14	74.45	70.10	70.27	82.10	82.94	77.63	54.81	56.11	
Spessartine	28.36	12.33	14.28	13.98	5.64	2.07	3.14	30.37	26.38	
Grossular	0.72	2.51	2.27	2.16	1.53	1.74	1.61	10.21	12.43	

Note: FW*: Unaltered footwall; FW: Altered footwall; Garn: garnet; Mol: molciular and AP5_22A [P3_Garn (FW)] means borehole AP5_sample No. 22A_[analysis point No_in garnet (from the footwall zone)].

Table B.12: Chemical composition and unit formulae of biotite grains near the ore zone (Areachap and Kantienpan)

	Biotite Analyses												
Sample No.	AP5_23 [P3_Bio (FW)]	AP5_22A [P3_Bio (FW)]	AP5_30B [P2_Bio (FW)]	AP5_32 [P4_Bio (FW)]	AP5_35 [P8_Bio (FW*)]	KN11_20 [P5_Bio (HW)]	KN11_27B [P2_Bio (HW)]	KN11_28 [P4_Bio (HW)]	KN11_38 [P3_Bio (Ore Zone)]	KN11_39 [P2_Bio (FW)]	KN11_41 [P2_Bio (FW)]	KN11_43 [P2_Bio (FW)]	KN11_44 [P1_Bio (FW)]
Mineral	Biotite	Biotite	Phlogopite	Phlogopite	Annnite	Phlogopite	Biotite	Phlogopite	Phlogopite	Biotite	Phlogopite	Phlogopite	Biotite
SiO₂	36.19	36.32	38.32	37.33	35.23	35.07	37.97	35.79	36.86	38.12	36.94	36.76	37.83
TiO₂	1.46	1.56	1.48	0.39	2.40	4.20	2.79	2.76	1.17	0.25	1.02	1.06	2.43
Al₂O₃	18.09	18.42	17.94	18.53	15.45	14.93	16.85	17.48	17.86	16.41	19.10	18.68	15.93
FeO	16.74	18.27	12.42	13.46	25.00	9.07	15.68	12.74	13.78	18.39	12.96	13.34	17.10
MgO	12.29	11.07	15.34	15.57	6.12	21.90	11.56	14.88	14.40	10.39	15.49	14.67	11.32
MnO	0.10	0.06	0.13	0.21	0.83	0.14	0.35	0.49	0.15	0.09	0.12	0.20	0.21
CaO	0.00	0.00	0.01	0.00	0.01	0.05	0.00	0.00	0.00	0.00	0.01	0.02	0.00
K₂O	7.87	8.07	8.21	7.04	8.76	8.49	9.56	8.51	8.82	8.45	8.47	7.95	8.84
Na₂O	0.63	0.41	0.42	0.44	0.13	0.05	0.05	0.09	0.15	0.25	0.31	0.31	0.14
F	0.55	0.51	0.74	0.53	0.12	0.24	1.00	0.27	1.45	2.00	0.92	1.11	1.27
Total	93.94	94.73	95.10	93.55	94.21	94.18	95.85	93.12	94.63	94.40	95.44	94.19	95.15
Based on 22(O)													
Si	5.51	5.51	5.64	5.57	5.62	5.19	5.69	5.42	5.56	5.90	5.46	5.51	5.76
Al	2.49	2.49	2.36	2.43	2.38	2.81	2.31	2.58	2.44	2.10	2.54	2.49	2.24
Al	0.75	0.81	0.74	0.82	0.53	-0.21	0.67	0.53	0.73	0.89	0.78	0.81	0.61
Ti	0.17	0.18	0.16	0.04	0.29	0.47	0.31	0.31	0.13	0.03	0.11	0.12	0.28
Fe⁺²	2.13	2.32	1.53	1.68	3.34	1.12	1.97	1.61	1.74	2.38	1.60	1.67	2.18
Mg	2.79	2.50	3.36	3.46	1.46	4.83	2.58	3.36	3.24	2.40	3.41	3.28	2.57
Mn	0.01	0.01	0.02	0.03	0.11	0.02	0.04	0.06	0.02	0.01	0.02	0.03	0.03
Ca	0.00	0.00	0.00	0.00	0.00	0.01	0.00	0.00	0.00	0.00	0.00	0.00	0.00
K	1.53	1.56	1.54	1.34	1.78	1.60	1.83	1.64	1.70	1.67	1.60	1.52	1.72
Na	0.37	0.24	0.24	0.25	0.08	0.03	0.03	0.05	0.09	0.15	0.18	0.18	0.08
Mg/Fe	1.31	1.08	2.2	2.06	0.44	4.3	1.31	2.08	1.86	1.01	2.13	1.96	1.18

FW: Altered footwall, FW*: Unaltered footwall, HW: hanging wall and AP5_22A [P3_Bio (FW)] means borehole AP5_ sample No 22A_[analysis point No_ in biotite (from the footwall zone)].

Appendix C

Sample preparation and whole rock analysis

C.1. Sample preparation for XRF Analysis

The remainder of quarter-core samples after making thin sections was crushed in a jaw crusher before being milled in a carbon-steel mill. The samples were milled to a particle size of <63 micron. To minimize possible cross contamination, the mill was cleaned after every sample by milling clean quartz, washing the mill pots, and drying with acetone, followed by pre-contaminating the mill with the sample to be milled.

3 grams of each sample powder were weighed and dried at 100°C overnight before being roasted at 1000°C overnight to determine the absorbed (H_2O^-) and the percentage loss on ignition (H_2O^+), respectively.

Major elements were determined on fused beads, prepared following the standard method used in the analytical laboratory of the Department of Geology, University of Pretoria, as adapted from Bennett and Oliver (1992). One gram of pre-roasted sample powder and 6 grams of flux (Lithium tetra-borate) mixed in a Pt crucible is fused at 1050°C for 15

minutes in a muffle furnace with occasional swirling. The fused mixture is poured into a pre-heated Pt/Au mould and left to cool at room temperature in a desiccator. The bottom surface of the glass disk is analysed by x-ray fluorescence spectroscopy (XRF) using an ARL 9400XP+ wavelength dispersive XRF Spectrometer.

Trace elements were determined on pressed powder briquettes prepared following the method of Watson (1996). Approximately 16-20ml of sample powder is mixed with less than 1 volume % of a liquid binder (Mowiol: polyvinyl alcohol). This mixture is loaded into aluminium cups to increase the stability and strength before being pressed at \pm 7 tons/in².

C.1.1. CALIBRATION

The XRF Spectrometer was calibrated with certified reference materials. The NBSGSC fundamental parameter program was used for matrix correction of major elements as well as for Cl, Co, Cr, V, Sc and S. The Rh Compton peak ratio method was used for the other trace elements.

C.3. XRF analytical precision and accuracy

Standard deviations and detection limits are listed in Table C.1.

C.4. Results of XRF analyses

The results of XRF analysis are given below in Tables C.2 to C.6. The word “Fused” in the table refers to fused bead analysis and ‘‘Powder’’ to pressed powder briquette analysis. The first three columns in Table C.2 (LIT, GSN, and NIMN) are standard reference samples.

The sulphide samples were analysed as pressed powder briquettes using the UNIQUANT software, a fundamental parameter based programme, calibrated with pure metals and oxides (Samples KN12/22 to KN12/25 and KN11/34 to KN11/37). This software

analyses samples by specifying a sulphide matrix. In this case S is analysed at a different peak position and Fe, Mn, Cu, Ni, Zn and Pb expressed as elements.

Table C.1: Standard deviation and detection limit of XRF analysis

wt %	Standard deviation (%)	LOD
SiO₂	0.4	0.02
TiO₂	0.03	0.0032
Al₂O₃	0.3	0.01
Fe₂O₃	0.3	0.0097
MnO	0.0065	0.0013
MgO	0.1	0.0118
CaO	0.07	0.01
Na₂O	0.11	0.0265
K₂O	0.06	0.005
P₂O₅	0.08	0.01
ppm	Standard deviation (%)	LOD
Cl*	100	11
Co	6	3
Cr	40	15
F*	500	400
S*	300	40
Sc	5	1
V	10	1
As*	10	3
Cu	3	2
Ga	2	2
Mo	1	1
Nb	3	2
Ni	6	3
Pb	3	3
Rb	4	2
Sr	4	3
Th	2	3
U	2	3
W*	10	6
Y	4	3
Zn	4	4
Zr	6	10
Ba	14	5
La	24	5
Ce	14	6

Values for elements indicated with an *should be considered semi-quantitative

Table C.2: XRF analytical results for samples from borehole AP5 (Areachap)

Fused	LIT	GSN	NIMN	AP5/1	AP5/2	AP5/3	AP5/4	AP5/5	AP5/6	AP5/7	AP5/8	AP5/9	AP5/10	AP5/11	AP5/12	AP5/13
Depth (m)	-	-	-	79.2	29.7	33.5	46.2	60.8	84.8	108.6	120.8	145.8	154.6	177.9	176.2	176.5
Rock Name	Standard	Standard	Standard	Bt-Hbl Gn	Hbl-Gn	Bt-Hbl Gn	Amph.	Amph.	Hbl-Bt-Gn	Amph.	Garnet-Bt-Gn	Hbl-Gn	Garnet-Bt-Gn	Chl-Schist	Granite rock	Granite rock
SiO₂(wt%)	0.01	65.87	52.5	64.68	52.11	56.69	47.74	54.18	66.1	52.04	75.36	53.54	71.27	70.71	75.84	69.16
TiO₂	n.d.	0.65	0.19	0.68	1.1	0.74	0.77	0.89	0.42	0.88	0.26	0.92	0.34	0.41	0.21	0.53
Al₂O₃	0.01	14.85	16.71	14.6	17.43	16.51	19.69	16.73	15.09	14.58	12.29	14.56	12.16	13.92	11.73	14.39
Fe₂O₃	n.d.	3.67	9.01	7.65	11.23	10.41	10.84	10.52	5.97	12.14	4.52	11.7	5.37	4.44	2.68	3.69
MnO	0.01	0.05	0.18	0.2	0.18	0.19	0.19	0.22	0.16	0.13	0.16	0.26	0.14	0.05	0.02	0.06
MgO	n.d.	2.22	7.63	1.53	3.82	3.64	4.78	3.28	1.48	6.78	0.57	5.2	1.04	1.21	0.22	1.79
CaO	n.d.	2.69	11.38	5.42	9.31	3.71	10.43	7.55	4.01	7.76	1.21	9.28	1.69	0.57	0.63	0.75
Na₂O	0.23	3.83	2.63	3.08	2.89	4.02	2.2	3.17	3.41	3.59	4.84	2.96	3.96	6.7	6.5	6.83
K₂O	n.d.	4.74	0.24	0.87	1.24	1.45	1.29	1.32	1.98	0.68	1.31	0.74	1.8	0.54	0.35	0.58
P₂O₅	0.01	0.3	0.03	0.23	0.43	0.19	0.2	0.28	0.15	0.12	0.07	0.2	0.09	0.16	0.07	0.18
LOI	n.d.	1.29	0.00	0.52	0.83	2.48	1.36	0.92	0.58	0.89	0.3	0.78	0.58	1.19	0.91	1.63
Total:		100.16	100.28	99.45	100.57	100.03	99.49	99.04	99.37	99.56	100.89	100.14	98.44	99.90	99.16	99.59

Hbl: hornblende, Bt: biotite, Gn: gneiss, Chl: chlorite, Amph.: amphibolite and n.d.: Not detected.

Table C.2: Continued

Powder	SIO2	GSN	NIMN	AP5/1	AP5/2	AP5/3	AP5/4	AP5/5	AP5/6	AP5/7	AP5/8	AP5/9	AP5/10	AP5/11	AP5/12	AP5/13
Cl* (ppm)	90	536	57	12	84	41	56	9	91	110	29	217	8	40	26	71
Co	2	39	49	42	47	41	49	43	33	51	28	51	30	28	32	32
Cr	16	51	36	10	40	27	62	27	11	34	10	62	10	10	10	10
F*	584	4789	100	100	100	100	100	100	528	100	551	100	1218	191	288	190
S*	16	108	16	350	132	16	16	45	16	16	16	454	16	16	16	16
Sc	1	5	20	14	15	31	9	20	11	33	8	28	10	14	4	10
V	3	55	200	57	247	169	210	185	76	339	5	322	1	37	36	46
As	3	9	3	3	3	3	3	3	3	3	4	3	3	3	3	3
Cu	2	23	11	46	186	3	44	35	26	4	19	40	4	7	2	5
Ga	2	20	17	16	16	16	16	17	14	16	18	16	16	14	10	13
Mo	1	1	1	1	2	1	1	1	1	1	1	1	2	1	1	1
Nb	2	22	2	5	6	3	3	4	4	2	8	3	8	5	2	10
Ni	3	36	109	6	19	10	43	9	6	24	6	32	5	6	4	6
Pb	3	55	3	8	7	4	6	7	8	5	8	4	15	4	3	3
Rb	2	181	5	21	27	64	54	38	56	21	26	17	109	20	22	18
Sr	3	583	264	309	417	309	431	401	427	190	86	331	167	77	24	35
Th	3	43	3	5	3	3	4	3	6	3	4	3	5	10	4	3
U	3	13	3	3	3	3	3	3	3	3	3	3	4	5	3	3
W*	6	452	6	316	112	100	95	118	228	85	325	146	299	281	463	369
Y	4	18	6	33	27	24	16	25	19	24	87	23	65	23	14	28
Zn	11	54	59	92	89	103	76	92	70	30	126	90	100	36	11	41
Zr	10	213	12	105	96	58	42	67	79	44	265	55	217	139	159	220
Ba	5	1443	81	506	573	351	378	400	1009	123	231	269	703	131	47	133
La	5	49	19	31	47	32	31	42	15	43	32	55	23	18	29	13
Ce	28	122	10	44	45	25	18	24	42	6	54	35	46	27	52	37

*: Semi-quantitative analysis.

Table C.2: Continued

Fused	AP5/14	AP5/15	AP5/16	AP5/17	AP5/18	AP5/19	AP5/20	AP5/21	AP5/22	AP5/23	AP5/24	AP5/25	AP5/26	AP5/27	AP5/28	AP5/29
Depth (m)	188.1	196.6	206.9	219.3	228	243.2	253.4	269.9	282.7	277.6	281.4	298.5	311.5	306.1	318.8	317.4
Rock Name	Amph.	Hbl-Gn	Amph.	Hbl-Gn	Hbl-Gn	Sil-Crd-Bt-Gn	Bt-Gn	Garnet-Sil-Crd-Bt-Gn	Garnet-Sil-Crd-Bt-Gn	Sil-Crd-Bt-Gn	Sil-Crd-Bt-Gn	Garnet-Sil-Crd-Bt-Gn	Garnet-Sil-Crd-Bt-Gn	Garnet-Sil-Crd-Bt-Gn	Garnet-Sil-Crd-Bt-Gn	Garnet-Sil-Crd-Bt-Gn
SiO₂ (wt%)	47.51	58.37	48.51	55.14	53.54	65.7	66.89	65.25	70.51	67.44	75.03	72.59	64.25	56.41	70.12	78.07
TiO₂	0.47	0.76	1.07	1.16	0.95	0.8	0.4	0.37	0.47	0.3	0.25	0.25	0.56	0.55	0.27	0.25
Al₂O₃	15.21	15.35	14.52	14.06	14.67	13.75	13.91	13.23	11.85	10.89	11.6	11.63	14.9	14.11	15.02	9.2
Fe₂O₃	8.96	7.64	12.85	13.42	12.62	9.26	6.62	9.61	7.01	13.55	4.51	7.32	7.69	12.61	9.91	4.5
MnO	0.16	0.14	0.33	0.43	0.33	0.19	0.14	0.1	0.08	0.08	0.05	0.13	0.11	0.17	0.13	0.06
MgO	8.94	4.25	7.06	5.51	4.66	2.67	2.55	5.98	4.21	3.86	3.24	2.34	4.68	7.27	3.12	2.65
CaO	12.99	6.11	5.14	3.66	5.71	2.31	0.56	0.05	0.34	n.d.	0.23	0.01	0.76	0.56	0.02	0.07
Na₂O	1.55	3.79	3.91	3	5.03	3.56	5.47	0.32	0.82	0.23	1.42	0.38	2.23	1.51	0.1	1.03
K₂O	1.28	1.34	0.36	0.87	0.68	0.79	0.32	2.65	2.15	1.54	1.42	1.57	1.47	1.25	0.91	1.34
P₂O₅	0.09	0.21	0.15	0.17	0.15	0.27	0.13	0.12	0.18	0.04	0.06	0.04	0.21	0.07	0.06	0.05
LOI	1.78	1.58	6.08	2.43	1.08	0.96	2.18	2.26	2.47	2.59	2.14	1.79	3.37	1.25	0.24	1.61
Total:	98.96	99.55	99.97	99.87	99.43	100.26	99.20	99.93	100.11	100.52	99.94	98.05	100.23	95.78	99.91	98.84

Hbl: hornblende, Bt: biotite, Gn: gneiss, Sil: sillimanite, Crd: cordierite, Amph.: amphibolite and n.d.: Not detected.

Table C.2: Continued

Powder	AP5/14	AP5/15	AP5/16	AP5/17	AP5/18	AP5/19	AP5/20	AP5/21	AP5/22	AP5/23	AP5/24	AP5/25	AP5/26	AP5/27	AP5/28	AP5/29
Cl* (ppm)	130	131	13	15	78	8	8	15	18	8	8	8	8	8	8	17
Co	47	39	58	50	49	42	28	39	33	50	27	39	33	54	48	38
Cr	323	58	25	15	19	10	10	10	10	10	10	10	10	16	10	16
F*	100	100	100	100	567	100	1032	1438	945	1615	913	887	231	467	281	733
S*	16	404	16	16	16	381	637	1139	16	27647	16	16	92	247	16	16
Sc	41	11	41	34	36	19	11	18	16	13	9	13	18	23	12	12
V	241	136	279	325	343	6	1	31	12	1	6	1	27	174	1	1
As	3	3	5	3	3	3	3	4	3	3	3	3	3	3	4	4
Cu	5	28	2	8	2	22	9	57	3	137	2	3	3	16	2	2
Ga	11	15	25	19	17	17	16	14	14	19	12	16	15	24	21	10
Mo	1	1	1	1	1	1	1	21	3	1	1	2	1	1	1	1
Nb	2	7	2	4	2	5	6	6	8	5	6	5	5	6	4	3
Ni	106	39	24	6	15	5	3	3	3	3	3	3	4	7	3	9
Pb	8	6	13	31	5	6	49	3	3	3	3	3	29	3	3	15
Rb	74	61	29	52	30	25	70	63	46	31	31	36	37	24	17	43
Sr	264	477	56	142	132	158	28	9	29	9	48	8	66	52	6	30
Th	5	3	5	3	3	3	3	3	3	3	3	6	3	7	6	3
U	4	3	19	3	3	3	3	3	3	3	3	6	3	3	5	3
W*	75	133	32	116	116	339	279	184	213	362	210	355	147	237	500	377
Y	9	20	31	34	27	40	51	34	60	56	67	67	25	21	89	43
Zn	63	72	184	144	156	68	257	49	49	38	32	53	48	109	34	51
Zr	22	81	53	71	48	144	209	150	197	195	241	161	107	175	225	150
Ba	511	633	26	292	130	336	656	1423	1328	1474	881	1008	967	623	1115	659
La	28	34	35	33	39	29	8	5	7	14	6	13	17	28	14	5
Ce	11	35	23	18	12	28	37	39	39	25	46	29	22	62	54	40

*: Semi-quantitative analysis.

Table C.2: Continued

Fused	AP5/30	AP5/31	AP5/32	AP5/33	AP5/34	AP5/35	AP5/36	AP5/37	AP5/38	AP5/39	AP5/40	AP5/41	AP5/42	AP5/43	AP5/44	AP5/45	AP5/46
Depth (m)	318.9	322.7	326.8	336.8	335.7	334.2	331.3	328.4	327.4	339	338	341.4	343.7	344.7	349	354.8	360.1
Rock Name	Sil-Crd-Bt-Gn	Hbl-Schist	Sil-Crd-Gn	Amph.	Bt-Hbl Gn	Bt-Gn	Gneiss	Sil-Crd-Schist	Garnet-Hbl-Schist	Amph.	Bt-Hbl-Gneiss	Hbl-Gneiss	Garnet-Bt-Gn	Hbl-Garnet-Bt-Gneiss	Hbl-Gn	Hbl-Bt-Gn	Amph.
SiO ₂ (wt%)	73.05	53.1	71.03	51.14	60.7	68.26	74.38	66.37	55.85	49.57	51.69	56.38	73.83	59.51	70.5	69.61	46.85
TiO ₂	0.29	1.3	0.25	0.89	0.96	0.31	0.29	0.49	0.51	1.04	0.89	1.2	0.23	0.46	0.32	0.44	1.9
Al ₂ O ₃	11.64	13.92	11.84	14.62	14.12	13.05	11.23	12.74	15.31	14.56	14.63	13.8	12.32	12.43	12.12	12.67	13.44
Fe ₂ O ₃	6.36	18.78	7.69	14.64	11.88	6.28	4.92	8.91	10.59	15.08	14.09	13.34	4.23	10.17	5.86	6.47	17.02
MnO	0.09	0.23	0.11	0.29	0.36	0.15	0.11	0.16	0.22	0.34	0.4	0.33	0.17	0.24	0.14	0.16	0.26
Mg	3.99	8.86	4.7	4.65	1.39	1.92	0.5	4.88	5.89	4.54	4.55	2.4	0.41	2.39	0.91	1.26	7.1
CaO	n.d.	1.01	0.03	7.94	4.22	3.26	1.09	n.d.	4.99	8.2	7.37	6.12	1.73	7.09	2.22	3.66	10.12
Na ₂ O	0.49	0.9	0.35	4.22	4.56	4.36	5.52	0.33	2.92	3.87	3.9	4.31	4.83	2.54	4.15	3.12	1.82
K ₂ O	1.48	0.37	1.55	1.35	1.11	1.13	0.41	2.32	1.32	1.65	0.99	1.21	0.64	2.22	0.96	1.42	0.77
P ₂ O ₅	0.05	0.27	0.05	0.13	0.48	0.08	0.06	0.06	0.1	0.14	0.13	0.6	0.07	0.13	0.08	0.06	0.24
LOI	2.41	1.34	2.14	0.47	0.62	0.78	0.55	3.32	1.76	0.65	0.85	0.46	0.48	0.85	0.94	0.91	0.79
Total:	99.85	100.07	99.73	100.34	100.42	99.58	99.07	99.58	99.46	99.54	99.49	100.14	98.96	98.06	98.20	99.78	100.31

Hbl: hornblende, Bt: biotite, Gn: gneiss, Sil: sillimanite, Crd: cordierite, Amph.: amphibolite and n.d.: Not detected.

Table C.2: Continued

Powder	AP5/30	AP5/31	AP5/32	AP5/33	AP5/34	AP5/35	AP5/36	AP5/37	AP5/38	AP5/39	AP5/40	AP5/41	AP5/42	AP5/43	AP5/44	AP5/45	AP5/46
Cl* (ppm)	8	8	8	50	26	23	8	8	8	108	40	29	13	33	16	182	36
Co	40	60	38	61	43	35	34	35	46	60	57	45	30	44	36	39	68
Cr	10	15	10	19	10	18	10	10	52	23	18	10	10	17	10	12	143
F*	717	100	784	100	100	551	100	100	100	100	100	100	384	100	136	281	100
S*	1542	16	74	16	56	16	140	497	400	452	203	69	180	16	16	34	780
Sc	14	35	13	29	23	14	9	21	37	33	30	32	7	20	14	11	36
V	2	260	1	378	1	49	12	11	198	384	301	30	1	103	34	58	390
As	3	26	4	3	3	3	3	3	3	3	3	3	3	3	6	3	4
Cu	37	2	11	28	14	11	20	25	23	72	51	18	20	3	8	16	75
Ga	17	19	15	16	21	16	18	17	15	16	18	18	15	16	17	17	17
Mo	1	1	3	1	1	1	1	1	1	1	1	1	1	1	1	1	1
Nb	4	3	5	2	3	6	7	5	3	2	4	3	7	3	7	6	2
Ni	3	11	6	9	4	12	5	3	27	16	13	3	4	10	4	9	62
Pb	22	39	21	9	6	6	4	130	6	4	14	4	11	3	3	9	7
Rb	38	13	45	40	36	36	15	81	54	59	24	52	37	79	40	34	46
Sr	12	23	15	171	167	153	71	13	95	136	174	151	169	337	177	190	86
Th	5	3	3	3	3	5	3	4	3	3	5	3	5	3	3	4	3
U	3	3	3	3	3	4	3	3	3	3	3	3	3	3	3	3	3
W*	408	162	281	111	253	238	389	165	114	95	119	154	329	190	362	300	94
Y	61	29	49	22	45	55	82	46	27	25	40	36	53	35	57	65	36
Zn	101	96	92	99	151	95	54	181	111	105	129	114	99	96	90	125	170
Zr	187	80	203	43	80	232	241	201	71	47	68	55	167	76	180	200	72
Ba	751	237	705	325	535	604	157	959	1496	456	327	302	376	490	381	482	90
La	23	44	18	47	33	34	25	26	5	41	34	42	13	44	17	32	31
Ce	48	8	42	6	26	45	45	41	15	15	19	19	46	33	40	44	10

*: Semi-quantitative analysis.

Table C.3: XRF analytical results for samples from borehole AP2 (Areachap)

Fused	AP2/1	AP2/2	AP2/3	AP2/4	AP2/5	AP2/6	AP2/7	AP2/8	AP2/9	AP2/10	AP2/11	AP2/12	AP2/13	AP2/14	AP2/15	AP2/16	AP2/17
Depth (m)	62.2	71.2	74.4	81.2	82.5	87.1	91.1	92.2	92.5	105.7	106.3	97.8	91.1	92.6	118	113.2	112.2
Rock Name	Garnet-Schist	Amph.	Garnet-mica-Gn	Bt-Hbl-Gn	Bt-Gn	Hbl-Gn	Highly altered rock	Highly altered rock	Gossan Zone	Gossan Zone	Gossan Zone	Granite(?)	Granite(?)	Hbl-Bt-Gn	Gneiss	Gossan Zone	
SiO₂ (wt%)	62.72	33.98	54.41	62.63	76.33	46.63	53.46	45.83	48.82	72.14	73.63	49.75	54.31	77.66	53.15	53.22	39.43
TiO₂	0.61	0.62	0.97	0.63	0.05	1.07	0.96	0.53	0.64	0.25	0.05	0.04	0.04	0.03	2.05	1.49	1.64
Al₂O₃	15.52	12.3	16.75	15.84	13.38	17.31	15.58	17.91	20.45	11.63	12.89	10.03	9.07	12.87	14.37	12.27	14.25
Fe₂O₃	7.65	9.93	11.57	7.2	0.93	10.23	12.06	15.63	11.84	4.97	3.49	26.32	0.53	0.66	13.64	13.69	26.51
MnO	0.18	0.19	0.25	0.18	0.01	0.26	0.22	0.21	0.21	0.19	0.03	0.11	n.d.	0.01	0.24	0.3	0.33
MgO	2.86	3.77	4.11	2.82	0.08	7.51	4.13	6.93	5.85	3.51	1.07	2.29	n.d.	n.d.	4.83	5.71	6.34
CaO	1.28	6.29	3.1	1.03	0.59	4.37	5.69	0.7	0.95	0.29	n.d.	n.d.	0.02	n.d.	5.6	7.26	0.98
Na₂O	5.71	2.49	4.18	5.63	3.66	5.03	3.47	4.97	5.22	1.6	6.75	1.01	3.79	7.6	4.06	2.91	1.06
K₂O	0.8	0.77	1.53	1.06	4.92	0.76	1.22	0.73	1.33	2.43	0.03	4.98	2.26	0.12	0.54	0.57	2.87
P₂O₅	0.23	0.12	0.24	0.17	0.04	0.31	0.23	0.09	0.08	0.06	0.03	0.05	0.02	0.05	0.83	0.16	0.18
LOI	2.31	29.65	3.14	2.28	0.45	6.74	1.72	5.22	4.45	2.61	1.42	4.44	29.65	0.42	0.89	1.81	5.89
Total:	99.84	100.10	100.24	99.46	100.45	100.24	98.2	98.75	99.83	99.70	99.41	99.01	99.71	99.41	100.22	99.40	99.48

Hbl: hornblende, Bt: biotite, Gn: gneiss, Amph.: amphibolite and n.d.: Not detected.

Table C.3: Continued

Powder	AP2/1	AP2/2	AP2/3	AP2/4	AP2/5	AP2/6	AP2/7	AP2/8	AP2/9	AP2/10	AP2/11	AP2/12	AP2/13	AP2/14	AP2/15	AP2/16	AP2/17
Cl* (ppm)	36	8	40	45	27	8	8	8	40	33	47	39	30	41	50	38	8
Co	44	58	46	36	28	46	48	63	54	38	41	81	36	43	46	56	96
Cr	11	19	17	14	10	24	26	24	49	10	10	11	10	10	12	96	164
F*	100	100	100	100	432	100	100	100	100	100	462	108	485	431	100	100	100
S*	16	16	351	16	16	16	16	16	16	16	16	16	16	16	44	16	16
Sc	22	26	29	30	1	34	28	18	25	14	1	6	2	1	29	38	65
V	87	341	182	105	3	222	221	141	164	54	11	121	5	6	155	317	395
As	3	6	3	3	3	3	7	5	3	3	4	3	3	3	3	3	3
Cu	45	11	56	12	2	3	53	175	83	80	64	572	7	5	11	87	4
Ga	15	17	17	15	11	19	18	16	15	12	10	14	9	8	17	15	23
Mo	1	1	1	1	1	1	1	1	1	1	1	25	1	1	1	3	1
Nb	5	4	4	4	2	4	4	3	3	4	4	3	4	2	4	4	5
Ni	7	6	9	4	3	15	16	15	19	5	4	4	3	3	9	38	75
Pb	21	6	34	8	41	9	38	10	8	3	3	35	22	3	4	9	31
Rb	23	34	53	21	122	21	45	34	84	15	2	114	76	6	20	13	161
Sr	111	295	179	73	96	88	223	125	205	100	27	57	62	34	167	77	93
Th	8	3	3	3	43	6	3	20	3	5	28	17	25	48	3	3	3
U	5	3	3	12	5	9	3	10	8	8	4	23	3	7	3	3	40
W*	298	122	135	141	397	22	116	19	12	234	489	110	544	615	168	92	25
Y	23	18	30	15	47	15	26	39	8	13	17	24	13	49	43	36	45
Zn	236	109	165	280	211	247	83	5414	2409	2404	1558	5761	275	267	111	346	3026
Zr	85	39	88	60	14	51	64	78	23	72	58	11	10	86	84	98	84
Ba	339	357	857	354	234	194	588	273	242	34	5	694	272	5	155	96	538
La	22	19	24	11	13	18	39	52	30	14	10	18	5	5	47	46	66
Ce	37	25	38	28	55	31	28	41	17	39	10	10	18	30	33	25	88

*: Semi-quantitative analysis.

Table C.3: Continued

Fused	AP2/18	AP2/19	AP2/20	AP2/21	AP2/22	AP2/23	AP2/24	AP2/25	AP2/26	AP2/27
Depth (m)	112.4	111.7	108.7	107.5	120.1	124.1	122.1	141.1	153.7	165
Rock Name	Amph.	Hbl-Gn	Amph.	Amph.	Bt-Hbl-Gn	Bt-Gn	Hbl-Gn	Bt-Schist	Hbl-Gn	Amph.
SiO₂ (wt%)	52.01	46.95	47.62	47.07	69.81	70.85	53.67	62.46	56.44	50.27
TiO₂	1.34	1.85	1.01	0.85	0.44	0.42	1.05	0.83	0.57	0.81
Al₂O₃	13.56	14.02	17.42	18	11.88	12.32	15.22	12.47	14.99	14.64
Fe₂O₃	15.68	16.39	14.84	12.59	6.81	6.76	12.48	9.51	8.23	11.38
MnO	0.3	0.28	0.25	0.24	0.14	0.19	0.21	0.15	0.18	0.21
MgO	6.44	7.02	5.33	5.67	1.48	1.31	4.41	5.67	4.38	6.54
CaO	3.19	6.51	5.17	8.59	4.18	1.86	8.5	1.14	7.45	10.83
Na₂O	2.55	3.41	4.54	3.46	3.17	4.37	3.32	2.25	3.39	2.56
K₂O	0.8	0.9	1.07	1	0.56	0.95	0.63	3.63	1.67	0.78
P₂O₅	0.16	0.2	0.16	0.14	0.09	0.07	0.18	0.24	0.14	0.2
LOI	3.67	2.29	2.82	3.02	0.42	1.12	0.48	1.39	1.32	1.16
Total:	99.70	99.83	100.21	100.61	98.97	100.22	100.17	99.74	98.73	99.40

Hbl: hornblende, Bt: biotite, Gn: gneiss, Amph.: amphibolite and n.d.: Not detected.

Table C.3: Continued

Powder	AP2/18	AP2/19	AP2/20	AP2/21	AP2/22	AP2/23	AP2/24	AP2/25	AP2/26	AP2/27
Cl* (ppm)	8	30	15	42	8	8	8	14	77	70
Co	68	63	57	54	39	30	54	38	43	54
Cr	120	108	38	37	10	10	19	10	69	150
F*	100	100	100	100	110	1388	100	1196	100	1238
S*	16	16	16	16	216	16	43	16	132	313
Sc	48	51	38	28	9	18	27	30	19	27
V	266	379	313	299	82	42	311	95	201	300
As	3	4	3	4	4	3	3	3	7	3
Cu	10	5	5	6	17	2	25	4	21	44
Ga	17	19	15	16	14	18	17	18	14	15
Mo	1	1	1	1	1	1	1	3	1	1
Nb	6	5	3	3	3	6	2	7	5	3
Ni	55	55	24	25	3	6	8	5	28	50
Pb	13	8	6	3	7	9	4	7	6	3
Rb	34	32	50	52	22	30	15	314	93	24
Sr	77	97	186	194	145	68	157	45	252	257
Th	4	3	4	3	8	4	3	3	7	3
U	8	5	4	3	4	3	3	3	3	3
W*	64	55	45	44	311	205	173	82	188	173
Y	29	36	19	16	52	64	27	56	23	18
Zn	1228	622	293	229	99	155	90	133	65	86
Zr	100	96	29	28	168	230	66	157	55	39
Ba	224	209	196	140	146	368	72	288	432	122
La	41	53	37	41	18	25	19	32	19	22
Ce	35	18	17	20	45	40	20	54	33	26

*: Semi-quantitative analysis.

Table C.4: XRF analytical results from surface (Kantienpan).

Fused	KPR5/1	KPR5/2	KPR5/3	KPR5/4	KPR5/5
Depth (m)	Surface	Surface	Surface	Surface	Surface
Rock Name	Amph.	Bt-Crd-Gn	Crd-Sil-Bt-Gn	Amph.	Hbl-Gn to Amph.
SiO₂ (wt%)	46.05	48.31	73.26	47.15	53
TiO₂	0.7	0.82	0.21	0.66	0.53
Al₂O₃	14.27	20.56	12.89	12.81	14.45
Fe₂O₃	10.66	10.56	4	8.62	7.56
MnO	0.19	0.19	0.13	0.24	0.22
MgO	6.54	3.78	5.14	8.3	3.95
CaO	19.99	10.39	n.d.	20.51	17.72
Na₂O	1.32	3.33	0.34	0.96	1.97
K₂O	0.11	1.04	3.03	0.25	0.6
P₂O₅	0.09	0.24	0.04	0.09	0.13
LOI	0.61	1.21	1.02	0.56	0.56
Total:	100.54	100.42	100.06	100.16	100.70

Bt: biotite, Gn: gneiss, Sil: sillimanite, Crd: cordierite, Amph.: amphibolite and n.d.: Not detected.

Table C.4: Continued

Powder	KPR5/1	KPR5/2	KPR5/3	KPR5/4	KPR5/5
Cl* (ppm)	8	23	8	8	8
Co	47	35	30	45	39
Cr	273	10	10	614	173
F*	100	968	4094	100	100
S*	16	16	16	26	159
Sc	6	5	9	9	1
V	250	1	3	191	150
As	3	3	3	3	11
Cu	190	2	2	35	13
Ga	13	16	19	13	16
Mo	1	1	1	1	1
Nb	2	16	20	8	4
Ni	81	4	7	136	139
Pb	5	5	6	3	3
Rb	6	56	63	16	21
Sr	291	34	18	242	228
Th	4	13	11	3	3
U	3	3	3	3	3
W*	99	372	314	88	124
Y	12	14	27	34	18
Zn	77	69	140	69	82
Zr	24	302	297	35	61
Ba	350	1366	993	226	384
La	41	14	31	43	37
Ce	12	87	75	18	25

*: Semi-quantitative analysis.

Table C.5: XRF analytical results for samples from borehole KN12 (Kantienpan)

Fused	KN12/1	KN12/2	KN12/3	KN12/4	KN12/5	KN12/6	KN12/7	KN12/8	KN12/9	KN12/10	KN12/11	KN12/12	KN12/13	KN12/14
Depth (m)	175.68	179.78	188.27	190.12	194.67	203.23	209.93	216.76	221.15	228.83	233.67	239.8	253.95	250.62
Rock Name	Bt-Hbl-Gn	Amph.	Bt-Hbl-Gn	Amph.	Amph.	Amph.	Bt-Gn	Bt-Gn	Amph.	Amph.	Bt-Hbl-Gn	Bt-Gn	Amph.	Amph.
SiO₂ (wt%)	76.08	45.72	48.2	47.25	48.54	49.75	49.29	69.69	48.91	49.46	48.97	65.01	50.39	48.42
TiO₂	0.19	0.89	0.78	0.77	0.79	0.98	0.97	0.45	1.02	1.31	1.02	0.59	0.84	1.43
Al₂O₃	11.54	20.16	19.91	19.69	18.04	17.79	19.62	14.39	18.82	15.83	18.14	14.18	18.97	15
Fe₂O₃	5.04	11.4	11.37	12.61	11.42	12.38	10.65	5.12	13.05	14.59	12.3	7.15	10.12	16.24
MnO	0.09	0.24	0.18	0.18	0.18	0.16	0.21	0.1	0.27	0.28	0.19	0.23	0.2	0.36
MgO	2.47	3.44	4.62	3.75	5.51	4.39	4.01	0.64	3.96	5.08	5.61	1.75	4.47	4.98
CaO	0.01	14.17	9.09	10.61	8.17	7.41	8.3	3.71	6.67	8.67	4.92	3.43	8.45	8.2
Na₂O	0.57	2.01	3.66	3.37	3.92	3.91	4.06	3.82	3.68	3.88	4.52	4.68	4.6	3.23
K₂O	3.57	1.26	1.06	0.66	1.53	1.58	1.69	1.38	1.55	1.11	3	1.02	0.77	1.26
P₂O₅	0.04	0.27	0.27	0.21	0.24	0.33	0.29	0.14	0.26	0.45	0.23	0.21	0.22	0.34
LOI	0.27	0.4	1.34	0.36	0.51	1.07	0.46	0.38	0.00	0.00	0.75	0.1	0.23	0.58
Total:	99.86	99.95	100.46	99.47	98.87	99.76	99.56	99.83	97.94	100.64	99.65	98.37	99.26	100.03

Hbl: hornblende, Bt: biotite, Gn: gneiss, Amph.: amphibolite and n.d.: Not detected.

Table C.5: Continued

Powder	KN12/1	KN12/2	KN12/3	KN12/4	KN12/5	KN12/6	KN12/7	KN12/8	KN12/9	KN12/10	KN12/11	KN12/12	KN12/13	KN12/14
Cl* (ppm)	48	18	76	55	44	59	27	21	38	50	57	8	16	8
Co	49	44	49	48	49	49	45	29	49	52	50	31	56	41
Cr	28	32	41	41	55	34	27	10	24	30	27	10	21	26
F*	100	100	100	100	100	2867	994	1217	1415	100	100	100	398	100
S*	51	136	267	1380	72	733	76	535	81	645	391	282	236	42
Sc	13	8	22	16	23	26	20	15	26	30	27	18	37	23
V	251	264	253	227	247	279	292	19	301	420	348	27	430	267
As	3	5	4	4	3	3	3	3	3	3	3	3	4	3
Cu	47	42	54	359	3	59	7	71	7	69	3	6	66	2
Ga	19	20	18	19	15	20	20	16	23	21	17	16	20	16
Mo	1	1	1	1	1	1	2	1	1	1	1	1	1	1
Nb	4	3	4	4	5	5	6	6	4	4	3	4	5	3
Ni	18	21	23	26	29	18	19	3	16	11	15	3	6	5
Pb	6	8	5	7	6	11	11	7	7	19	4	8	6	14
Rb	23	30	27	12	37	63	61	36	55	22	82	9	51	18
Sr	586	400	560	567	444	213	324	161	133	366	284	191	359	327
Th	3	3	3	3	3	3	4	4	3	3	3	3	3	7
U	3	3	3	3	3	5	3	3	3	3	3	3	3	3
W*	152	118	80	120	90	78	81	285	108	81	71	242	81	93
Y	21	20	20	22	20	32	26	34	26	30	22	28	31	22
Zn	76	93	83	82	73	112	99	73	98	76	59	100	184	59
Zr	58	37	50	52	51	63	73	156	56	58	45	110	59	46
Ba	501	496	320	260	508	533	610	481	723	235	602	639	815	326
La	38	24	45	35	28	16	40	23	38	42	37	17	37	36
Ce	28	33	28	29	31	45	38	45	22	41	28	32	34	30

*: Semi-quantitative analysis.

Table C.5: Continued

Fused	KN12/15	KN12/16	KN12/17	KN12/18	KN12/19	KN12/20	KN12/21	KN12/22	KN12/23	KN12/24	KN12/25	KN12/28
Depth (m)	255.82	262.1	266.8	274.8	278.7	276.5	277.97	278.5	279.41	280.28	280.74	281.8
Rock Name	Garnet-Bt-Crd-Gn	Sil-Crd-Bt-Gn	Sil-Crd-Bt-Gn	Bt-Hbl-Gn	Crd-Bt-Gn	Hbl-Gn	Bt-Hbl-Gn	Ore Zone	Ore Zone	Ore Zone	Ore Zone	Bt-Crd-Gn
SiO₂ (wt%)	63.98	66.5	68.6	53.79	60.77	55.33	51.45	41.27	24.86	15.47	23.46	35.6
TiO₂	0.38	0.37	0.45	0.95	0.88	1.06	1.29	0.11	0.0642	132	340	0.16
Al₂O₃	14.95	13.62	13.86	16.54	15.9	14.84	15.16	3.74	5.83	1.36	3.43	10.37
Fe₂O₃	5.45	5.71	5.3	11.96	9.26	13.41	15.21	24.04	37.98	45.82	36.40	29.09
MnO	0.06	0.13	0.11	0.31	0.14	0.26	0.29	0.14	0.18	0.13	0.18	0.42
MgO	4.06	2.17	1.41	4.52	2.97	2.97	3.7	1.46	2.61	1.86	2.60	6.4
CaO	1.29	2.11	2.34	8.01	4.56	7.17	8.02	0.43	0.93	0.98	0.28	1.04
Na₂O	1.92	2.45	4.19	2.42	3.8	3.03	2.83	<10 ppm	<10 ppm	<10 ppm	<10 ppm	0.72
K₂O	3.28	3.48	1.52	0.77	0.91	0.39	0.42	663	0.20	154	680	1.31
P₂O₅	0.07	0.08	0.06	0.28	0.23	0.37	0.47	247	675	370	413	0.09
LOI	3.46	1.75	0.98	0.73	0.64	n.d.	0.09	n.a.	n.a.	n.a.	n.a.	9.84
Total:	98.91	98	98.83	100.30	100.08	98.84	98.92	94.19 **	96.10**	92.96**	91.20**	95.06

n.a.: not applicable, Hbl: hornblende; Bt: biotite; Gn: gneiss; Sil: sillimanite; Crd: cordierite, n.d.: Not detected and **: recalculated total for sulphide riched samples (S, Cu, Zn and Pb) based on the powder disc analysis.

Table C.5: Continued

Powder	KN12/15	KN12/16	KN12/17	KN12/18	KN12/19	KN12/20	KN12/21	KN12/22	KN12/23	KN12/24	KN12/25	KN12/27
Cl* (ppm)	8	8	8	14	8	48	45	8	8	8	8	13
Co	25	28	33	51	42	51	55	63	76	111	85	60
Cr	10	10	10	10	15	10	12	10	10	22	16	10
F*	2233	1074	1225	1699	932	539	319	3227	3604	3915	3061	3199
S*	14913	10252	4014	720	1048	643	1121	127976	145676	181278	158576	90645
Sc	19	19	17	19	24	25	26	2	1	1	2	7
V	8	26	4	158	159	157	228	17	9	5	5	15
As	3	3	3	3	3	3	3	3	3	3	7	6
Cu	142	11	18	26	13	91	483	3425	4319	5442	4749	15955
Ga	17	14	15	20	19	18	20	3	5	2	2	35
Mo	2	1	1	1	1	1	1	16	25	27	57	22
Nb	7	5	4	6	3	6	4	4	6	2	2	7
Ni	3	3	4	6	8	5	5	15	14	25	22	9
Pb	12	18	12	24	39	10	45	341	532	406	589	1079
Rb	76	66	26	23	35	7	12	4	12	3	3	60
Sr	130	141	228	218	247	357	351	7	22	21	4	57
Th	7	6	6	4	3	3	3	3	9	5	5	14
U	4	3	3	3	3	3	3	3	7	8	3	3
W*	220	222	346	330	273	340	272	322	168	279	242	147
Y	44	37	35	46	23	43	32	4	18	6	5	78
Zn	111	86	81	126	168	160	183	97306	83299	85577	90797	2313
Zr	168	142	139	120	121	91	65	58	41	10	25	136
Ba	578	1115	529	332	434	382	528	117	926	2175	235	4542
La	30	5	26	51	39	37	34	64	43	11	72	5
Ce	56	50	43	48	39	40	40	9	33	10	10	105

*: Semi-quantitative analysis

Table C.5: Continued

Fused	KN12/28	KN12/29	KN12/30	KN12/31	KN12/32	KN12/33	KN12/34	KN12/35	KN12/36	KN12/37	KN12/38	KN12/39
Depth (m)	283.32	285.32	287.25	290.80	292	291.29	292.65	293.03	293.80	295.10	297.20	299.10
Rock Name	Bt-Crd-Gn	Crd-Bt-Gn	Bt-garnet-Crd-Gn	Bt-Crd-Gn	Ore Zone	Ore Zone	Bt-Crd-Gn	Ore Zone	Crd-Bt-Gn	Garnet-Bt-Crd-Gn	Bt-Gn	Crd-Bt-Gn
SiO₂ (wt%)	78.31	78.49	79.18	68.86	34.92	56.65	73.74	33.38	62.6	71	70.64	69.07
TiO₂	0.07	0.09	0.09	0.08	0.15	0.12	0.11	0.37	0.3	0.37	0.41	0.37
Al₂O₃	8.03	8.09	7.34	14.26	8.51	7.17	10.37	16.8	11.89	13.26	13.89	13.3
Fe₂O₃	6.53	8.12	7.67	7.85	30.65	20.22	6.46	24.14	12.69	5.74	4.7	5.77
MnO	0.09	0.04	0.12	0.04	0.09	0.07	0.04	0.17	0.19	0.18	0.13	0.22
MgO	3.48	3.15	2.28	2.17	5.48	4.97	1.65	10.59	5.15	1.29	1.14	1.11
CaO	0.08	n.d.	0.08	0.64	0.26	0.09	1.64	0.64	2.63	2.55	4.11	3.27
Na₂O	0.13	0.1	0.12	1.57	0.13	0.13	1.63	0.21	1.48	3.54	3.54	3.32
K₂O	0.52	0.63	0.41	1.61	1.64	1.38	1.17	2.54	1.81	1.2	0.49	1.09
P₂O₅	0.02	0.02	0.02	0.02	0.01	0.02	0.03	0.03	0.05	0.06	0.12	0.09
LOI	2.01	0.99	0.92	2.75	16.77	8.81	2.8	9.43	1.01	0.51	0.37	0.75
Total:	99.27	99.73	98.25	99.85	98.63	99.66	99.63	98.31	99.80	99.68	99.54	98

Hbl: hornblende, Bt: biotite, Gn: gneiss, Crd: cordierite and n.d.: Not detected.

Table C.5: Continued

Powder	KN12/28	KN12/29	KN12/30	KN12/31	KN12/32	KN12/33	KN12/34	KN12/35	KN12/36	KN12/37	KN12/38	KN12/39
Cl* (ppm)	9	8	8	8	8	8	8	11	8	8	8	20
Co	43	45	52	40	74	69	44	55	48	38	34	41
Cr	10	10	10	10	10	10	10	34	11	10	10	10
F*	2011	2210	1175	1113	4573	4265	1339	5063	2657	524	497	212
S*	9667	1689	4873	20996	108778	51831	12360	47767	6250	450	153	1975
Sc	2	5	5	1	8	6	2	18	12	10	10	7
V	2	1	2	8	9	6	8	64	76	23	40	29
As	3	3	3	3	3	3	5	3	3	3	3	3
Cu	315	38	165	1849	4707	1529	626	2352	184	6	3	70
Ga	19	15	12	22	39	32	14	37	18	14	14	14
Mo	1	1	1	2	19	19	10	10	1	1	1	1
Nb	4	4	3	3	7	5	3	8	7	7	3	4
Ni	5	4	4	4	12	4	5	5	13	5	4	3
Pb	91	11	16	91	17	12	53	19	13	13	8	13
Rb	20	21	19	37	61	71	40	109	86	25	12	21
Sr	12	8	11	57	5	7	115	73	167	183	334	244
Th	3	4	5	3	3	3	4	12	6	5	6	9
U	3	3	3	3	3	3	3	7	3	3	3	3
W*	438	480	571	360	413	444	545	109	338	418	368	39
Y	13	23	44	7	6	15	31	50	36	37	19	32
Zn	280	113	87	322	1238	971	247	2586	211	230	67	99
Zr	124	133	117	211	137	130	201	336	143	157	152	146
Ba	1011	458	389	806	482	420	312	1166	585	585	516	727
La	5	24	26	7	42	37	19	47	41	19	28	18
Ce	23	22	24	24	6	6	37	66	49	65	45	47

*: Semi-quantitative analysis.

Table C.6: XRF analytical results for samples from borehole KN11 (Kantienpan).

Fused	KN11/1	KN11/2	KN11/3	KN11/4	KN11/5	KN11/6	KN11/7	KN11/8	KN11/9	KN11/10	KN11/11	KN11/12	KN11/13	KN11/14
Depth (m)	24.20	22.10	27.20	42.00	48.90	42.80	60.54	68.40	72.00	78.13	84.66	90.00	97.65	101.28
Rock Name	Granite	Bt-Crd-Gn	Bt-Crd-Gn	Amph.	Amph.	Gneiss	Crd-Bt-Gn	Amph.	Amph.	Amph.	Bt-Gn	Spotty Gneiss	Amph.	Amph.
SiO₂ (wt%)	67.12	65.88	68.06	48.44	49.03	72.2	71.24	50.23	46.57	51.74	63.04	61.18	50.2	51.6
TiO₂	0.46	0.37	0.31	1.05	1.01	0.43	0.4	1.21	1.18	1.13	1.02	1.02	1.19	1.27
Al₂O₃	14.96	13.51	13.91	17.27	16.95	12.43	13.48	17.09	16.86	15.72	15.01	15.05	15.97	15.36
Fe₂O₃	5.31	6.48	6.42	12.94	12.59	4.76	4.41	13.48	15.95	12.92	8.59	8.63	13.42	11.75
MnO	0.14	0.11	0.13	0.2	0.21	0.11	0.11	0.43	0.52	0.33	0.23	0.27	0.34	0.38
MgO	2.52	1.87	2.18	4.97	4.37	0.66	0.67	4.07	4.61	3.1	1.91	1.76	3.9	3.46
CaO	1.77	1.62	1.89	8.95	6.72	2.08	1.2	5.44	4.32	5.7	3.72	3.39	8.49	8.15
Na₂O	2.55	2.92	2.87	4.03	4.56	4.76	4.68	4.54	3.95	4.01	4.35	3.58	4.32	4.86
K₂O	3.55	3.87	2.3	0.9	1.96	1.06	3.33	1.41	2.55	1.06	1.75	3.79	1.02	0.72
P₂O₅	0.08	0.07	0.06	0.26	0.3	0.09	0.1	0.54	0.52	0.46	0.38	0.39	0.58	0.6
LOI	0.82	2.35	1.19	0.23	0.73	0.1	0.17	0.13	0.41	0.00	0.00	0.15	0.00	0.00
Total:	99.29	99.06	99.32	99.24	98.42	98.68	99.80	98.58	97.45	96.17	99.98	99.19	99.37	97.94

Hbl: hornblende, Bt: biotite, Gn: gneiss, Crd: cordierite, Amph.: amphibolite and n.d.: Not detected.

Table C.6: Continued

Powder	KN11/1	KN11/2	KN11/3	KN11/4	KN11/5	KN11/6	KN11/7	KN11/8	KN11/9	KN11/10	KN11/11	KN11/12	KN11/13	KN11/14
Cl* (ppm)	8	13	8	21	16	8	8	29	8	60	10	8	15	8
Co	37	31	34	52	47	37	36	46	50	46	34	36	46	44
Cr	10	10	10	45	40	10	10	10	11	10	10	10	15	17
F*	504	626	1316	100	906	100	223	695	1738	787	249	274	296	100
S*	3121	8500	12305	107	200	545	365	163	5243	1368	838	4615	25	2160
Sc	17	20	12	22	17	11	12	26	30	27	18	19	17	22
V	19	26	21	329	304	1	1	149	197	134	42	33	252	248
As	3	3	3	3	3	3	3	3	3	3	3	3	4	3
Cu	5	64	14	84	28	159	24	24	1114	94	33	98	2	99
Ga	15	15	16	17	17	14	14	22	21	21	17	18	19	20
Mo	1	2	1	1	1	1	6	2	7	10	1	1	1	1
Nb	5	5	4	4	5	5	4	4	4	5	6	6	3	6
Ni	4	4	5	23	23	3	5	4	5	3	4	4	5	6
Pb	6	36	16	3	3	3	5	22	72	9	12	26	7	9
Rb	49	65	37	10	43	4	35	33	65	26	20	43	16	4
Sr	125	168	122	245	289	231	132	303	170	150	149	146	175	249
Th	4	11	8	3	3	6	6	3	4	3	4	3	3	3
U	3	4	4	4	3	3	3	3	4	3	3	3	3	3
W*	396	224	284	115	68	447	470	123	66	134	199	221	109	47
Y	37	41	39	23	22	27	50	38	31	36	38	24	35	42
Zn	75	103	108	81	70	54	46	370	472	297	202	149	140	208
Zr	143	154	158	46	49	175	183	85	77	81	158	141	61	23
Ba	1106	1079	954	315	630	373	960	730	775	882	842	1574	427	291
La	5	15	5	40	35	21	11	37	37	22	35	5	34	46
Ce	44	52	50	35	30	43	61	38	34	28	50	33	38	32

*: Semi-quantitative analysis.

Table C.6: Continued

Fused	KN11/15	KN11/16	KN11/17	KN11/18	KN11/19	KN11/20	KN11/21	KN11/22	KN11/23	KN11/24	KN11/25	KN11/26
Depth (m)	108.25	112.48	120.05	126.10	130.20	136.80	142.70	149.55	154.43	159.60	165.66	172.20
Rock Name	Gneiss	Amph.	Amph.	Bt-Hbl-Gn	Spotty Gneiss	Bt-Gn	Bt-Gn	Bt-Gn	Bt-Hbl-Gn	Bt-Hbl-Gn	Sil-Crd-Bt-Gn	Crd-Gn
SiO₂ (wt%)	69.47	50.32	47.7	49.42	72.92	73.2	72.5	72.24	47.61	49.88	64.71	68.22
TiO₂	0.73	0.8	1	0.76	0.33	0.47	0.47	0.21	0.81	0.71	0.46	0.35
Al₂O₃	12.48	19.47	17.4	18.74	12.69	12.72	13.97	12.8	17.9	18.14	14.15	14.29
Fe₂O₃	6.56	10.22	13.11	10.63	4.07	4.59	2.91	1.78	11.83	11.2	5.53	5.92
MnO	0.2	0.32	0.37	0.27	0.1	0.12	0.07	0.04	0.29	0.21	0.05	0.18
MgO	1.56	3.89	5.4	4.04	0.63	0.83	0.67	0.33	6.08	5.11	1.4	1.69
CaO	4.22	7.48	6.66	7.42	1.07	2.46	1.53	1.33	7.45	8.62	1.14	1.65
Na₂O	3.61	4.49	4.05	4.78	4.75	4.35	4.49	3.12	3.53	4.29	2.37	2.24
K₂O	0.62	1.91	1.93	1.46	2.59	0.91	2.7	5.45	2.08	0.94	3.01	2.75
P₂O₅	0.28	0.2	0.25	0.15	0.03	0.11	0.05	0.07	0.21	0.18	0.05	0.06
LOI	0.26	0.48	0.51	0.54	0.21	0.23	0.26	0.7	1.15	0.61	3.15	1.85
Total:	99.98	99.59	98.37	98.22	99.42	100.01	99.64	98.08	98.94	99.90	96.04	99.18

Hbl: hornblende, Bt: biotite, Gn: gneiss, Sil: sillimanite, Crd: cordierite, Amph.: amphibolite and n.d.: Not detected.

Table C.6: Continued

Powder	KN11/15	KN11/16	KN11/17	KN11/18	KN11/19	KN11/20	KN11/21	KN11/22	KN11/23	KN11/24	KN11/25	KN11/26
Cl* (ppm)	18	31	36	16	8	9	8	55	159	98	8	8
Co	37	43	50	43	31	37	27	27	50	48	29	36
Cr	10	28	30	34	10	10	10	10	52	46	10	10
F*	100	380	100	100	100	100	1086	579	100	100	305	359
S*	1591	24	1239	831	292	140	16	16	173	140	18678	13916
Sc	9	19	28	21	13	11	11	1	22	22	9	10
V	47	261	287	269	7	7	2	18	287	278	3	22
As	3	3	3	3	3	3	3	3	3	3	3	3
Cu	70	2	152	124	11	45	4	2	161	197	9	17
Ga	13	19	18	18	13	14	13	12	18	17	17	14
Mo	1	1	1	1	18	1	1	1	1	1	1	2
Nb	4	3	4	3	5	6	6	7	5	3	7	7
Ni	4	14	12	15	3	4	4	4	25	23	5	4
Pb	14	73	86	30	9	5	12	32	13	11	25	26
Rb	10	39	51	33	24	9	45	137	53	17	46	37
Sr	146	219	271	335	107	232	140	144	314	202	128	119
Th	5	3	3	4	7	5	7	20	3	3	6	4
U	3	3	3	3	3	3	3	6	3	3	3	3
W*	348	91	66	78	397	456	300	312	77	99	302	325
Y	23	19	23	19	43	31	33	25	18	15	41	40
Zn	115	296	223	126	51	60	41	40	115	77	92	100
Zr	108	46	54	47	195	165	189	152	44	38	163	145
Ba	495	956	769	700	706	485	676	1113	633	256	569	1044
La	20	23	37	43	21	16	22	20	43	43	22	23
Ce	28	24	33	21	61	46	66	83	37	22	56	49

*: Semi-quantitative analysis.

Table C.6: Continued

Fused	KN11/27	KN11/28	KN11/29	KN11/30	KN11/31	KN11/32	KN11/33	KN11/34	KN11/35	KN11/36
Depth (m)	175.80	182.40	188.32	195.35	196.84	198.80	205	206.57	206.95	208.25
Rock Name	Crd-Bt-Gn	Crd-Bt-Gn	Bt-Gn	Bt-Hbl-Gn	Bt-Hbl-Gn	Hbl-Gn to Amph.	Bt-Sil-Crd-Gn	Bt-Garnet-Crd-Gn	Ore Zone	Ore Zone
SiO₂ (wt%)	67.84	66.73	61.96	51.34	45.23	48.81	85.96	59.71	14.00	13.15
TiO₂	0.37	0.44	0.5	0.81	1.24	1.45	0.08	0.05	0.03	0.01
Al₂O₃	14.24	14.19	16.5	18.43	17.05	14.95	3.91	12.01	4.38	1.30
Fe₂O₃	5.77	6.12	8.37	9.87	15.35	16.32	3.95	9.87	35.67	43.24
MnO	0.16	0.1	0.21	0.25	0.28	0.28	0.06	0.13	0.28	0.19
MgO	2.74	1.48	1.94	3.75	5.26	4.34	1.72	1.99	3.18	2.82
CaO	2.02	1.4	5.65	8.39	11.94	9.31	0.05	3.26	2.98	0.90
Na₂O	2.52	3.21	2.61	3.91	2.01	2.81	0.17	0.78	n.d.	n.d.
K₂O	3.07	2.8	1.35	0.82	0.39	0.36	0.4	0.64	0.28	0.10
P₂O₅	0.08	0.09	0.14	0.24	0.22	0.31	0.03	0.062	0.04	0.04
LOI	1.25	2.46	0.7	1.69	0.65	0.55	1.87	n.a.	n.a.	n.a.
Total:	100.04	99.03	99.93	99.51	99.64	99.47	98.23	94.73 **	92.50 **	89.95 **

n.a.: not applicable; Hbl: hornblende; Bt: biotite; Gn: gneiss; Sil: sillimanite; Crd: cordierite, n.d.: Not detected, **: recalculated total for sulfide riched samples (S, Cu, Zn and Pb) based on the powder disc analysis and Amph.: amphibolite.

Table C.6: Continued

Powder	KN11/27	KN11/28	KN11/29	KN11/30	KN11/31	KN11/32	KN11/33	KN11/34	KN11/35	KN11/36
Cl* (ppm)	19	68	96	89	53	64	14	8	8	9
Co	33	29	39	39	56	54	41	64	93	97
Cr	10	10	19	40	41	26	10	10	17	10
F*	1047	393	1500	2049	100	272	1214	524	2506	4081
S*	8408	10108	1140	4602	1076	733	8384	52269	163606	159185
Sc	17	18	23	30	25	33	2	1	1	1
V	27	8	125	284	490	458	2	1	7	5
As	7	3	3	6	3	10	3	3	3	3
Cu	8	12	22	72	284	185	235	1461	9470	6724
Ga	15	15	17	21	20	19	10	34	2	2
Mo	1	1	1	1	1	1	1	1	13	62
Nb	5	5	5	8	3	3	2	4	3	3
Ni	5	3	11	14	16	8	3	7	27	21
Pb	20	31	23	182	27	12	233	1509	447	673
Rb	53	38	55	24	20	9	13	12	17	11
Sr	136	194	90	345	479	414	23	119	40	56
Th	7	3	6	5	3	3	3	13	11	3
U	3	3	4	6	3	3	3	3	8	5
W*	307	253	233	135	158	133	519	327	195	163
Y	37	45	29	32	19	26	23	40	13	6
Zn	113	82	128	262	200	189	214	7023	143196	113388
Zr	137	156	81	49	35	50	51	107	44	12
Ba	902	887	512	312	117	221	2260	3859	1328	2311
La	14	15	24	27	33	51	5	5	37	6
Ce	47	58	43	31	24	25	33	37	17	6

*: Semi-quantitative analysis.

Table C.6: Continued

Fused	KN11/37	KN11/38	KN11/39	KN11/40	KN11/41	KN11/42	KN11/43	KN11/44	KN11/45	KN11/46	KN11/47	KN11/48	KN11/49
Depth (m)	209.2	210.66	212.16	216.23	217.73	217.8	218.19	226.69	224.06	231.18	229.29	237.65	239.33
Rock Name	Ore Zone	Garnet-Bt-Crd-Gn	Bt-Crd-Gn	Bt-Crd-Gn	Sil-Bt-Crd-Gn	Sil-Crd-Bt-Gn	Sil-Bt-Crd-Gn	Sil-Bt-Gn	Amph.	Bt-Gn	Gneiss to granulite	Bt-Gn	Bt-Gn
SiO₂ (wt%)	13.66	78.43	76.69	75.12	75.22	75.86	79.52	68.55	44.7	70.72	67.15	56.57	65
TiO₂	0.02	0.09	0.09	0.12	0.13	0.13	0.09	0.36	0.86	0.36	0.57	0.55	0.47
Al₂O₃	1.42	8.85	9.33	9.67	10.77	10.56	7.47	11.19	19.15	12.94	15.1	16.42	13.47
Fe₂O₃	40.56	7.86	7.85	8.26	8.04	7.77	7.62	7.34	12.94	4.76	5.7	8.15	10.78
MnO	0.18	0.1	0.06	0.12	0.06	0.09	0.08	0.21	0.32	0.12	0.13	0.14	0.19
MgO	2.00	2.81	3.6	4.11	2.97	2.83	2.72	4.25	5.64	0.98	1.44	3.87	1.51
CaO	0.27	n.d.	n.d.	0.04	n.d.	n.d.	0.02	2.84	11.62	3.19	3.95	9.32	2.51
Na₂O	n.d.	0.13	0.13	0.16	0.18	0.26	0.23	2.16	2.16	3.62	3.66	2.78	3.36
K₂O	0.07	0.58	0.8	1.16	1.17	1.17	0.85	1.39	0.21	0.64	1.28	0.41	1.68
P₂O₅	0.03	0.02	0.02	0.03	0.02	0.03	0.02	0.05	0.24	0.08	0.15	0.19	0.07
LOI	n.a.	0.75	0.99	1.34	0.87	1.19	1.2	0.47	0.43	0.86	0.38	0.27	0.37
Total:	90.03 **	99.62	99.60	100.11	99.44	99.89	99.84	98.83	98.29	98.28	99.53	98.68	99.42

n.a.: not applicable; Hbl: hornblende; Bt: biotite; Gn: gneiss; Sil: sillimanite; Crd: cordierite, n.d.: Not detected, **: recalculated total for sulfide riched samples (S, Cu, Zn and Pb) based on the powder disc analysis and Amph.: amphibolite

Table C.6: Continued

Powder	KN11/37	KN11/38	KN11/39	KN11/40	KN11/41	KN11/42	KN11/43	KN11/44	KN11/45	KN11/46	KN11/47	KN11/48	KN11/49
Cl* (ppm)	8	214	279	247	254	416	286	296	247	257	408	135	211
Co	99	52	46	45	43	46	44	41	49	33	34	40	43
Cr	10	10	10	10	10	10	10	10	54	10	10	31	10
F*	3488	928	2131	3209	2001	1990	1687	2228	832	460	1465	401	354
S*	165953	3476	4959	4853	1272	6230	9094	430	1146	383	427	16	811
Sc	1	7	4	5	6	5	4	12	22	13	16	17	10
V	6	1	1	1	1	1	1	57	280	25	23	155	43
As	3	3	4	3	3	3	3	3	3	3	3	3	3
Cu	6885	192	54	71	39	141	274	10	45	15	19	8	21
Ga	2	17	17	16	16	16	14	15	19	12	16	15	15
Mo	54	1	1	1	1	1	1	1	1	1	1	1	1
Nb	4	4	4	5	4	4	3	17	3	4	5	2	4
Ni	15	3	4	4	3	4	3	9	27	4	4	19	4
Pb	634	3	12	3	8	10	11	5	13	8	11	7	5
Rb	5	16	24	35	28	31	23	38	9	14	30	5	23
Sr	4	10	13	13	13	11	18	142	428	274	226	365	259
Th	3	3	4	3	4	5	7	16	3	5	5	3	7
U	3	3	3	3	3	3	3	3	3	3	3	3	3
W*	157	585	486	398	388	435	421	308	143	307	275	184	318
Y	4	52	18	30	18	23	17	34	22	31	38	18	29
Zn	144803	111	85	263	133	903	111	125	226	51	74	50	118
Zr	15	143	135	161	173	169	118	185	35	147	134	63	175
Ba	31	1036	2940	494	714	944	1037	1048	86	291	884	255	1232
La	55	9	5	24	16	10	5	35	50	26	13	37	36
Ce	6	12	15	22	26	30	21	115	25	26	45	24	53

*: Semi-quantitative analysis.

Appendix D

Analytical methods and results of regolith analyses

D.1. Regolith samples

These samples were collected from the sand cover that was deposited by the wind, commonly referred to as the Kalahari sand. The sand samples were sieved to identify the best size fraction with the highest element content. For this, a few samples from within and outside of the assumed secondary dispersion haloes of the deposit were selected and sieved into five fractions:

- 1) -710 to +180 micron.
- 2) -180 to +125 micron.
- 3) -125 to +75 micron.
- 4) -75 to +45 micron; and
- 5) -45 micron.

Different extractions were prepared using ammonium nitrate (NH_4NO_3), ammonium acetate (NH_4OAC), ethylene diamine tetraacetic acid (NH_4EDTA) and calcium hydro phosphate ($\text{Ca}(\text{H}_2\text{PO}_4)_2$) before analyzing the solutions by Inductively Coupled Plasma Mass Spectrometry (ICP-MS) for the elements of interest including Cu, Zn, Pb, Cd, Mn, Fe, Ba and S.

D.1.1. NH₄NO₃ extraction

A 0.2 M NH₄NO₃ solution is used to remove weakly bound elements of interest from the sand particles. 50 ml of this solution is added to a small plastic container (100 ml), with 5 grams of the sand sample. The container is shaken for 30-minutes in a mechanical shaker. Two blank samples, comprising a plastic container with 50 ml of the 0.2 M NH₄NO₃ solution, were also shaken for 30-minutes. The blank samples are analyzed to determine the abundance of the elements of interest in the reagents.

The suspension was then poured into a centrifuging tube to separate the solid part of the sample. The solution is for analysis. The results of the ICP-MS analysis of these samples are given in Table D.1. Duplicate samples were also analyzed and later used for statistical analysis. Based on this table, most of the elements, except Ba and Mn, have very high blank contents. The finest sample fraction analyzed (-75 μ) shows the highest contents of the elements of interest. The -45 μ size fraction was analyzed for a limited number of samples, but as inadequate quantities of this fraction was available for most of the samples, it was decided to base the interpretation of the data on the -75 μ grain size fraction. When the samples from within (KP12/13) and outside (KP12/2) the assumed geochemical halo are compared to each other, samples from within the halo returned higher concentrations of the elements of interest.

The results of statistical validation exercises (regression and correlation procedures) for duplicated samples are summarized in Table D.2. The slope of the regression line between the duplicate analyses is close to one for only Ba and Mn where the null hypothesis ($H_0=0$) that the slope is equal to null may be rejected (probability values < 0.0001). Inaccuracy in the intercept is probably caused by the small number of duplicate pairs. However, inspection of the data reveals that the repeatability of both high and low concentrations is poor. In general, this is confirmed by the strong correlation coefficients determined for Ba and Mn. The results of Cu, Zn, Pb, Cd and Fe are rejected due to the high blank values for these elements and the poor repeatability of the determinations.

Table D.1: ICP-MS analytical results of wind blown sand samples (5 gram sample + 50 ml of 0.2 M NH₄NO₃ solution, 30minute shacking times)

Location	Sample No	Fraction (μ)	Cu (ppb)	Zn (ppb)	Pb (ppb)	Ba (ppb)	Mn (ppb)	Fe (ppb)	Cd (ppb)	T (°C) ¹ Extraxt.	pH ¹ Extract.	T (°C) ² solution	pH ² solution
Outside the halo	T2/290N From Areachap	-710 to +180	180 161	609 676	203 163	5518 5971	1291 1600	800 900	66 126	21.9 23.8	4.63 4.91	22.3 24.7	5.2 5
		-180 to +125	165 155	626 690	195 166	7638 10705	1283 2040	700 900	63 98	22 23.8	5.2 4.91	22.3 24.7	5 5.1
		-125 to +75	162 160	552 679	173 159	9861 7536	1637 1741	700 550	65 102	22 23.8	5.2 4.91	22.3 24.8	5.33 5.1
		-75 to +45	183 184	643 904	171 170	14897 16036	2642 3081	700 900	82 102	22 23.8	5.2 4.91	22.3 24.6	5.38 5.1
		-45	251 183	1085 651	186 169	21077 21646	7194 8453	740 800	91 128	22 23.8	5.2 4.91	22.3 24.7	5.27 5.2
		-710 to +180	158 141	401 519	174 177	5212 4913	1100 884	700 700	87 141	21.9 23.8	4.6 4.9	22 22.4	6.1 6.2
		-180 to +125	189 132	602 282	165 164	6766 6616	723 697	700 700	70 115	21.9 23.8	4.6 4.9	22 24.7	6.1 6.2
Outside the halo	KP12/2 From Kantienpan	-125 to +75	144 136	501 569	167 159	9019 9457	996 948	800 700	88 136	22 23.8	5.2 4.9	22.4 24.6	6.4 6.3
		-75 to +45	125 156	379 869	167 161	12903 13606	925 1071	700 120	75 108	22 23.8	5.2 4.9	22.5 24.6	6.7 6.5
		-45	130 144	221 286	163 173	15885 17683	1276 1452	700 700	82 131	22 23.8	5.2 4.9	22.7 24.7	7 6.9
		-710 to +180	231 166	1127 547	202 168	8075 8741	2274 1213	900 700	92 160	22 23.8	5.2 4.9	23.5 24.6	5.8 5.9
		-180 to +125	245 136	1282 447	202 166	11045 11561	2219 90.30	900 600	114 133	22 23.8	5.2 4.9	23.5 24.6	5.9 5.9
		-125 to +75	296 143	1629 424	201 168	14083 15050	2557 1089	1000 700	101 162	22 23.8	5.2 4.9	23.5 24.7	6 6
		-75 to +45	188 368	939 1838	172 218	17346 17907	1649 3709	700 900	84 120	24.1 23.8	5 4.9	24.4 24.5	6.1 5.3
		-45	159 149	702 524	168 174	22252 24030	3576 3105	700 700	104 127	24.1 23.8	5 4.9	24.1 24.7	6 6.3
Background	Blank		183 117	922 501	173 176	215 296	507 311	600 700	135 110	23.8 23.8	4.91 4.91	24.9 24.8	5.11 4.95

1. The temperature and pH of NH₄NO₃

2. The temperature and pH of the solution at the end of shacking time

Table D.2: Results of statistical analysis on duplicate samples and the null hypothesis ($0.2\text{ M NH}_4\text{NO}_3$ solution, 30 min shacking time, $n=16$)

Elements	Slope	$H_0=0$ ($\text{Pr}> t $)	Intercept	$H_0=0$ ($\text{Pr}> t $)	Correlation coefficient
Cu	0.02	0.9278	747	0.0025	0.05
Zn	0.04	0.8630	180	0.0003	0.02
Pb	-0.19	0.5236	213	0.0008	-0.17
Ba	0.92	<0.0001	363	0.5316	0.99
Mn	0.73	<0.0001	513	0.0823	0.89
Fe	-0.01	0.7858	1281	0.0476	-0.07
Cd	0.34	0.2045	45	0.1766	0.34

D.1.2. NH_4OAC extraction

The second solution tested for its ability to remove weakly-bound cations of the elements of interest from the sand, is $1\text{ M NH}_4\text{OAC}$ solution. For this, 45 ml of this solution is added to a plastic container with 2.5 grams of the sand sample. This container is shaken for 30, 60 and 120-minutes. Two blank samples, contain only the reagents, were also shaken for 120-minutes as references samples.

The results of ICP-MS analyses of these samples and their duplicates are given in Table D.3. Again, Ba and Mn are concentration show the lowest contents in the reagents. The finest sample fraction (-75μ) returned the highest contents, and samples from within the halo have higher element concentrations.

The statistical validation for duplicate samples is summarized in Table D.4. The slope of the regression line between the duplicate analyses is close to one for Ba and Mn. Inaccuracy in the intercept is probably caused by the small number of duplicate pairs. The null hypothesis ($H_0=0$) that the slope equal to null is only rejected for Ba and Mn, (probability values < 0.0001). This is confirmed by the high correlation coefficients determined for Ba and Mn.

Inspection of the data reveals that the repeatability of both low and high concentrations is poor.

Table D.3: ICP-MS analytical results of sand samples (2.5 gram sample + 45 ml of 1 M NH₄OAC solution, different shacking times)

<75-45μ fraction											
Location	Sample No	Shacking Time	Cu (ppb)	Zn (ppb)	Pb (ppb)	Ba (ppb)	Mn (ppb)	pH ¹ of Extract	T (°C) ¹	pH ² of Solution	T (°C) ²
Outside the halo	T2/290N	30	351	752	56	19721	2912	7.2	22.3	7.2	22
			313	787	74	20772	3395	7.2	22.3	7.2	22
		60	304	590	54	21181	3470	7.2	22.3	7.2	22.1
			517	1264	63	21807	4750	7.2	22.3	7.1	22.3
		120	308	479	77	24457	3517	7.2	22.3	7.2	22.4
			297	760	31	21058	3710	7.2	22.3	7.3	22.3
Inside the halo	KP12/14	30	320	846	50	39704	3474	7.2	22.3	7.2	21.6
			329	1008	76	38954	4140	7.2	22.3	7.2	21.9
		68	356	972	68	40115	4262	7.2	22.3	7.21	21.9
			342	630	68	41584	4349	7.2	22.3	7.21	21.8
		125	432	1494	97	41260	4106	7.2	22.3	7.1	22.2
			326	792	13	40099	4455	7.2	22.3	7.2	21.7
<710-180 μ fraction											
Outside the halo	T2/290N	30	265	918	65	6991	1546	7.2	22.3	7	21.9
			257	504	45	8383	1624	7.2	22.3	7.2	21.9
		60	236	486	22	6228	1562	7.2	22.3	7.2	21.8
			245	612	65	6561	1823	7.2	22.3	7.1	22.1
		120	241	342	70	6926	1991	7.2	22.3	7.2	22.2
			265	1044	38	6755	1867	7.2	22.3	7.1	22.3
Inside the halo	KP12/14	30	241	378	94	11844	1472	7.2	22.3	7.2	21.5
			254	774	79	12033	1561	7.2	22.3	7.2	21.7
		68	263	594	112	13057	3706	7.2	22.3	7.2	21.7
			319	1602	97	12524	3274	7.2	22.3	7.2	21.7
		125	277	810	135	12874	2106	7.2	22.3	7.2	21.9
			274	522	83	11930	1908	7.2	22.3	7.2	22.9
Background	Blank	120	265	918	65	6991	1546	7.2	22.3	7	21.9
			257	504	45	8383	1624	7.2	22.3	7.2	21.9

1. The temperature and pH of NH₄OAC

2. The temperature and pH of the solution at the end of shacking time

Table D.4: Results of statistical analysis on duplicate samples and null hypothesis ($1\text{ M NH}_4\text{OAC}$ solution, different shaking time, $n=13$)

Elements	Slope	$H_0=0$ ($\text{Pr}> t $)	Intercept	$H_0=0$ ($\text{Pr}> t $)	Correlation coefficient
Cu	0.32	0.1754	198	0.0159	-0.30
Zn	-0.29	0.3221	975	0.0022	0.40
Pb	0.20	0.6006	62	0.0215	0.16
Ba	1.01	<0.0001	-267	0.7167	0.99
Mn	0.80	<0.0001	362	0.2102	0.94

Using different shaking times for extracting the cations of interest did not result in any meaningful improvement of the results.

D.1.3. NH_4EDTA extraction

A $0.02\text{ M NH}_4\text{EDTA}$ solution may also be used to remove weakly bound cations of the elements of interest from the finest parts of sand (here -75μ). 50 ml of this solution was added to a plastic container, with 2 grams of the sand sample. These different duplicates were shaken for 30, 60, 120 and 240-minutes. Two blank samples, with 50 ml of $0.02\text{ M NH}_4\text{EDTA}$ solution, were also shaken for 240-minutes.

The solution was analyzed by ICP-MS (Table D.5). The blank $0.02\text{ M NH}_4\text{EDTA}$ solution contains low contents of Cu, Zn, Pb, Mn and Ba (see the blank sample contents in Table D.5). Samples from within the halo (KP12/13) have significantly higher element contents than the samples from outside the halo (KP12/2).

The results of the statistical validation are summarized in Table D.6. The slopes of the regression lines between duplicate analyses are in all cases close to one. The hypothesis that there is no correlation can be rejected with probability values of less than 0.0005. This is confirmed by the high correlation coefficients. Inaccuracy in the intercept is probably caused by the small number of duplicate pairs. Inspection of the data reveals that the repeatability of high concentrations is poorer than that of lower concentrations. The numbers of duplicate pairs are too small to infer anything from the differences between the elements.

Table D.5: ICP-MS analytical results of sand samples (2 gram sample + 50 ml of 0.02 M NH₄EDTA solution, different shacking times)

<75-45μ fraction												
Location	Sample No	Shacking Time	Cu (ppb)	Zn (ppb)	Pb (ppb)	Ba (ppb)	Mn (ppb)	pH¹	T (°C)¹	pH²	T (°C)²	
Outside the halo	KP12/2	30	2270	3858	1770	19840	65913	4.49	22.4	4.14	22.6	
			2833	4200	1965	18535	58348	4.49	22.4	4.16	24.3	
		75	2570	3748	1843	21578	66305	4.49	22.4	4.16	22.9	
			2690	4675	2450	19495	54878	4.49	22.4	4.12	24.4	
		125	2955	4588	2530	24248	71298	4.49	22.4	4.16	22.8	
			2848	4468	2350	20380	55583	4.49	22.4	4.18	24.6	
		240	3145	4845	2908	23175	54425	4.49	22.4	4.2	23	
			3230	6180	2863	21970	55153	4.49	22.4	4.24	24.5	
Inside the halo	KP12/13	30	3853	6023	3923	32665	68833	4.5	24	4.11	24.4	
			4553	6160	4505	34830	79068	4.5	24	4.13	24.8	
		60	4103	6225	4805	34370	74235	4.5	24	4.11	24.6	
			4703	6395	5135	34420	79970	4.5	24	4.15	24.5	
		120	5390	8563	4813	34355	86328	4.5	24	4.11	24.9	
			4825	7625	5355	34900	81153	4.5	24	4.11	24.9	
		180	6758	8743	7255	43313	97883	4.5	24	4.17	24.4	
			5100	7175	5735	36488	79765	4.5	24	4.18	24.3	
Background	Blank	240	439	1645	175	618	2148	4.49	22.4	4.5	24.9	
			361	1839	163	410	1046	4.49	22.4	4.5	25.1	

1. The temperature and pH of NH₄EDTA

2. The temperature and pH of the solution at the end of shacking time

Table D.6: Results of statistical analysis on duplicate samples and null hypothesis ($1\text{ M NH}_4\text{EDTA}$ solution, different shaking time, $n=9$)

Elements	Slope	$H_0=0$ ($\text{Pr} > t $)	Intercept	$H_0=0$ ($\text{Pr} > t $)	Correlation coefficient
Cu	1.12	0.0004	-366	0.5971	0.94
Zn	1.20	0.0002	-1150	0.2674	0.92
Pb	1.07	<0.0001	-280	0.5906	0.95
Ba	1.01	0.0002	1200	0.6151	0.98
Mn	0.99	<0.0001	5504	0.5709	0.93

In Figure D.1, variations in the concentrations of Zn, Cu and Pb following different shaking times are shown. Zn (Fig. D.1, A and C) shows an optimum time of 180 minutes for both samples from within and outside of the halo. Cu (Fig. D.1B) and Pb (Fig. D.1 E) shows the same optimum times for samples outside the halo. For samples from within the halo, Cu (Fig. D.1 D) shows an increasing trend, whereas Pb (Fig. D.1 F) shows two increases, one from 30 to 60 and the other from 120 minutes. The latter may suggest that after this shaking time, another phase hosting Pb may begin to be leached. Based on Figures D.1, NH₄EDTA could be used as a solution for the extraction of mobile metal ions with a shaking time of 180-minutes.

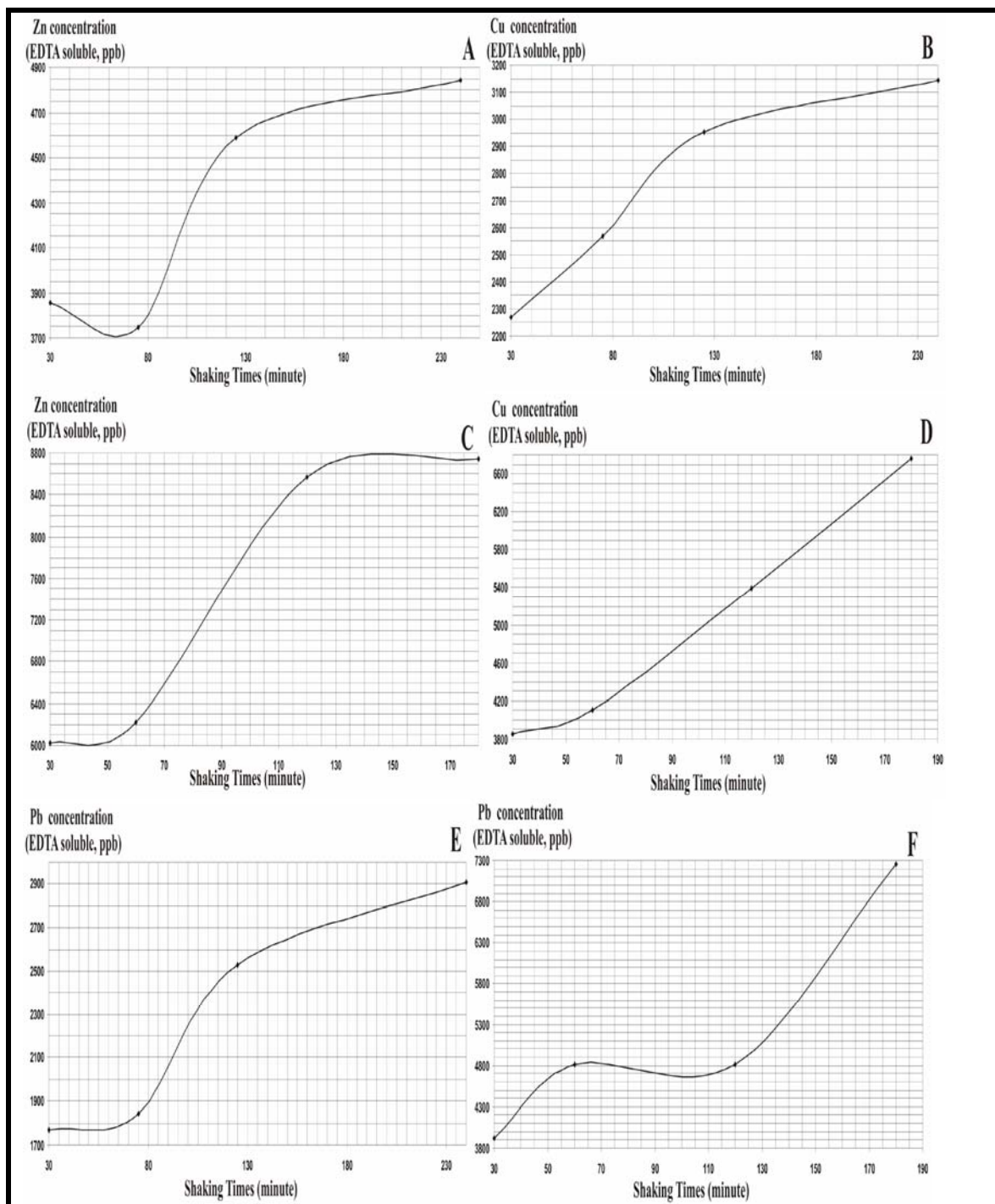


Figure D.1: Optimization of the shacking times and concentrations for Zn (A and C), Cu (B and D) and Pb (E and F) within and outside of the halo, NH₄EDTA method

D.1.4. Ca (H_2PO_4)₂ extraction

A 0.02 M Ca (H_2PO_4)₂ solution is used to remove S that is weakly bound to the sand. 50 ml of this solution was added to a plastic container (100 ml), with 5 grams of the -75 μ of the sand sample. The container is shaken for 120-minutes. Two blank samples were also shaken for 120-minutes.

The solution together with the blank samples was analyzed by ICP-MS (Table D.7). The S content in the reagents is lower than that of the sample solutions. Based on this table, samples within the halo show high contents of S when compared to the rest of the samples.

The results of the statistical calculations of duplicate samples are summarized in Table D.8. The slope of the regression lines between duplicate analyses is close to the ideal slope of one. The hypothesis that there is no correlation is rejected, with probability values of < 0.0001. This is confirmed by the good correlation coefficients determined. Inaccuracy in the intercept is probably caused by the small number of duplicate pairs. Inspection of the data reveals that the repeatability of high concentrations is poorer than that of lower values.

Table D.7: ICP-MS analytical results of sand samples for sulphur (5 grams sample + 50 ml of 0.02 M Ca (H_2PO_4)₂ solution, 120-minute shacking times)

<75 μ fraction							
Location	Sample No	Sulphur (mg/l)	S (ppb)	PH ¹ Extract.	T (°C) ¹ Extract.	PH ² Solution	T (°C) ² Solution
Outside the halo	KP12/3	0.84 1.44	8400 14400	3.3 3.3	25 25		
Inside the halo	KP12/12	0.87 0.8	8700 8000	3.3 3.3	25 25	4.6 4.6	25 25
Inside the halo	KP12/13	0.84 0.95	8400 9500	3.3 3.3	25 25		
Inside the halo	KP12/14	0.82 1.04	8200 10400	3.3 3.3	25 25		
Inside the halo	KP12/15	0.78 0.83	7800 8300	3.3 3.3	25 25	4.2 4.2	25 25
Outside the halo	KP12/19	0.78 0.98	7800 9800	3.3 3.3	25 25	3.9 3.9	25 25
Background	Blank	0.59 0.571	5900 5710	3.4 3.4	25.9 25.9	3.1 2.9	25.1 24.7
Inside the halo	KP12/1	1.291 1.564	12910 15640				
Inside the halo	KP12/7	1.016 1.137	10160 11370				
Inside the halo	KP12/10	6.085 6.636	60850 66360				
Inside the halo	KP12/18	1.581 1.658	15810 16580				
Background	Blank	0.699 0.680	6990 6800				

1. The temperature and pH of Ca (H_2PO_4)₂

2. The temperature and pH of the solution at the end of shacking time

Table D.8: Results of statistical analysis on duplicate samples and null hypothesis (0.02 M Ca (H_2PO_4)₂ solution, different shacking times, n=12)

Elements	Slope	H ₀ =0 (Pr> t)	Intercept	H ₀ =0 (Pr> t)	Correlation coefficient
S	0.92	<0.0001	-460	0.52	0.99

To optimize the shaking times, one sample within the halo at Kantienpan (KP12/13) was analyzed at different shaking times (Table D.9) and the variation of S versus shaking times shown in Figure D.2. S contents increase until it reaches a peak (~

12400 ppb) after 60-minutes of shaking, then decreases to 11300 ppb for a shaking time of 120-minute. The error calculated for duplicate pairs of sulphur analyses amounts to 6.7%. The difference observed between a shaking period of 60 minutes and 120 minutes approximates the same amount and it was decided to use a 120 minutes period for the routine sample preparation.

Table D.9: ICP-MS analytical results of sand samples for S for different shacking times (5 gram sample + 50 ml of 0.02 M Ca (H_2PO_4)₂ solution)

Location	Sample No	Shaking Time (Minute)	S (ppb)
Inside of the halo	KP12/13/1	20	8721
		20	12880
	KP12/13/2	40	11143
		40	12368
	KP12/13/3	60	12344
		60	9545
	KP12/13/4	120	11316
		120	11173
Blank	Background	120	5888
		120	5706

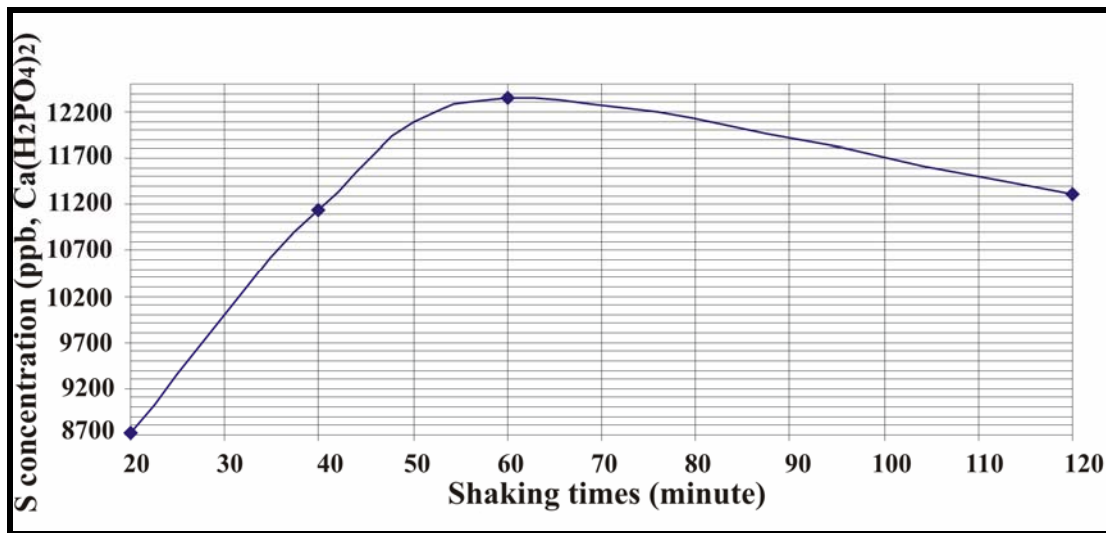


Figure D.2: Optimization of the shacking times and concentrations of S for sample from inside of the halo, Ca (H_2PO_4)₂ method.

D.1.5. XRF total analyses

The samples collected from two regolith sampling traverses, one from Kantienpan (KP12) and the other from Areachap (T2), were analyzed by x-ray fluorescence spectroscopy (XRF) to compare the results with those from the partial extraction methods. The same sample preparation and analytical method (XRF) as the one used for whole rock sample analyses was used for the analyses of regolith samples except that only pressed powder pellets were analyzed. The analytical results are presented in Tables D. 10 and D.11. Note that the major element concentrations in these samples are semi-quantitative in nature.

Table D.10: XRF analytical results of regolith sampling traverse KP12 for the <75 µ size fraction

Sample No.	%	ppm																			
	MnO	Cu	Zn	Pb	S	Rb	Sr	Cl	Co	Sc	V	As	Ga	Mo	Nb	Ni	Th	U	Y	Zr	Cr
KP 12/1	0.08	22	98	9	128	90	124	67	24	17	106	7	14	1	18	29	18	3	41	986	48
KP 12/2	0.09	22	94	15	38	97	116	244	27	20	126	11	14	1	19	32	22	3	43	989	70
KP 12/3	0.09	22	91	16	16	101	112	12	26	20	113	4	14	1	18	32	20	3	43	876	48
KP 12/4	0.10	24	96	13	16	102	109	8	30	24	117	11	16	1	18	34	19	3	44	851	64
KP 12/5	0.09	27	94	15	16	101	115	74	28	23	116	12	14	1	17	31	20	3	43	920	47
KP 12/6	0.09	29	90	13	16	101	109	55	27	22	116	8	15	1	19	32	20	3	46	929	55
KP 12/7	0.11	27	103	17	16	109	102	43	32	24	122	11	16	1	19	35	19	3	45	833	71
KP 12/8	0.09	23	97	14	16	99	111	8	28	21	115	9	14	1	19	32	21	3	46	1044	55
KP 12/9	0.12	33	120	20	66	124	89	183	38	28	130	10	17	1	17	44	22	3	45	564	75
KP 12/10	0.09	20	99	13	204	95	118	115	25	19	114	11	13	1	18	29	21	3	42	1036	35
KP 12/11	0.09	21	113	14	16	97	114	21	28	20	117	10	14	1	19	30	22	3	46	1113	57
KP 12/12	0.12	31	138	18	16	111	103	50	35	26	128	9	18	1	19	37	21	3	46	783	68
KP 12/13	0.07	13	86	21	56	96	89	182	31	89	98	12	9	1	12	20	11	3	19	274	10
KP 12/14	0.10	26	133	22	16	103	103	104	28	22	121	10	14	1	19	33	17	3	44	895	68
KP 12/15	0.10	29	135	16	16	109	103	39	32	25	127	9	17	1	20	36	20	3	49	969	76
KP 12/16	0.10	28	127	16	16	110	101	23	32	26	122	9	16	1	20	35	23	3	44	804	59
KP 12/17	0.12	30	131	22	81	111	100	142	34	25	122	9	17	1	19	38	22	3	43	837	66
KP 12/18	0.09	24	106	15	16	102	105	85	30	23	120	13	15	1	21	37	20	3	49	1047	80
KP 12/19	0.10	25	102	15	16	111	101	8	30	26	118	13	16	1	19	35	22	3	44	819	66

Table D.11: XRF analytical results of regolith sampling traverse T2 for the <75 µ finest size fraction

	%	ppm																				
Sample No.	MnO	Cu	Zn	Pb	Fe ₂ O ₃	S	Rb	Sr	Cl	Co	Sc	V	As	Ga	Mo	Nb	Ni	Th	U	Y	Zr	Cr
T2/390N	0.07	21	65	18	5.30	40	86	124	8	16	13	111	8	12	1	23	23	16	5	55	1413	137
T2/290N	0.09	29	83	23	5.87	185	97	113	8	21	17	108	3	14	1	21	30	12	4	45	976	138
T2/190N	0.08	26	79	19	5.60	124	89	121	8	18	14	111	8	14	1	23	27	16	4	53	1318	135
T2/140N	0.06	25	67	22	5.24	71	82	123	8	15	13	109	7	14	1	24	24	18	5	54	1494	128
T2/90NB	0.06	24	70	20	5.20	20	82	124	8	14	11	106	3	13	1	24	22	17	5	53	1539	134
T2/90NA	0.08	29	85	19	5.55	109	86	120	40	18	14	110	16	15	1	24	24	17	4	53	1387	130
T2/50N	0.06	29	86	21	5.04	78	82	122	8	14	13	100	3	13	1	23	21	15	3	51	1345	122
T2/30N	0.10	86	174	53	6.55	1895	93	114	8	24	17	114	12	16	1	20	29	15	3	49	1038	142
T2/20N	0.09	45	119	26	6.04	369	88	121	8	21	16	117	6	15	1	23	27	17	5	54	1300	138
T2/10N	0.08	38	103	27	5.68	337	84	123	8	20	13	112	3	14	1	24	25	18	5	58	1551	136
T2/0 (T3/240)	0.12	56	143	31	6.70	403	98	120	8	26	17	119	3	17	1	18	34	11	3	43	711	135
T2/10S	0.09	57	154	29	6.04	569	90	118	8	22	16	108	3	15	1	21	28	15	3	49	1092	144
T2/20S	0.08	43	99	26	5.74	332	88	117	8	18	16	112	3	14	1	23	26	16	4	51	1339	136
T2/40S	0.08	43	90	28	5.89	304	85	122	8	20	15	117	6	13	1	25	25	19	5	57	1560	149
T2/60S	0.07	39	84	22	5.55	228	84	121	8	17	13	112	16	13	1	25	25	18	6	57	1662	142
T2/80S	0.07	31	73	21	5.33	172	85	123	8	16	13	107	8	12	1	24	23	18	4	53	1496	131
T2/100S	0.06	29	71	21	5.38	93	86	125	8	16	12	110	3	14	1	24	22	17	5	57	1549	134
T2/150S	0.06	24	65	18	4.98	59	82	122	8	15	11	102	8	12	1	23	22	15	4	54	1438	114
T2/200S	0.06	25	66	21	4.95	69	82	125	8	14	12	104	3	12	1	22	22	14	4	52	1364	116
T2/300S	0.08	29	79	21	5.86	69	90	123	8	19	14	119	8	15	1	24	27	17	5	56	1393	139
T2/350S	0.07	25	93	22	5.57	53	89	122	8	17	13	117	8	13	1	24	26	17	5	57	1468	137
T2/190N	0.08	28	81	22	5.61	106	89	120	8	20	14	112	3	14	1	23	27	15	3	50	1235	129
T2/30N	0.10	86	175	49	6.66	1885	94	115	8	25	17	113	8	16	1	20	29	14	3	47	1017	138
T2/10S	0.09	59	152	30	6.05	576	87	117	8	22	15	109	5	15	1	21	29	13	4	48	1057	130
T2/300S	0.08	29	79	22	5.85	71	93	125	8	20	15	120	3	16	1	24	27	17	4	55	1381	134

D.1.6. Regolith data set of the Kantienpan traverses

Table D.12: ICP-MS results of regolith sampling traverse KP12 (0.02 M Ca (H_2PO_4)₂ solutions for S, shaking time: 120-minutes, and 0.02 M NH₄EDTA solutions for the rest of the elements shaking time 180-minutes)

Sample No.	Sample interval (m)	Cu (ppb)	Zn (ppb)	Pb (ppb)	Ba (ppb)	Mn (ppb)	S (mg/l) (Duplicate)	S (mg S/Kg soil) (ppm)
KP12/1	0	4712 4267	6931 6245	29984 3024	20101 19272	79674 66012	1.291 1.564	13 16
KP12/2	20	3230	6181	2861	21967	55153	0.972	10
KP12/3	40	2716	2329	28720	22064	83073	0.84	8
KP12/4	60	3517	2866	28905	21923	98921	0.832	8
KP12/5	80	3609 3449	2151 2176	8424 3578	26216 23697	105322 80709	1.186 -	12 -
KP12/6	100	2190	1351	5416	18605	101596	1.24	12
KP12/7	120	3611	5527	7474	27026	143786	1.016(1.137)	10(11)
KP12/8	140	2519	3294	120681	22117	104948	0.963	10
KP12/9	150	4754	4216	7807	29775	138939	18.43	184
KP12/10	160	2910 2699	4959 3592	3431 2785	22779 20010	102246 69948	6.085 6.636	61 66
KP12/11	170	2421	3448	3656	26426	102942	1.018	10
KP12/12	180	5477	6486	5761	46845	142653	1.44	14
KP12/13	190	5100	7175	5736	36488	79764	0.87	9
KP12/14	200	3258	9552	4240	23363	193172	0.8	8
KP12/15	210	4282 4443	6501 6864	5862 4931	38136 32897	132096 93406	0.84 -	8 -
KP12/16	220	3382	4693	5660	34671	133881	2.067	21
KP12/17	240	4274	6606	5831	33177	113758	8.594	86
KP12/18	260	3309	3962	3995	28089	85337	1.581(1.658)	16(17)
KP12/19	300	3409	2938	4290	31478	87442	0.78	78
Blank		68	218	84	266	2144	0.699(0.68)	7(7)

Table D.13: ICP-MS results of regolith sampling traverse KP5 (0.02 M NH₄EDTA solutions for Cu, Zn, Pb, Ba, Mn and Fe, shaking time: 180-minutes)

Sample No.	Sample interval (m)	Cu (ppb)	Zn (ppb)	Pb (ppb)	Ba (ppb)	Mn (ppb)	Fe (ppb)
KP5/1	0	4838	3030	2089	16784	211	132
		4072	2419	2593	16518	213	136
KP5/2	20	4201	5121	2140	19209	199	88
KP5/3	40	3805	3812	1727	17006	187	86
KP5/4	60	3594	3820	2503	21121	246	155
KP5/5	70	3526	4581	2942	20802	231	123
		3591	4584	1898	21063	229	121
KP5/6	80	6897	11078	3075	28241	379	150
KP5/7	90	3880	5654	2270	21546	220	96
KP5/8	100	3658	5086	2351	20143	167	107
KP5/9	110	4603	6014	2275	20320	185	102
KP5/10	120	4342	5654	2602	18084	173	103
		4169	5798	2669	17521	177	103
KP5/11	130	4672	5177	2886	19588	232	112
KP5/12	140	4688	5858	2851	21543	212	114
KP5/13	160	3703	5153	2935	20782	219	127
KP5/14	180	2413	4200	2667	17849	211	112
KP5/15	200	3253	5549	3532	22430	236	142
		3318	5710	3185	21832	233	138
KP5/16	220	4487	4892	3413	23608	354	147
KP5/17	240	3784	2709	3594	21388	255	133
KP5/18	270	3409	4096	3274	20775	292	160
		3458	4007	3015	20499	297	153

Table D.14: ICP-MS results of regolith traverse KP8 (0.02 M NH₄EDTA solutions for Cu, Zn, Pb, Ba, Mn and Fe, shaking time: 180-minutes)

Sample No.	Sample interval (m)	Cu (ppb)	Zn (ppb)	Pb (ppb)	Ba (ppb)	Mn (ppb)	Fe (ppb)
KP8/1	0	4268 4178	4875 5195	1961 1720	14271 12916	185 177	84 79
KP8/2	20	5535	5263	3221	25316	312	145
KP8/3	40	9756	7233	4217	25787	354	92
KP8/4	60	7991	7233	3678	29336	453	149
KP8/5	80	5159 5313	6633 8413	2042 1941	22664 20902	235 231	75 72
KP8/6	100	7990	11349	3503	29159	366	132
KP8/7	120	5562	10792	4164	31777	364	149
KP8/8	140	4608	7280	3400	25945	345	171
KP8/9	170	3620 3679	3391 4379	2652 2594	20683 20002	252 260	115 105
KP8/10	180	3004 3060	3804 3622	2783 2468	17849 16795	254 263	139 133
KP8/11	190	3548	3677	3595	21887	366	192
KP8/12	200	3152	4592	3654	20060	332	182
KP8/13	230	4552	4355	4575	22798	501	254
KP8/14	260	4665	4191	4541	25041	435	164
KP8/15	290	3948 3887	5009 4894	2593 2536	19193 19148	222 221	110 112
KP8/16	340	6815	4830	2661	16571	239	142

Table D.15: MMI results of regolith traverses 7700NW and 7800NW for Cu and Zn (Rossouw, 2003)

Regolith Traverse 7700NW					Regolith Traverse 7800NW				
Sample No.	Zn (ppb)	R/R ¹ (B=98)	Cu (ppb)	R/R ² (B=16)	Sample No.	Zn (ppb)	R/R ¹ (B=98)	Cu (ppb)	R/R ² (B=16)
800	175	1.8	46.5	2.9	800	45	0.5	1.9	0.1
825	260	2.7	25.9	1.6	825	135	1.4	28.6	1.8
850	60	0.6	1.9	0.1	850	125	1.3	1.9	0.1
875	75	0.8	1.9	0.1	875	200	2.0	41.1	2.6
900	175	1.8	62.4	3.9	900	70	0.7	1.9	0.1
925	100	1.0	1.9	0.1	925	300	3.1	86.5	5.4
950	295	3.0	78.7	4.9	950	255	2.6	70.4	4.4
975	205	2.1	62.9	3.9	975	115	1.2	1.9	0.1
1000	225	2.3	45.2	2.8	1000	300	3.1	83.6	5.2
1025	80	0.8	2.1	0.1	1025	540	5.5	51.5	3.2
1050	270	2.8	89.1	5.6	1050	295	3.0	83	5.2
1075	420	4.3	71.7	4.5	1075	370	3.8	30.2	1.9
1100	160	1.6	130	8.1	1100	100	1.0	12	0.8
1125	295	3.0	104.1	6.5	1125	5265	53.7	69	4.3
1150	75	0.8	1.9	0.1	1150	400	4.1	83.9	5.2
1175	180	1.8	111.5	7.0	1175	1980	20.2	46.2	2.9
1200	540	5.5	60.6	3.8	1200	980	10.0	269.7	16.9
1225	1380	14.1	1.9	0.1	1225	400	4.1	118.3	7.4
1250	270	2.8	120	7.5	1250	1345	13.7	99.6	6.2
1275	100	1.0	1.9	0.1	1275	430	4.4	33.9	2.1
1300	270	2.8	111.2	7.0	1300	955	9.7	83.7	5.2
1325	520	5.3	35.3	2.2	1325	200	2.0	82.8	5.2
1350	320	3.3	105.4	6.6	1350	420	4.3	78.7	4.9
1375	290	3.0	67.6	4.2	1375	270	2.8	61.7	3.9
1400	145	1.5	93.2	5.8	1400	300	3.1	82.9	5.2
1425	220	2.2	113.7	7.1	1425	270	2.8	96.8	6.1
1450	320	3.3	88.1	5.5	1450	385	3.9	89.9	5.6
1475	545	5.6	23.2	1.5	1475	40	0.4	1.9	0.1
1500	405	4.1	67.3	4.2	1500	340	3.5	44.1	2.8

 Note: R/R¹=[(peak/background) _{Zn}, Background= 98 ppb]; R/R²=[(peak/background) _{Cu}, Background= 16 ppb]

D.1.7. Regolith data set of the Areachap traverses

Table D.16: ICP-MS results of regolith sampling traverse T1 (0.02 M NH₄EDTA solutions for Cu, Zn, Pb, Ba, Mn and Fe, shaking time: 180-minutes; <75µ size fraction)

Sample No.	Sample interval (m)	Cu (ppb)	Zn (ppb)	Pb (ppb)	Ba (ppb)	Mn (ppb)	Fe (ppm)
T1/390N	390	647 636	2294 2251	1199 1140	8586 8359	68531 68084	58 52
T1/290N	290	1785	2312	1773	15534	122906	77
T1/190N	190	1572	3027	1572	11950	99999	64
T1/140N	140	2203	6664	2147	14419	136571	88
T1/90N	90	1471	1928	1671	10876	117036	71
T1/70N	70	1925	3465	2046	15040	125658	72
T1/50N	50	1710	3231	2127	9957	149248	94
T1/30N	30	2209	3130	1928	12460	118183	70
T1/20N	20	2813	3402	2180	12840	137797	74
T1/10N	10	2420	3907	1853	11626	118671	70
T1/0	0	2430	2987	2191	13908	140861	89
		2350	3991	2108	13059	142242	88
		2480	4112	2261	13725	148332	87
T1/10S	-10	1360	2706	1708	9393	102775	68
		1388	3132	1666	9633	105520	68
		1566	3689	1750	10548	108189	74
T1/20S	-20	1492	2745	1762	9438	103259	64
T1/30S	-30	1490	2996	1461	8589	78532	56
T1/50S	-50	1693	3420	1537	8526	90973	54
T1/70S	-70	1405	2937	1541	10606	97924	60
T1/90S	-90	1270	2544	1675	10283	99216	74
T1/140S	-140	1812	3530	1574	9974	97244	59
T1/190S	-190	1425	6016	1412	9894	78391	59
T1/250S	-250	1720	12134	1790	8321	105853	76
T1/250S		1736	12269	1764	8260	104247	78
Blank		74 47	819 670	17 <1	478 392	1345 308	61 2

Table D.17: ICP-MS results of regolith sampling traverse T3 (0.02M NH₄EDTA solutions for Cu, Zn, Pb, Ba, Mn and Fe, shaking time: 180-minutes; <75µ size fraction)

Sample No.	Sample interval	Cu (ppb)	Zn (ppb)	Pb (ppb)	Ba (ppb)	Mn (ppb)	Fe (ppm)
T3/0 (T1/0)	0	2480	4112	2261	13725	148332	87
T3/30	30	1704	3496	1590	10825	119164	67
T3/60	60	2772	4679	1635	9908	109543	64
T3/90	90	2270	4424	1592	9992	105432	62
T3/120	120	3315	3845	2030	12362	133356	53
T3/150	150	4038	5180	2119	12549	128565	79
T3/180	180	8667	9054	3082	14858	180343	102
T3/210	210	7120	10174	3378	12520	109333	62
T3/240	240	14821	13789	6963	19647	351	114

Table D.18: ICP-MS results of regolith sampling traverse T2 (0.02M NH₄EDTA solutions for Cu, Zn, Pb, Ba, Mn and Fe, shaking time: 180-minutes; <75µ size fraction)

Sample No.	Sample interval (m)	Cu (ppb)	Zn (ppb)	Pb (ppb)	Ba (ppb)	Mn (ppb)	Fe (ppm)	S (mg/l)	S (ppm)
T2/0 (T3/240)	0	14821 15870	13789 12899	6963 5494	19647 21585	350500 345750	114 112	1.35	14
T2/10N	10	20715 19484	26877 25012	4849 4918	21348 20328	261750 264000	135 135	1.43	14
T2/20N	20	2141 1626	4197 3638	1384 1443	13790 13370	154500 145750	81 76	0.62	6
T2/30N	30	30810 34590	28977 33638	4281 7327	11201 13084	207007 185374	152 157	1.13	11
T2/50N	50	3864	11272	2590	7208	44475	69	1.04	10
T2/70N	70	3472	7955	2809	10078	54697	85	0.86	9
T2/90N	90	1851	6010	2315	7558	39784	61	0.83	8
T2/140N	140	1821	5069	2360	7237	42203	64	0.93	9
T2/190N	190	2888	6051	3159	10992	66796	101	0.91	9
T2/290N	There was no enough sample left							0.95	10
T2/390N	390	2440 2399	17236 17294	1997 1873	16876 16996	191250 188750	84 83	0.77	8
T2/10S	-10	8781 9038	9691 9744	4853 3765	18491 18627	175000 173000	95 92	2.02	20
T2/20S	-20	9475 10808	10836 10603	5434 4297	10796 11020	65924 57963	94 97	1.75	18
T2/40S	-40	3518 4342	8900 8393	2062 2817	7548 8251	38009 47603	60 70	1.22	12
T2/60S	-60	9226	15092	3301	10788	52391	72	1.43	14
T2/80S	-80	4710	9477	2864	6505	43577	75	1.25	13
T2/100S	-100	8727 7849	12469 10468	3677 3864	10351 9293	57630 55527	82 80	0.76	8
T2/150S	-150	2087	6954	2034	6893	45026	66	1.25	13
T2/200S	-200	2107	4611	2422	6650	42958	59	1.48	15
T2/300S	-300	2966 3086	7176 8326	2967 3575	9865 9253	62205 63899	78 93	0.95	10
T2/350S	-350	11414 11400	9726 9511	3580 3334	22563 21940	242250 240500	112 112	1.36	14

D.2. Calcrete samples

Calcrete material collected from the cover above the ore deposits contains pieces of gossan. To distinguish the source of the elements of interest in the calcrete samples analyzed by XRF, the magnetic component was separated by using a hand magnet followed by a Frantz isodinamic magnetic separator (a procedure explained in Fig. D.3). For this purpose, the whole procedure was done on sample (KP12/4), a calcrete sample collected from above the ore zone in the Kantienpan area. Both the magnetic and non-magnetic parts of the sample were analyzed. The sample numbers given in brackets in this figure indicate those fractions that were analyzed by XRF. The results of XRF analysis on the magnetic and non-magnetic parts of the samples are given in Table D.18.

For the other calcrete samples, the magnetic part was removed and the original and magnetic parts were analyzed by XRF (Tables D.19 and D.23).

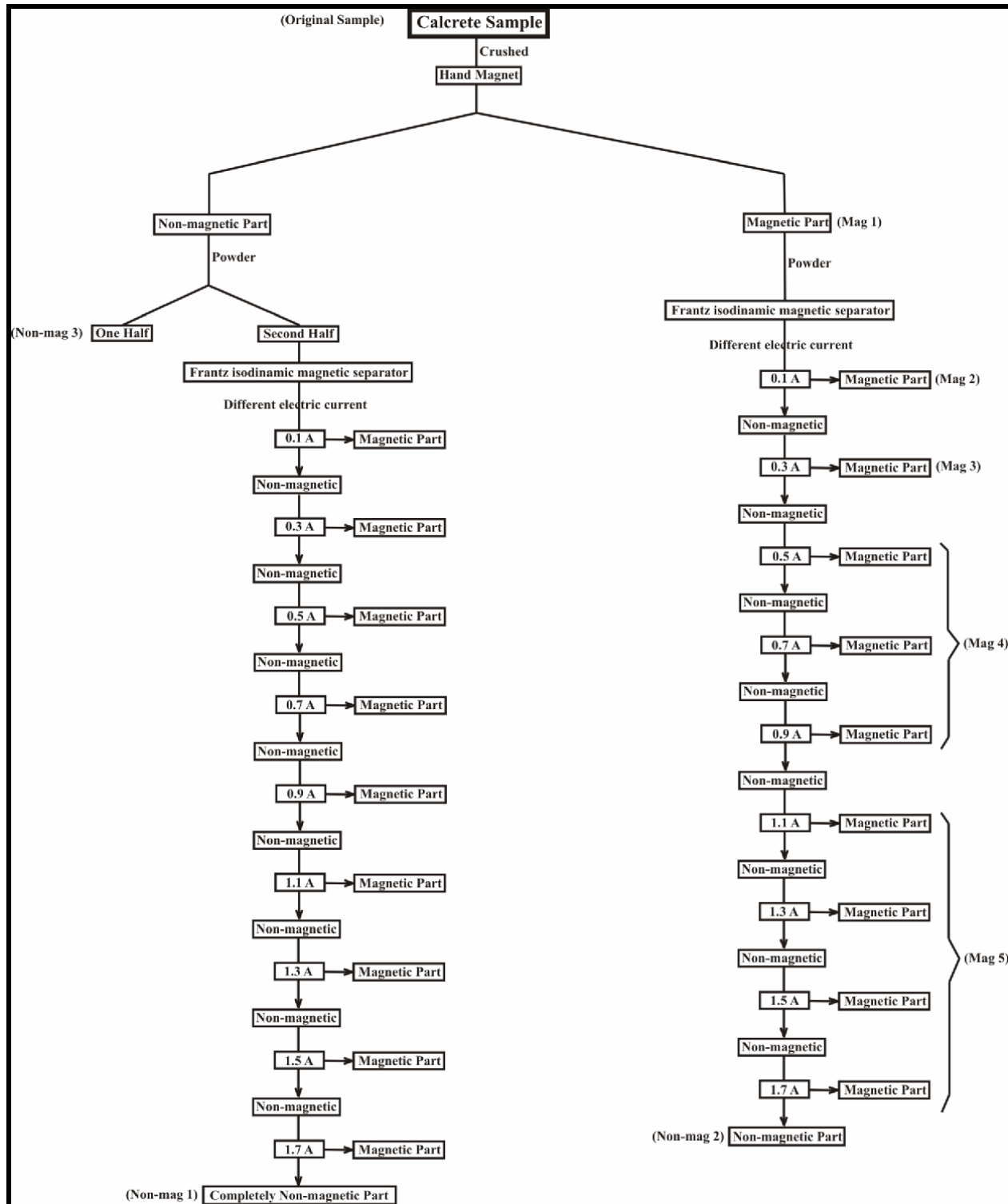


Figure D.3: Flow chart of the separation of magnetic and non-magnetic parts of calcrite samples [(in bracket): sample number for XRF analysis, A: ampere].

Table D.19: XRF results of the magnetic, non-magnetic and visually cleaned parts of the calcrete sample KPR12/4, Kantienpan (major elements: wt. %)

%	KPR 12/4	Non-Mag1	Non-Mag2	Non-Mag3	Mag1	Mag2	Mag3	Mag4	Mag5
SiO₂ *	18.43	16.84	13.84	15.56	12.67	12.71	12.42	13.79	14.69
TiO₂ *	0.22	0.09	0.1	0.15	0.21	0.51	1.1	0.98	0.53
Al₂O₃ *	2.54	1.99	1.91	2.05	1.91	1.92	1.94	2.35	2.66
Fe₂O₃ *	1.52	0.74	0.74	1	1.61	9.99	3.2	3.3	2.14
MnO *	0.05	0.04	0.04	0.05	0.04	0.06	0.08	0.08	0.06
MgO *	2.23	2.10	2.04	2.19	2.12	2.35	2.14	2.34	2.43
CaO *	39.34	39.81	42.0	39.96	42.42	39.92	40.77	40.73	40.58
Na₂O *	0.23	0.24	0.24	0.23	0.23	0.27	0.27	0.28	0.28
K₂O *	0.71	0.66	0.58	0.64	0.57	0.41	0.44	0.49	0.56
P₂O₅ *	0.17	0.21	0.11	0.22	0.11	0.09	0.09	0.12	0.17
TOTAL	65.44	62.72	61.57	62.04	61.90	68.23	62.46	64.45	64.10

Note: KPR12/4 is the original sample, Non-Mag: non-magnetic part of sample; Mag: magnetic part of samples.

*: Semi-quantitative XRF powder analyses

Table D.19: Continued

Trace elements (ppm)	KPR 12/4	Non-Mag1	Non-Mag2	Non-Mag3	Mag1	Mag2	Mag3	Mag4	Mag5
As	9	12	8	5	6	16	8	11	6
Cu	20	12	8	12	5	6	11	14	13
Ga	2	2	2	2	2	3	2	2	2
Mo	1	1	1	1	1	1	1	1	1
Nb	4	2	3	3	5	6	13	10	7
Ni	6	4	4	5	4	9	5	8	9
Pb	4	3	3	6	3	16	3	4	3
Rb	24	20	19	20	19	16	18	18	22
Sr	180	218	242	219	240	233	233	237	238
Th	4	4	3	6	5	4	3	6	6
U	3	3	3	3	3	3	3	3	3
W *	82	156	104	68	54	6	11	19	22
Y	10	8	8	9	8	9	10	16	16
Zn	45	42	39	52	42	70	86	68	62
Zr	85	69	73	87	76	65	94	90	92
Cl *	552	528	287	486	441	172	197	174	197
Co	9	9	4	2	2	31	3	5	3
Cr	10	10	10	10	10	10	10	10	10
F *	268	491	274	471	419	100	1452	560	651
S *	513	578	363	1142	446	289	300	299	329
Sc	1	1	1	1	1	1	1	1	1
V	35	16	18	19	37	305	72	63	46

Note: KPR12/4 is the original sample; Non-Mag: non-magnetic part of sample; Mag: magnetic part of samples.

*: Semi-quantitative analyses

Table D.20: XRF results of calcrete samples and magnetic parts, Kantienpan (major elements: wt. %, A: ampere)

	Original	0.1A	0.3 - 0.9A	Original	0.1- 0.3A	0.5- 0.9A	Original	0.1 - 0.3A	0.5 - 0.9A
%	KPR12/1	KPR12/1	KPR12/1	KPR12/2	KPR12/2	KPR12/2	KPR12/3	KPR12/3	KPR12/3
SiO₂ *	14	16.78	17.82	11.79	13.58	13.06	9.44	9.81	12.08
TiO₂ *	0.1	0.47	0.97	0.15	0.88	0.83	0.12	0.77	0.77
Al₂O₃ *	1.22	2.11	2.26	1.68	2.36	2.23	1.23	1.7	2.28
Fe₂O₃ *	0.79	8.08	3.14	1.48	10.72	4.22	1.54	12.23	5.77
MnO *	0.05	0.04	0.06	0.05	0.08	0.14	0.04	0.07	0.07
MgO *	2.51	1.95	1.96	2.53	2.48	2.28	1.73	1.85	1.69
CaO *	43.30	37.20	39.70	44.17	39.11	39.37	46.63	37.60	40.75
Na₂O *	0.18	0.45	0.4	0.19	0.44	0.35	0.19	0.23	0.4
K₂O *	0.33	0.38	0.45	0.51	0.4	0.47	0.29	0.24	0.27
P₂O₅ *	0.11	0.11	0.12	0.18	0.16	0.16	0.08	0.07	0.06
TOTAL	62.59	67.56	66.87	62.72	70.20	63.12	61.28	64.56	64.15

Note: *: Semi-quantitative XRF powder analyses

Table D.20: Continued

	Original	0.1 - 0.2A	0.35- 0.8A	Original	0.1- 0.2A	0.4 - 0.85A
%	KPR12/5	KPR12/5	KPR12/5	KPR12/6	KPR12/6	KPR12/6
SiO₂ *	16.59	14.18	15.81	11.34	14.01	13.51
TiO₂ *	0.19	0.95	0.88	0.16	0.98	1.54
Al₂O₃ *	2.42	2.36	2.86	2.01	2.75	2.87
Fe₂O₃ *	2.31	8.36	5.46	3.05	11.91	10.54
MnO *	0.05	0.08	0.1	0.06	0.09	0.15
MgO *	2.48	2.62	2.73	1.73	1.98	1.88
CaO *	39.72	35.85	35.81	44.35	37.23	34.84
Na₂O *	0.24	0.23	0.24	0.2	0.26	0.26
K₂O *	0.72	0.43	0.55	0.45	0.45	0.47
P₂O₅ *	0.12	0.1	0.14	0.18	0.17	0.19
TOTAL	64.84	65.15	64.58	63.52	69.82	66.25

Note: *: Semi-quantitative XRF powder analyses

Table D.20: Continued

	Original	0.1A	0.3- 0.9A	Original	0.1 - 0.3A	0.5 - 0.9A	Original	0.1 - 0.3A	0.5 - 0.9A
ppm	KPR12/1	KPR12/1	KPR12/1	KPR12/2	KPR12/2	KPR12/2	KPR12/3	KPR12/3	KPR12/3
As	12	6	6	7	6	3	6	14	3
Cu	9	15	15	19	30	27	32	35	42
Ga	2	5	3	2	6	2	2	3	2
Mo	1	1	1	1	6	1	2	1	1
Nb	3	8	10	3	17	2	2	7	2
Ni	3	3	3	6	11	3	3	7	3
Pb	3	4	7	5	7	7	9	8	22
Rb	14	18	13	17	25	2	12	14	2
Sr	154	138	134	158	182	86	207	225	123
Th	7	5	3	3	15	3	3	3	3
U	3	5	3	3	13	3	3	3	3
W[*]	6	14	16	13	10	17	6	6	20
Y	5	7	7	7	16	3	4	6	3
Zn	40	31	36	95	118	124	117	156	107
Zr	33	61	77	47	67	68	35	58	59
Cl[*]	485	8	8	8	8	8	8	260	8
Co	2	20	2	2	34	10	2	42	14
Cr	10	75	44	10	118	73	10	10	52
F[*]	635	1069	3358	290	219	2573	276	100	2184
S[*]	532	412	418	488	555	453	601	654	849
Sc	1	1	1	1	1	1	1	1	1
V	26	203	51	28	282	61	28	395	94

Note: *: Semi-quantitative analyses

Table D.20: Continued

	Original	0.1 - 0.2A	0.35 - 0.8A	Original	0.1- 0.2A	0.4 - 0.85A
ppm	KPR12/5	KPR12/5	KPR12/5	KPR12/6	KPR12/6	KPR12/6
As	8	9	14	9	10	15
Cu	17	14	42	49	37	106
Ga	2	2	3	2	4	2
Mo	1	1	1	2	1	2
Nb	4	12	11	4	8	16
Ni	6	7	12	4	9	13
Pb	7	4	12	4	6	19
Rb	23	19	22	16	18	18
Sr	251	241	234	187	170	181
Th	4	7	6	3	6	6
U	3	3	3	3	3	3
W*	32	15	9	8	11	33
Y	12	14	24	10	11	22
Zn	62	100	124	210	191	409
Zr	76	109	102	46	101	105
Cl*	238	11	26	8	8	8
Co	2	28	18	2	42	46
Cr	10	10	10	10	171	10
F *	256	100	189	182	100	100
S *	469	398	330	495	428	702
Sc	1	1	1	1	1	1
V	37	234	98	60	370	201

Note: *: Semi-quantitative analyses

Table D.21: XRF results of calcrete samples and magnetic parts, Kantienpan (major elements: wt. %, A: ampere)

	Original	0.1 - 0.3A	0.5 - 0.9A		Original	0.1A	0.3-0.9A
%	Vcal2	Vcal2	Vcal2	Vcal3	Vcal3	Vcal3	Vcal3
SiO₂ *	18.19	17.47	15.04	12.87	22.26	19.11	
TiO₂ *	0.16	0.88	0.62	0.17	0.8	0.98	
Al₂O₃ *	2.52	2.57	2.33	1.82	5.19	3.48	
Fe₂O₃ *	1.14	10.21	2.5	1.42	15.44	4.9	
MnO *	0.04	0.08	0.04	0.05	0.16	0.16	
MgO *	3.13	3.43	2.51	3.13	4.36	4.37	
CaO *	38.99	36.53	37.06	42.66	27.71	34.09	
Na₂O *	0.32	0.32	0.45	0.18	0.79	0.45	
K₂O *	0.54	0.39	0.37	0.39	0.51	0.49	
P₂O₅ *	0.14	0.1	0.07	0.13	0.33	0.29	
TOTAL	65.17	71.99	60.99	62.82	77.56	68.33	

Note: *: Semi-quantitative XRF powder analyses

Table D.21: Continued

	Original	0.1 - 0.3A	0.5 - 0.9A		Original	0.1A	0.3-0.9A
ppm	Vcal2	Vcal2	Vcal2	Vcal3	Vcal3	Vcal3	Vcal3
As	9	7	4	6	22	5	
Cu	2	2	12	2	7	10	
Ga	2	4	3	2	8	4	
Mo	1	1	1	1	2	1	
Nb	3	8	2	4	5	9	
Ni	6	10	3	6	21	15	
Pb	3	3	4	3	4	3	
Rb	18	17	2	16	31	25	
Sr	149	144	96	236	366	364	
Th	3	7	3	4	5	3	
U	3	3	3	3	3	3	
W *	44	14	25	9	12	14	
Y	8	10	3	8	27	22	
Zn	29	43	26	30	101	76	
Zr	66	93	62	41	71	85	
Cl *	102	8	8	8	363	305	
Co	2	35	2	2	73	28	
Cr	10	10	37	10	17	10	
F *	100	100	3110	366	100	340	
S *	294	258	200	231	359	338	
Sc	1	1	1	1	1	1	
V	24	275	20	41	502	103	

Note: *: Semi-quantitative analyses

Table D.22: XRF results of calcrete samples and magnetic parts, Areachap (major elements: wt. %, A: ampere, Sample set Calc1)

	Original	<0.9 A	>0.9A	Original	0.1 – 1.7A	Original	0.1 – 1.7A
%	Calc1-1	Calc1-1	Calc1-1	Calc1-2	Calc1-2	Calc1-3	Calc1-3
Depth of sample: 6 m							
Depth of sample: 3 m							
SiO₂ *	26.52	47.61	35.41	19.83	30.80	10.01	20.11
TiO₂ *	0.26	0.60	0.46	0.17	0.38	0.15	1.22
Al₂O₃ *	6.24	16.57	9.31	4.01	7.62	1.43	4.24
Fe₂O₃ *	4.77	16.60	6.78	2.70	8.18	0.91	6.44
MnO *	0.12	0.23	0.17	0.05	0.07	0.05	0.10
MgO *	2.37	4.42	3.62	1.99	2.54	1.40	2.13
CaO *	30.79	12.26	25.39	40.31	28.54	46.67	36.68
Na₂O *	0.11	0.05	0.05	0.09	0.05	0.14	0.37
K₂O *	1.00	1.93	1.52	0.62	1.13	0.25	0.56
P₂O₅ *	0.06	0.05	0.05	0.03	0.03	0.03	0.06
TOTAL	72.23	100.31	82.75	69.80	79.34	61.05	71.92

Note: *: Semi-quantitative XRF powder analyses

Table D.22: Continued

	Original	<0.9 A	>0.9A	Original	0.1 – 1.7A	Original	0.1 – 1.7A
%	Calc1-1	Calc1-1	Calc1-1	Calc1-2	Calc1-2	calc1-3	Calc1-3
Depth of sample: 6 m							
As	11	9	4	10	5	5	6
Cu	761	1998	1148	152	439	52	88
Ga	8	31	14	2	12	2	2
Mo	1	6	2	1	1	1	1
Nb	4	9	9	3	2	2	2
Ni	7	22	13	4	6	3	8
Pb	5	37	21	3	12	3	5
Rb	30	58	50	20	28	14	2
Sr	118	83	122	55	38	114	43
Th	3	7	6	3	3	4	3
U	3	3	3	3	3	3	3
W *	19	9	6	12	25	14	6
Y	18	37	23	8	18	10	3
Zn	527	1117	570	163	400	36	59
Zr	98	147	121	45	93	70	92
Cl *	648	157	202	144	8	8	8
Co	16	85	28	2	35	2	21
Cr	10	111	77	10	90	10	199
F *	301	100	1849	508	846	177	1738
S *	1332	141	231	148	81	229	386
Sc	1	1	1	1	1	1	1
V	85	264	110	46	94	19	114

Note: *: Semi-quantitative analyses

Table D.23: XRF results of calcrete samples and magnetic parts, Areachap (major elements: wt. %, A: ampere, Sample set Calc2)

	Original	0.1 – 1.7 A	Original	<0.9 A	>0.9 A	Original
%	Calc2-1	Calc2-1	Calc2-2	Calc2-2	Calc2-2	Calc2-3
Depth of sample: 4 m						
SiO₂ *						
	25.80	24.01		22.83	28.90	20.83
TiO₂ *						
	0.07	1.09		0.11	0.23	0.09
Al₂O₃ *						
	7.29	5.59		4.06	8.72	4.29
Fe₂O₃ *						
	11.36	12.40		6.24	18.45	6.05
MnO *						
	0.08	0.08		0.07	0.08	0.07
MgO *						
	2.73	2.54		2.17	3.12	2.23
CaO *						
	27.38	31.80		34.47	25.82	36.11
Na₂O *						
	0.05	0.21		0.10	0.05	0.10
K₂O *						
	0.58	0.49		0.48	0.64	0.52
P₂O₅						
	0.05	0.05		0.04	0.03	0.04
TOTAL						
	75.38	78.25		70.57	86.04	70.35

	Original	Depth of sample: 2 m	Depth of sample: surface
Calc2-2	<0.9 A	22.83	8.12
Calc2-2	>0.9 A	0.11	0.19
Calc2-2		4.06	1.68
Calc2-2		6.24	1.41
Calc2-2		0.07	0.05
Calc2-2		2.17	1.34
Calc2-2		34.47	46.98
Calc2-2		0.10	0.19
Calc2-2		0.48	0.33
Calc2-2		0.04	0.09
Calc2-2		70.57	60.37
Calc2-3			

Note: *: Semi-quantitative XRF powder analyses

Table D.23: Continued

	Original	0.1 – 1.7 Å
ppm	Calc2-1	Calc2-1
Depth of sample: 4 m		
As	12	4
Cu	125	61
Ga	14	3
Mo	2	1
Nb	5	2
Ni	3	3
Pb	17	3
Rb	22	2
Sr	98	19
Th	14	3
U	3	3
W *	57	6
Y	14	3
Zn	1047	176
Zr	68	65
Cl *	8	8
Co	78	59
Cr	10	118
F *	100	100
S *	149	236
Sc	1	1
V	116	268

Original	<0.9 Å	>0.9 Å
Calc2-2	Calc2-2	Calc2-2
Depth of sample: 2 m		
11	5	12
169	335	191
5	23	6
1	5	1
4	15	5
3	13	5
7	33	9
18	31	20
141	116	144
10	23	12
3	12	3
28	56	32
11	26	12
480	1204	504
85	73	81
8	8	349
33	122	33
10	37	10
173	100	300
327	358	330
1	1	1
85	186	84

Original
Calc2-3
11
159
2
1
3
3
3
14
158
4
3
6
9
81
145
40
2
10
310
699
1
28

Note: *: Semi-quantitative analyses

Table D.24: Chemical composition of calcretes near the ore zone (Calc1-3 and Calc2-3) and further away from ore zone (Vcal2 and Vcal3)

	Original	Original	Original	Original
%	Calc1-3	Calc2-3	Vcal2	Vcal3
SiO₂ *	10.01	8.12	18.20	12.90
TiO₂ *	0.15	0.19	0.20	0.20
Al₂O₃ *	1.43	1.68	2.50	1.80
Fe₂O₃ *	0.91	1.41	1.10	1.40
MnO *	0.05	0.05	0.00	0.00
MgCO₃ *	3.36	3.22	7.44	7.44
CaCO₃ *	83.34	83.89	69.64	76.25
Na₂O *	0.14	0.19	0.30	0.20
K₂O *	0.25	0.33	0.50	0.40
P₂O₅ *	0.03	0.09	0.10	0.10
TOTAL	99.67	99.17	99.98	100.69

Note: *: Semi-quantitative XRF powder analyses

Table D.24: Continued

	Original	Original	Original	Original
ppm	calc1-3	Calc2-3	Vcal2	Vcal3
As	5	11	9	6
Cu	52	159	2	2
Ga	2	2	2	2
Mo	1	1	1	1
Nb	2	3	3	3.7
Ni	3	3	6	6
Pb	3	3	3	3
Rb	14	14	18	16
Sr	114	158	149	236
Th	4	4	3	3.5
U	3	3	3	3
W *	14	6	44	9
Y	10	9	8	8
Zn	36	81	29	30
Zr	70	145	66	41
Cl *	8	40	102	8
Co	2	2	2	2
Cr	10	10	10	10
F *	177	310	100	366
S *	229	699	294	231
Sc	1	1	<1	<1
V	19	28	24	41

Note: *: Semi-quantitative analyses

Table D.25: Chemical composition of magnetic parts of calcretes near the ore zone (Calc1-3) and further away from ore zone (Vcal2 and Vcal3) (A: ampere in)

	0.1 – 1.7A	0.1 – 0.3A	0.5 – 0.9A	0.1A	0.3 – 0.9A
%	Calc1-3	Vcal2	Vcal2	Vcal3	Vcal3
SiO₂ *	20.11	17.50	15.00	22.30	19.10
TiO₂ *	1.22	0.90	0.60	0.80	1.00
Al₂O₃ *	4.24	2.60	2.30	5.20	3.50
Fe₂O₃ *	6.44	10.20	2.50	15.40	4.90
MnO *	0.10	0.10	0.00	0.20	0.20
MgCO₃ *	5.11	8.16	6.00	10.56	10.56
CaCO₃ *	65.50	65.18	66.25	49.46	60.89
Na₂O *	0.37	0.30	0.50	0.80	0.40
K₂O *	0.56	0.40	0.40	0.50	0.50
P₂O₅ *	0.06	0.10	0.10	0.30	0.30
TOTAL	103.71	105.44	93.65	105.52	101.35
Depth	surface	Surface	Surface	Surface	Surface

Note: *: Semi-quantitative XRF powder analyses

Table D.25: Continued

	0.1 – 1.7A	0.1– 0.3A	0.5 – 0.9A	0.1A	0.3– 0.9A
ppm	Calc1-3	Vcal2	Vcal2	Vcal3	Vcal3
As	6	7	4	22	5
Cu	88	2	12	7	10
Ga	2	4	3	8	4
Mo	1	1	1	2	1
Nb	2	8	2	5	9
Ni	8	10	3	21	16
Pb	5	3	4	4	3
Rb	2	17	2	31	25
Sr	43	144	96	366	364
Th	3	7	3	5	3
U	3	3	3	3	3
W *	6	14	25	12	14
Y	3	10	3	27	22
Zn	59	43	26	101	76
Zr	92	93	62	71	85
Cl *	8	8	8	363	305
Co	21	35	2	73	28
Cr	199	10	37	17	10
F *	1738	100	3109.7	100	340.3
S *	386	258	200	359	338
Sc	1	<1	<1	<1	<1
V	114	275	20	502	103
Depth	surface	Surface	Surface	Surface	Surface

Note: *: Semi-quantitative analyses

Table D.26: Chemical composition of calcretes near and further away from ore zone analyzed by the XRF method (Vermaak, 1984).

Vermaak Data set (1984)					
Major Oxides (%)	Copperton Cu-Zn deposit		Areachap Cu-Zn deposit		No Mineralization
	Calcrete	Complex samples	Calcrete	Complex samples	Average
No. of Samples	12	5	26	7	24
SiO₂	21.18	29.24	20.00	24.71	28.94
Fe₂O₃	2.75	11.35	1.29	12.89	1.82
MgCO₃	8.81	7.20	4.83	3.35	6.06
CaCO₃	61.46	52.09	67.72	52.80	53.43
Na₂O	0.03	0.06	0.00	0.03	0.25
K₂O	0.25	0.27	0.29	0.39	1.30
Trace elements (ppm)					
Sr	344	378	195	173	242
V	151	628	13	101	22
Cu	1850	20883	325	5945	14
Zn	372	1792	140	1018	13

Appendix E

Quantitative X-Ray Diffractometry (XRD) analyses results

Samples for quantitative x-ray diffractometry analyses are milled in a carbon-steel mill and then analyzed in a Siemens D-501 instrument (Table E.1). Utilizing Bruker AXS GmbH (Bruker AXS, 2003), the different mineral phases present are identified. This is followed by a calculation of the quantitative abundance of these minerals using the Rietveld method (Young, 1996).

TABLE E.1: Instrument and data collection parameters

Instrument	Siemens D-501
Radiation	Cu <i>K</i> (1.5418 Å)
Temperature	25EC
Specimen	flat-plate, rotating (30 RPM)
Power Setting	40 kV, 40 mA
Soller slits	2E (diffracted beam side)
Divergence slits	1E
Receiving slits	0.05E
Monochromator	secondary, graphite
Detector	scintillation counter
Range of 22	5-70E22?
Step width	0.04E 22
Time per step	1.5s

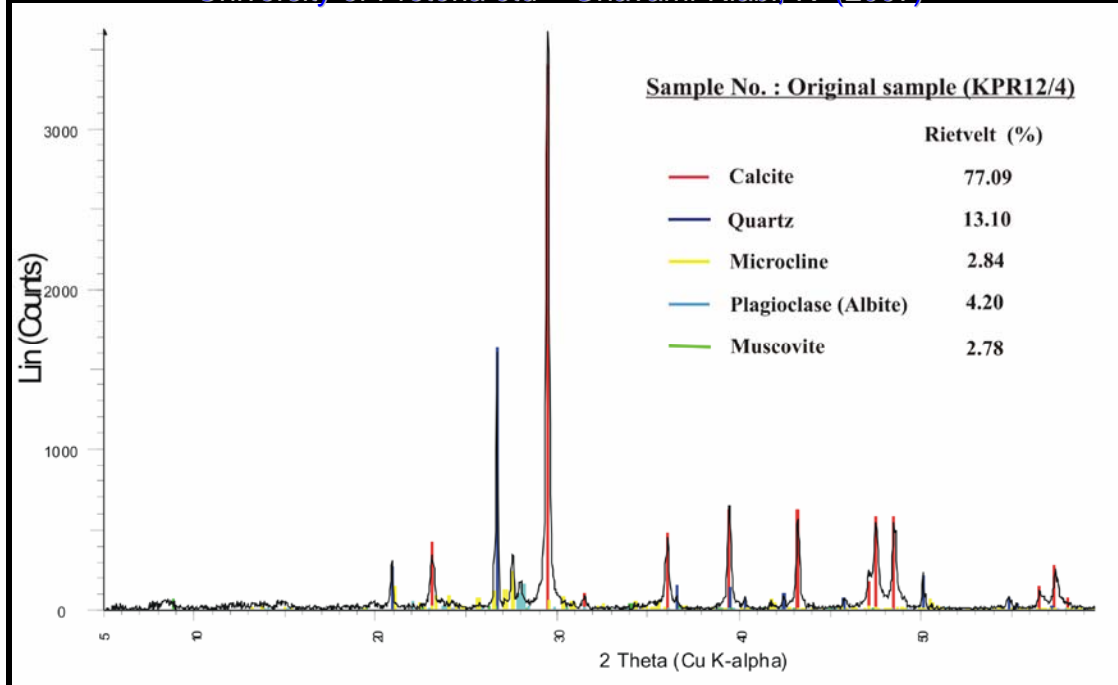


Figure E.1: XRD result for original sample KPR12/4

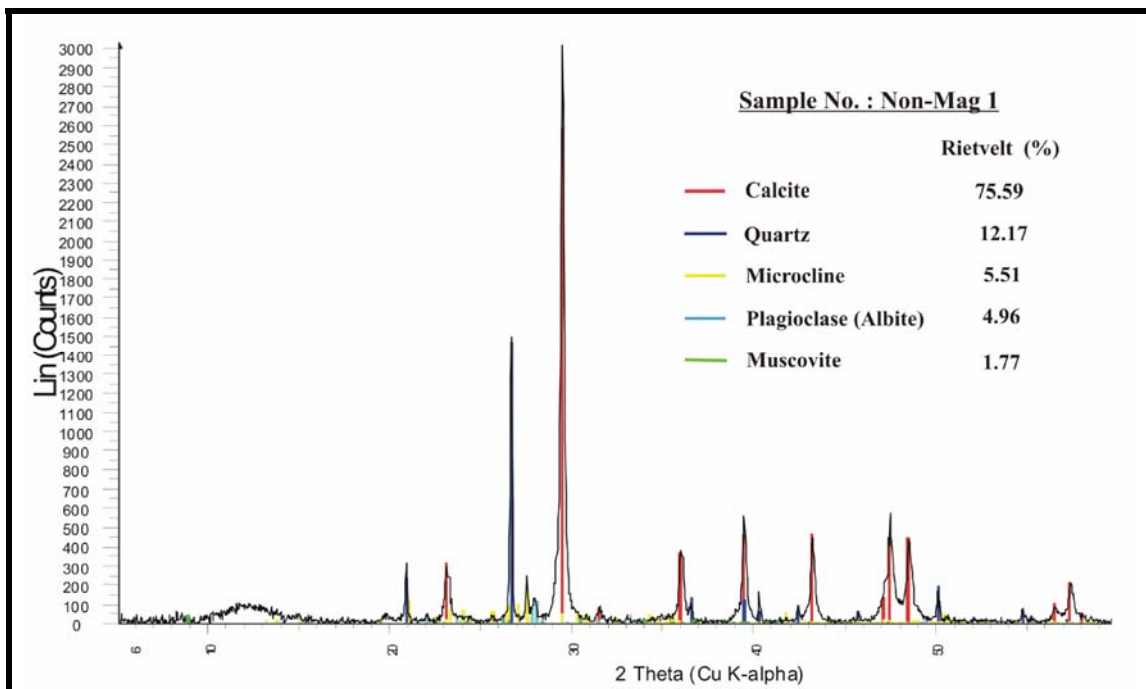


Figure E.2: XRD result for sample Non-Mag 1

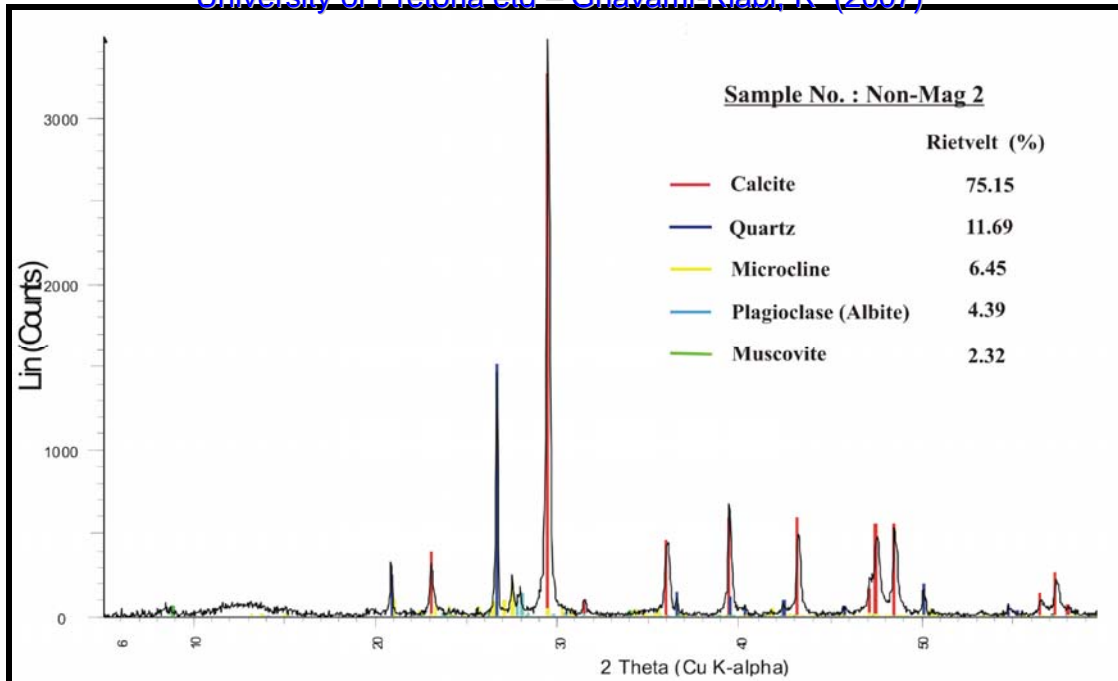


Figure E.3: XRD result for sample Non-Mag 2

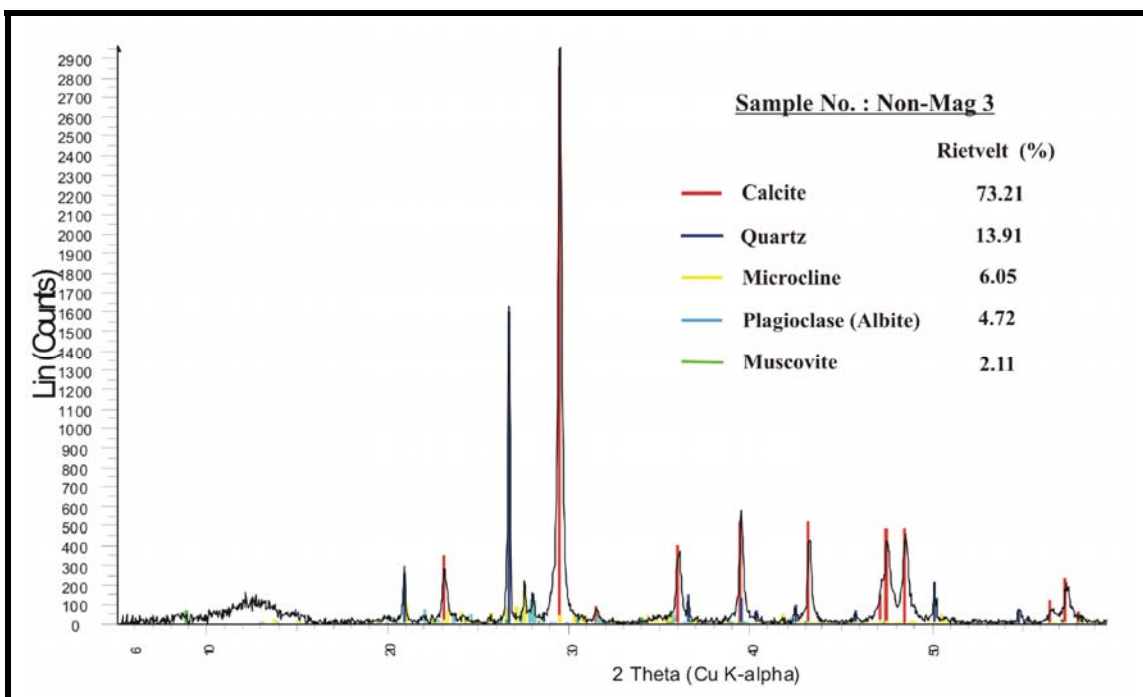


Figure E.4: XRD result for sample Non-Mag 3

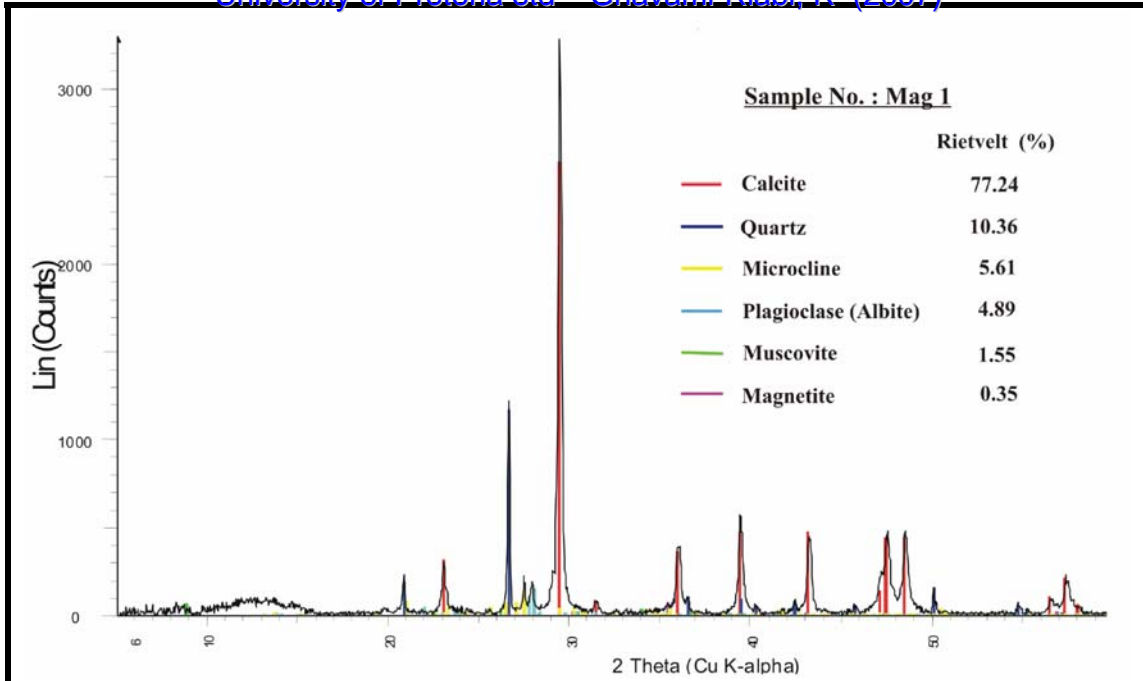


Figure E.5: XRD result for sample Mag 1

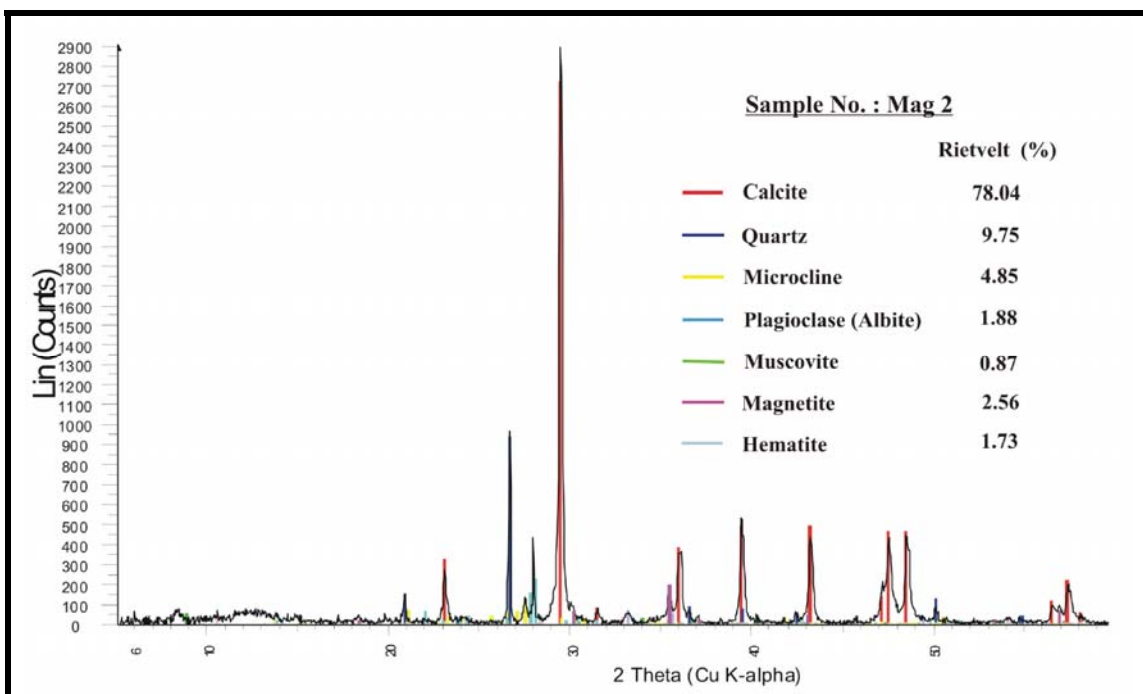


Figure E.6: XRD result for sample Mag 2

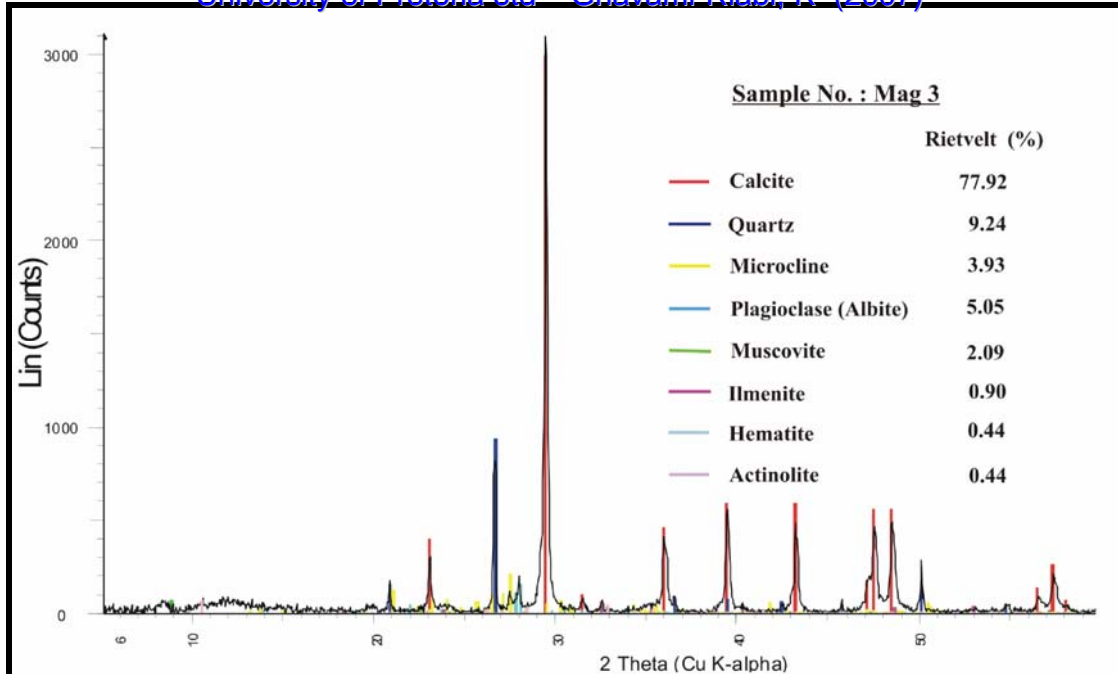


Figure E.7: XRD result for sample Mag 3

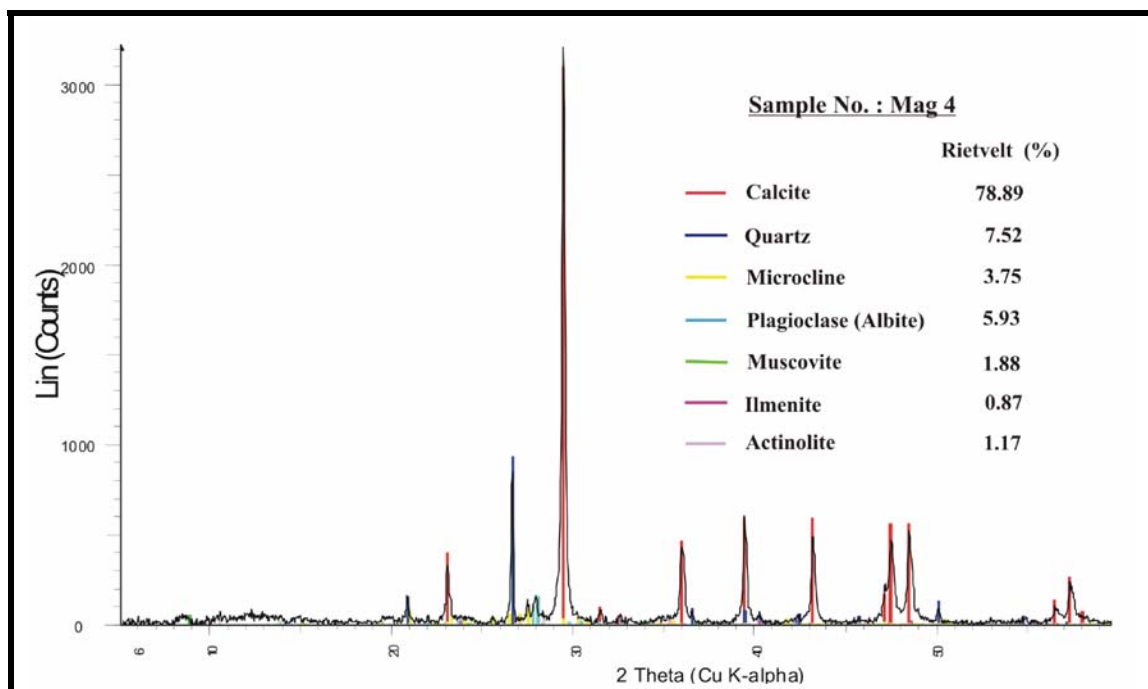


Figure E.8: XRD result for sample Mag 4

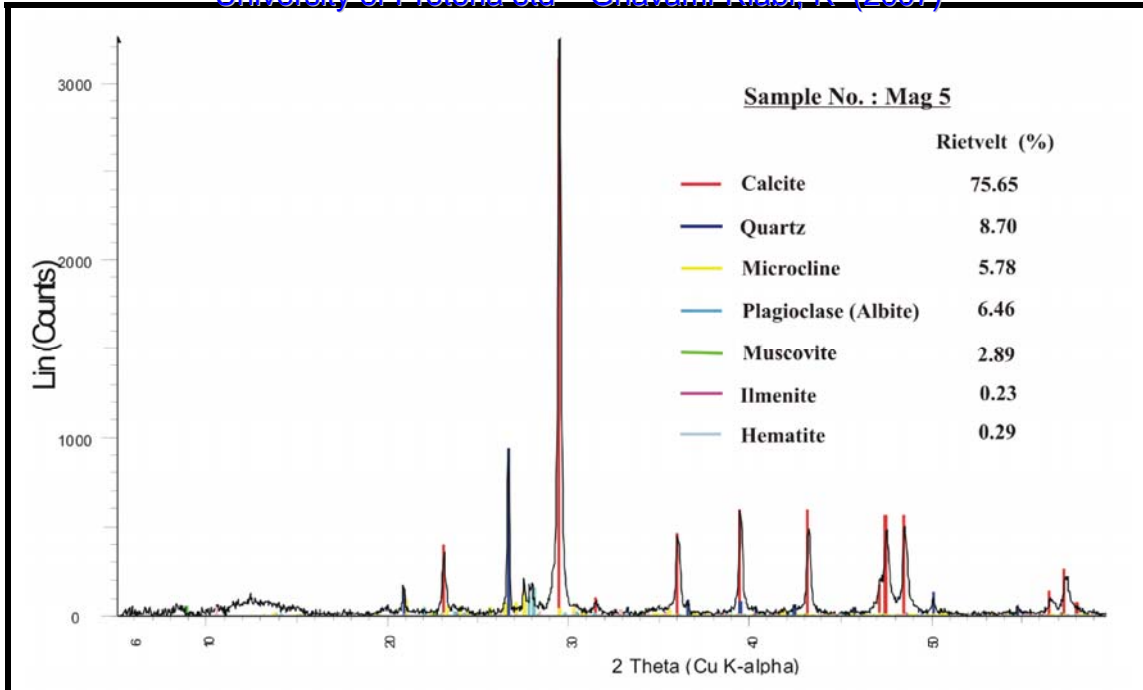


Figure E.9: XRD result for sample Mag 5

Appendix F

Confidentiality agreement with Kumba Resources Limit



Universiteit van Pretoria

Pretoria 0002 Republiek van Suid-Afrika Tel 012-420-2454
Faks 012-362-5219 <http://www.up.ac.za>

20th June 2003

Fakulteit Natuur- en Landbouwetenskappe

Prof Hennie Theart
Department of Geology
Pretoria, 0002
Tel. 012 420 3613
Fax 012 362 5219
e-mail: htheart@postino.up.ac.za

Mr H J van den Berg
General Manager Geology
Kumba Resources Limited
P O Box 9229
Pretoria, 0001

Dear Mr van den Berg,

Department of Geology, University of Pretoria, Namaqua Project: Mr Reza Ghavami-Riabi

Following our discussion on Thursday 19 June 2003, I wish to confirm the following:

- 1) Kumba Resources Limited (the Company) gave Mr Ghavami-Riabi permission to utilize the results of a lithogeochemical survey the company conducted between Areachap and Copperton in his research towards his PhD degree. The Company would also permit him to sample the core from boreholes drilled on the farms Kantlenpan and Areachap, which is kept at a storage facility on the farm Areachap.
- 2) In return Mr Ghavami-riabi undertakes to inform the company of his findings with regard this material and not to publish or publicly present these findings or the supplied information, until two years after the completion of this research project without prior permission from the Company's General Manager Geology. He and his Supervisor would treat the Company's information as confidential during this period.

Please accept our sincere appreciation for the Company's support of Mr Ghavami-Riabi's studies in this way.

Yours truly,

Mr Reza Ghavami-Riabi

Supervisor: Prof Hennie Theart